

Title: The Physics of Unification

Author: Steven Howard Snyder

Email: steveinternetemail@yahoo.com

Abstract:

To date, a unification is needed with the application of Planck units which unifies not only the force of Newtonian gravity with the electromagnetic force and the strong and weak nuclear forces, but also one which includes quantum field theory and relativity. Herein, a unification as such is accomplished in which the mathematical terms of the conventional fields and the corresponding forces are unified into one general function in Planck units, and the geometry (including internal structure) and functionality of certain aspects of the respective unified field constructed therefrom are described. Accordingly, the geometry and functionality of the unified field are applied for describing certain aspects of electromagnetic, gravitational, and nuclear interaction along with certain aspects of elementary particles (including antiparticles), atoms, molecules, and at the macroscopic scale, astronomical bodies.

GENERAL FUNCTION OF THE UNIFIED FIELD:

A general function of a unified field is formulated herein complemented by a theoretical internal structure which has been constructed for the posited unified field unlike the functions of the conventional forces of Newtonian gravity, the electromagnetic force, the strong and weak nuclear forces, and the functions of conventional spacetime. Wherein, first, equation (1A), which was designed especially for the purposes of the theory herein, is rewritten as a general exponential function which has the form shown in equation (1B):

$$f = z = \pm e^{\frac{1}{N}[n_1 \pm x + n_2 \pm y]} \quad \text{Eq. (1A)}$$

$$f = z = \pm e^{\left[\frac{1}{N}n_1 \pm x + \frac{1}{N}n_2 \pm y \right]} \quad \text{Eq. (1B)}$$

In which case, $1/N$ is a constant such that $N=1, 2, 3, \dots$; and n_1 and n_2 are constants such that $1 < n_1 < 2$, and $0 < n_2 < 1$.

Now, substituting $\frac{2\pi(qvr)}{h_q}$ and $\frac{2\pi(mvr)}{h}$ for (x) and (y), respectively, in equation (1B) results in

the following more specific function:

$$f = \pm e^{\left[\frac{1}{N} n_1 \frac{\pm 2\pi(qvr)}{h_q} + \frac{1}{N} n_2 \frac{\pm 2\pi(mvr)}{h} \right]}. \quad \text{Eq. (2)}$$

Here, (q) is charge, (v) is velocity, (r) is radius, (m) is mass, (π) is Pi, and (h) is Planck's constant as applied for the mass aspect of the unified field, and (h_q) is a variation of sorts on Planck's constant which is applied theoretically for the charge aspect of the unified field as will be described more so below.

Equation (2) is expressed as follows when $v=c$:

$$f = \pm e^{\left[\frac{1}{N} n_1 \frac{\pm 2\pi(qcr)}{h_q} + \frac{1}{N} n_2 \frac{\pm 2\pi(mcr)}{h} \right]}. \quad \text{Eq. (3A)}$$

The (x) and (y) terms in the exponent (neglecting signs) can each be made approximately equal to a dimensionless value of one when using terms which include Planck units in both variables of the exponent, when $h \approx 2\pi mcr$, and when applying the following charge to mass ratio in the (x) variable of the exponent:

$$\frac{\frac{(q_p)}{(m_p)}}{\frac{(q_p)}{(m_p)}} = \frac{\frac{(1.8755 \times 10^{-18} \text{ C})}{(2.1764 \times 10^{-8} \text{ kg})}}{\frac{(1.8755 \times 10^{-18} \text{ C})}{(2.1764 \times 10^{-8} \text{ kg})}} = 1$$

Wherein, $\frac{2\pi(qcr)}{h_q} = \frac{2\pi(mcr)}{h}$ as exemplified in figures (1A) and (1B) as follows:

$$x = \frac{2\pi(qcr)}{h_q} = \frac{2\pi(2.1764 \times 10^{-8} \text{ kg}) \frac{(1.8755 \times 10^{-18} \text{ C}) (1.6162 \times 10^{-35} \text{ m})}{(2.1764 \times 10^{-8} \text{ kg}) (5.3912 \times 10^{-44} \text{ s})} (1.6162 \times 10^{-35} \text{ m})}{\frac{(1.6162 \times 10^{-35} \text{ m})^2 (2.1764 \times 10^{-8} \text{ kg}) \frac{(1.8755 \times 10^{-18} \text{ C})}{(2.1764 \times 10^{-8} \text{ kg})} (5.3912 \times 10^{-44} \text{ s})}{(5.3912 \times 10^{-44} \text{ s})^2}} \approx 1$$

FIG. 1A

$$y = \frac{2\pi(mcr)}{h} = \frac{2\pi(2.1764 \times 10^{-8} \text{ kg}) \frac{(1.6162 \times 10^{-35} \text{ m})}{(5.3912 \times 10^{-44} \text{ s})} (1.6162 \times 10^{-35} \text{ m})}{\frac{(1.6162 \times 10^{-35} \text{ m})^2 (2.1764 \times 10^{-8} \text{ kg}) (5.3912 \times 10^{-44} \text{ s})}{(5.3912 \times 10^{-44} \text{ s})^2}} \approx 1$$

FIG. 1B

Here, the (x) variable of the exponent in equation (3A) is made to represent the "charge" aspect of the function with the application of the respective charge to mass ratio, and, as will be shown later, the ratio will be useful for constructing an expression for theoretical and conventional electromagnetic potentials, etc.

Now, equation (3A) is made into unified field function (4A) by first taking equation (3A)

$$f = \pm e^{\left[\frac{1}{N} n_1 \frac{\pm 2\pi(qcr)}{h_q} + \frac{1}{N} n_2 \frac{\pm 2\pi(mcr)}{h} \right]} \quad \text{Eq. (3A)}$$

and rewriting it as Eq. (3B)

$$f = \pm e^{\left[\frac{1}{N} n_1 \frac{\pm 2\pi(qcr)}{h_q} \right]} * \pm e^{\left[\frac{1}{N} n_2 \frac{\pm 2\pi(mcr)}{h} \right]}, \quad \text{Eq. (3B)}$$

and then reflecting the (x) variable (which relates to charge) while treating (c) and 1/N as constants, such that

$$f = \pm c \frac{1}{N} * \ln \left[\frac{n_1 * 2\pi(qr)}{h_q} \right] * e^{\left[\frac{1}{N} n_2 \frac{\pm 2\pi(mcr)}{h} \right]}.$$

Here, the reflection of the function is considered to be a mathematical representation of an important physical aspect of the oscillatory trajectory of the flow of mass-energy in the unified field as will be indicative later.

Then, upon taking one partial derivative by keeping the exponential portion of the function which relates to the (y) variable (mass) constant the following function is produced:

$$f_x(x, y) = {}^{\pm}c * \frac{1}{N} \frac{1}{n_1 * 2\pi(qr)} * e^{\left[\frac{1}{N} \frac{n_2 * {}^{\pm}2\pi(mcr)}{h} \right]},$$

which then can be expressed as Eq. (4A)

$${}^{\pm}f_x(x, y) = \frac{1}{N} \frac{h_q c}{n_1 * 2\pi(qr)} * e^{\left[\frac{1}{N} \frac{n_2 * {}^{\pm}2\pi(mcr)}{h} \right]}. \quad \text{Eq. (4A)}$$

In result, equation (4A) is a general unified field function which provides families of functions for the potential of the unified field presented herein.

Equation (4A) will be applied next to describe electromagnetic, gravitational, and nuclear potentials. However, the essential difference between the function of equation (4A) and the functions of Newtonian and Coulombic potentials resides in the presence of the exponential term.

In convention, the exponential term is present along with the inverse function in the function which describes the nuclear potential. In which case, the exponential term in the function of the nuclear potential is considered to approach a value of one as the mass in the exponent approaches a value of zero. While, the exponential term is absent in the functions which conventionally describe Newtonian gravitational and Coulombic (electrostatic) potentials.

However, to the contrary, the exponential term is applied with the inverse function in the unified field

function herein, and thus is included in the definition of not only the nuclear potential, but also included in the definition of the gravitational and electromagnetic potentials. Wherein, in the present theory, the exponential term only approximates a value of zero in the expressions for gravitational and electromagnetic potentials.

While, in physical terms, the exponential term plays an important role in the unified field function in allowing for the three dimensional spatial aspect of the function (i.e., the three dimensional physical aspect of the oscillatory trajectory of the flow of mass-energy in the unified field) as will be described more so later.

Next, a theoretical "nuclear" field potential equation (4B), which can be related to both the conventional strong and weak fields, is arrived at by applying the following member functions from the families of functions in equation (4A)

$$f = \frac{1}{N} \frac{h_q c}{n_1 * 2\pi(qr)} * e^{\left[\frac{1}{N} \frac{n_2 * -2\pi(mcr)}{h} \right]},$$

and then taking the negative of the functions for convention as shown in equation (4B)

$$f = - \frac{1}{N} \frac{h_q c}{n_1 * 2\pi(qr)} * e^{\left[\frac{1}{N} \frac{n_2 * -2\pi(mcr)}{h} \right]} \quad \text{Eq. (4B)}$$

(Note that the signs used for the families of functions in equation 4A pertain to the signs on the axes which relate to the functions, while the sign of the function in equation 4B relates to the direction of potential in

conventional terms.)

Next, the value of the theoretical nuclear potential function in equation (4B) approximately equals

$\frac{1}{2}c^2$ when $1/N$ is considered equal to one, and $n_1 \approx 2$ and $n_2 \approx 0$,

$$f = \frac{-h_q c}{\approx 4\pi(qr)} * e^{\left[\frac{\approx -0\pi(mcr)}{h} \right]} \approx \frac{1}{2}c^2 \quad \text{Eq. (4C)}$$

or

$$f = \frac{-h_q c}{\approx 4\pi(qr)} * e^{\left[\frac{\approx -0*2\pi(mcr)}{h} \right]} \approx \frac{1}{2}c^2 .$$

Wherein, equation (4C) is considered to represent one half of one portion of the family of nuclear potential functions as will also be described more so later.

Now, since $\frac{2\pi qcr}{h_q} = \frac{2\pi mcr}{h} \approx 1$, then $\frac{q}{h_q} = \frac{m}{h}$ and $\frac{h_q}{q} = \frac{h}{m}$. Wherein, after taking the

gradient of equation (4C), breaking the result down into vector components, and then substituting $\frac{h}{m}$ for $\frac{h_q}{q}$

in one term, equation (4C) can be written in terms of vector components in the form of mass and electric charge gradients as follows in equation (5):

$$\begin{aligned} \frac{1}{2} \nabla \varphi \text{ (nuclear gradient portion)} &= \left(\frac{1}{\sqrt{2}} \frac{-h_q c}{\approx 4\pi(qr^2)} * e^{\left[\frac{\approx -0\pi(mcr)}{h} \right]} \right)^2 + \left(\frac{1}{\sqrt{2}} \frac{-hc}{\approx 4\pi(mr^2)} * e^{\left[\frac{\approx -0\pi(mcr)}{h} \right]} \right)^2 \\ &= \left(\frac{-h_q c}{\approx 4\pi(qr^2)} * e^{\left[\frac{\approx -0\pi(mcr)}{h} \right]} \right)^2 \end{aligned}$$

Eq. (5)

Here (∇) is gradient, and $\varphi = -\frac{K_T q}{r} * e^{\left[\frac{\approx -0\pi(mcr)}{h} \right]} = \frac{-h_q c}{\approx 2\pi(qr)} * e^{\left[\frac{\approx -0\pi(mcr)}{h} \right]}$ wherein K_T is a

theoretical precursor to the conventional electrostatic constant K_C as will also be explained more so later.

Next, one portion of the theoretical gravitational mass gradient for what is considered herein as the “extranuclear” field of the unified field (i.e., a theoretical gravitational field gradient which can be related to the conventional Newtonian gravitational potential at weak field and low velocity) is represented by one vector component, i.e., the (y) component, in equation (5). Wherein, in terms of theoretical gravitational potential,

$$\frac{1}{\sqrt{2}} \frac{-hc}{\approx 4\pi(mr)} * e^{\left[\frac{\approx -0\pi(mcr)}{h} \right]} \approx \frac{-1}{2\sqrt{2}} c^2 \text{ when}$$

$$h \approx 2\pi mcr = 2\pi(2.1764 \times 10^{-8}) \left(\frac{1.6162 \times 10^{-35}}{5.3912 \times 10^{-44}} \right) (1.6162 \times 10^{-35}) \approx 6.6253 \times 10^{-34} \text{ such that } e^{\left[\frac{\approx -0\pi(mcr)}{h} \right]} \approx 1, \text{ in}$$

$$\text{which case the units in } e^{\left[\frac{\approx -0\pi(mcr)}{h} \right]} \text{ cancel, and such that } \frac{1}{\sqrt{2}} * \frac{-hc}{\approx 4\pi(mr)} = \frac{1}{\sqrt{2}} * \frac{-2\pi mc^2 r}{\approx 4\pi(mr)} \approx \frac{-1}{2\sqrt{2}} c^2.$$

Also, figure (2A) shows the production of approximately one half of the conventional gravitational potential,

i.e., $\approx \frac{1}{2} G_T * \frac{m}{r}$, after the cancellation of certain units in $\frac{hc}{\approx 4\pi(mr)}$ (while neglecting the sign).

$$\frac{hc}{\approx 4\pi(mr)} \Rightarrow \frac{(kg * m^2 * \cancel{s}) (m)}{(s)^2 (\cancel{s}) (kg * m)} \Rightarrow \frac{(m^3)}{(kg * s^2)} \frac{(kg)}{(m)} \Rightarrow \approx \frac{1}{2} G_T \frac{(kg)}{(m)}$$

FIG. 2A

In which case, (G_T) takes on the same numerical value as the conventional gravitational constant, i.e.,

6.6×10^{-11} , using Planck units as shown below:

$$G_{Planck} = \frac{(m)^3}{(kg)(s)^2} = \frac{(l_p)^3}{(m_p)(t_p)^2} = \frac{(1.6162 \times 10^{-35})^3}{(2.1764 \times 10^{-8})(5.3912 \times 10^{-44})^2} = 6.6730 \times 10^{-11} .$$

Similarly, one portion of the theoretical electric charge gradient for the extranuclear field of the unified field, (i.e., a theoretical electric field gradient which can be related to the conventional electrostatic, i.e., Coulomb, potential at weak field and low velocity) is represented by the other vector component, i.e., the (x) component, in equation (5). In which case, an equivalent argument for the theoretical electromagnetic potential which relates to the theoretical electric charge gradient component in equation (5) can be made, wherein

$$\frac{1}{\sqrt{2}} \frac{h c}{q} * e^{\left[\frac{\approx -0\pi(mcr)}{h} \right]} \approx \frac{-1}{2\sqrt{2}} c^2 \text{ when } h_q = h \approx 2\pi mcr, \text{ such that } e^{\left[\frac{\approx -0\pi(mcr)}{h} \right]} \approx 1, \text{ and such that}$$

$$\frac{1}{\sqrt{2}} * \frac{\bar{h}qc}{\approx 4\pi(qr)} = \frac{1}{\sqrt{2}} * \frac{\bar{h}c}{\approx 4\pi(mr)} = \frac{1}{\sqrt{2}} * \frac{\bar{2}\pi mc^2 r}{\approx 4\pi(mr)} \approx \frac{1}{2\sqrt{2}} c^2). \text{ In which case,}$$

$$\frac{1}{\sqrt{2}} \frac{\bar{h}c}{\approx 4\pi(qr)} * e^{\left[\frac{\approx -0\pi(mcr)}{h} \right]}$$

is considered the theoretical electromagnetic potential counterpart to the

theoretical gravitational potential shown before. Moreover, similarly, figure (2B) shows the conversion of the

units of theoretical electromagnetic potential $\frac{\bar{h}qc}{\approx 4\pi(qr)}$ into the units of conventional electrostatic potential,

including the units of the conventional electrostatic constant, i.e., the units of $\frac{N * m^2}{C^2}$, for the production of a

theoretical approximation of one half of the conventional electrostatic potential, i.e., $\approx \frac{1}{2} K_C * \frac{q}{r}$, after the

cancellation of certain units while again applying the following charge to mass ratio $\frac{(q_p)}{(m_p)}$ which has the

units $\frac{(C)}{(kg)}$ (also while neglecting the sign):

$$\frac{hc \frac{(q_p)}{(m_p)}}{\approx 4\pi(mr) \frac{(q_p)}{(m_p)} \frac{(q_p)}{(m_p)}} \Rightarrow \frac{h_q c}{\approx 4\pi(qr) \frac{(q_p)}{(m_p)}} \Rightarrow \frac{\frac{(\cancel{kg}) (C)}{(\cancel{kg})} (m)^2 \frac{(s)}{(s)} (m)}{(s)^2 \frac{(\cancel{kg})}{(\cancel{kg})} \frac{(C)}{(kg)} \frac{(C)}{(kg)} (m)} \Rightarrow \frac{(N) * (m)^2 (C)}{(C)^2 (m)} \Rightarrow \approx \frac{1}{2} K_C \frac{(C)}{(m)}$$

FIG. 2B

Now, substituting $\approx \frac{1}{2} K_T \frac{q}{r}$ for $\frac{-hc}{\approx 4\pi(qr)}$ in equation (4C) provides for a different expression

for theoretical nuclear potential:

$$f \approx \frac{1}{2} K_T \frac{q}{r} * e^{\left[\frac{\approx -0\pi(mcr)}{h} \right]} \approx \frac{1}{2} c^2$$

which can be rewritten as Eq. (6)

$$f \approx \frac{1}{2} K_T (q) * \frac{e^{\left[\frac{\approx -0\pi(mcr)}{h} \right]}}{r} \approx \frac{1}{2} c^2. \quad \text{Eq. (6)}$$

Here, equation (6) is considered to be another expression which represents one half of a given portion of the theoretical nuclear potential. Wherein, a whole portion of theoretical nuclear potential is arrived at by adding two equivalent portions of the function from equation (6) as shown in equation (7A) as follows:

$$V_{(\text{whole nuclear potential portion})} \approx \frac{1}{2} K_T(q) * \frac{e^{\left[\frac{\approx -0\pi(mcr)}{h} \right]}}{r} + \frac{1}{2} K_T(q) * \frac{e^{\left[\frac{\approx -0\pi(mcr)}{h} \right]}}{r} \approx$$

$$K_T(q) * \frac{e^{\left[\frac{\approx -0\pi(mcr)}{h} \right]}}{r} \approx 1c^2$$

Eq. (7A)

or

$$V_{(\text{whole nuclear potential portion})} \approx K_T \left(\frac{q}{2} + \frac{q}{2} \right) * \frac{e^{\left[\frac{\approx -0\pi(mcr)}{h} \right]}}{r} \approx K_T(q) * \frac{e^{\left[\frac{\approx -0\pi(mcr)}{h} \right]}}{r} \approx 1c^2$$

Next, substituting $\approx \frac{1}{2} K_T \frac{q}{r^2}$ for $\frac{\approx h_q c}{\approx 4\pi(qr^2)}$ and $\approx \frac{1}{2} G_T \frac{m}{r^2}$ for $\frac{\approx hc}{\approx 4\pi(mr^2)}$ for the

components in equation (5), and substituting $\approx \frac{1}{2} K_T \frac{q}{r^2}$ for the respective sum $\frac{\approx h_q c}{\approx 4\pi(qr^2)}$ in equation

(5) such that $K_T = G_T$, the resulting equation (8A) provides for an expression for gravitational plus electromagnetic charge gradients:

$$-\frac{1}{2} \nabla \varphi_{\text{(extranuclear gradient portion)}} \approx \left(-\frac{1}{2\sqrt{2}} K_T(q) * \frac{e}{r^2} \frac{\left[\frac{\approx -0\pi(mcr)}{h} \right]}{r^2} \right)^2 + \left(-\frac{1}{2\sqrt{2}} G_T(m) * \frac{e}{r^2} \frac{\left[\frac{\approx -0\pi(mcr)}{h} \right]}{r^2} \right)^2 \approx$$

$$\left(-\frac{1}{2} K_T(q) * \frac{e}{r^2} \frac{\left[\frac{\approx -0\pi(mcr)}{h} \right]}{r^2} \right)^2$$

Eq. (8A)

Here, equation (8A) is considered to represent one half of the total theoretical electric field plus gravitational field gradient for the given portion of the extranuclear field. While a whole theoretical electric field plus gravitational field gradient for the given portion of the extranuclear field is considered to be arrived at by adding two equivalent portions of the function from equation (8A) as follows:

$$-\nabla \varphi_{\text{(whole extranuclear gradient portion)}} \approx$$

$$\left(-\frac{1}{2\sqrt{2}} K_T(q) * \frac{e}{r^2} \frac{\left[\frac{\approx -0\pi(mcr)}{h} \right]}{r^2} - \frac{1}{2\sqrt{2}} K_T(q) * \frac{e}{r^2} \frac{\left[\frac{\approx -0\pi(mcr)}{h} \right]}{r^2} \right)^2 +$$

$$\left(-\frac{1}{2\sqrt{2}} G_T(m) * \frac{e}{r^2} \frac{\left[\frac{\approx -0\pi(mcr)}{h} \right]}{r^2} - \frac{1}{2\sqrt{2}} G_T(m) * \frac{e}{r^2} \frac{\left[\frac{\approx -0\pi(mcr)}{h} \right]}{r^2} \right)^2 \approx \left(-K_T(q) * \frac{e}{r^2} \frac{\left[\frac{\approx -0\pi(mcr)}{h} \right]}{r^2} \right)^2$$

such that

$$\begin{aligned}
 -\nabla \varphi_{(\text{whole extranuclear gradient portion})} \approx & \\
 & \left(-\frac{1}{\sqrt{2}} K_T(q) * \frac{e}{r^2} e^{\left[\frac{\approx -0\pi(mcr)}{h} \right]} \right)^2 + \\
 & \left(-\frac{1}{\sqrt{2}} G_T(m) * \frac{e}{r^2} e^{\left[\frac{\approx -0\pi(mcr)}{h} \right]} \right)^2 \approx \left(-K_T(q) * \frac{e}{r^2} e^{\left[\frac{\approx -0\pi(mcr)}{h} \right]} \right)^2
 \end{aligned} \tag{Eq. (8B)}$$

The addition of two equivalent functions in equation (8B) involves the vector addition of two portions of the unified field which can be more clearly understood by referring to the geometry of the unified field described later as with respect to, in particular, figures 7A, 7B, 7C, and 7D.

Nevertheless, the total potential of a static elementary particle can be considered to be arrived at by the following summation shown in equation (9A) (for eight octants):

$$V_{(\text{particle total})} = 4 * \sum \left(\frac{-h_q c}{n_1 * 2\pi(qr)} * e^{\left[\frac{n_2 * -2\pi(mcr)}{h} \right]} + \frac{-h_q c}{n_1 * 2\pi(qr)} * e^{\left[\frac{n_2 * -2\pi(mcr)}{h} \right]} \right) + \dots$$

Eq. (9A)

Wherein (V) is potential, and n_1 goes from ≈ 2 to ≈ 1 as n_2 goes from ≈ 0 to ≈ 1 for each term of the summation.

While furthermore, the total potential of a system (e.g., a system of bonded nucleons) can be considered to be arrived at by the following shown summation in equation (9B):

$$V_{(\text{system total})} = 4 * \sum \left(\frac{1}{N_a} \frac{-hqc}{n_1 * 2\pi(qr)} * e^{\left[\frac{1}{N_a} \frac{n_2 * -2\pi(mcr)}{h} \right]} + \frac{1}{N_a} \frac{-hqc}{n_1 * 2\pi(qr)} * e^{\left[\frac{1}{N_a} \frac{n_2 * -2\pi(mcr)}{h} \right]} \dots \right) +$$

$$\left(\frac{1}{N_a} \frac{-hqc}{n_1 * 2\pi(qr)} * e^{\left[\frac{1}{N_a} \frac{n_2 * -2\pi(mcr)}{h} \right]} + \frac{1}{N_a} \frac{-hqc}{n_1 * 2\pi(qr)} * e^{\left[\frac{1}{N_a} \frac{n_2 * -2\pi(mcr)}{h} \right]} \dots \right) \dots$$

Eq. (9B)

Wherein $1/N_a$ is a constant with the same value for all terms inside the parentheses and changes from one parenthetical term to another in the summation shown such that $a=1, 2, \dots$, i.e., $N_a=1, 2, \dots$; and n_1 goes from ≈ 2 to ≈ 1 as n_2 goes from ≈ 0 to ≈ 1 progressively for each term inside the parentheses in the summation shown. In which case, here, $1/N_a$ is considered to relate to a macroscopic form of the quantization of potential as will be described more so later.

Moreover, the resultant gradient extending out from an elementary particle or a system of particles can be considered to be arrived at by the following summation:

$$\nabla \varphi_{(\text{system})} = \frac{\partial \varphi}{\partial x} \hat{i} + \frac{\partial \varphi}{\partial y} \hat{j} + \frac{\partial \varphi}{\partial z} \hat{k}$$

and the respective Laplacian is:

$$\nabla^2 \varphi = \left(\frac{\partial^2}{\partial x^2} + \frac{\partial^2}{\partial y^2} + \frac{\partial^2}{\partial z^2} \right) \varphi$$

Wherein ∇ is gradient and ∇^2 is the Laplacian such that in both cases $\varphi = \frac{1}{N_a} \frac{-hqc}{n_1 * 2\pi(qr)} * e^{\left[\frac{1}{N_a} \frac{n_2 * -2\pi(mcr)}{h} \right]}$;

N_a equals 1, 2, ...; and $1 < n_1 < 2$, and correspondingly $1 > n_2 > 0$.

Note here how the form of the terms of a time independent particle in quantum mechanics supports the form of the potential of the unified field presented herein:

$$\psi(x) = Ae^{-ikx} = \frac{-i2\pi mcx}{h} = Ae^{\frac{-i2\pi mcr}{h}} \quad (\text{when } k=2\pi mc/h \text{ and } x=r)$$

Wherein, (A) can be a scalar amplitude, such that, for example, $A=1/2kx^2 \equiv mgh$ which pertains to $\approx G_T m/r$ (when the other mass is positioned at infinity) which, herein, is equivalent to $\approx K_T q/r$; or (A) can be a vector amplitude, e.g., E (electric vector strength), i.e., $K_C q/r^2$, which is the gradient of the potential $K_C q/r$ which herein relates to $\approx K_T q/r$ which again, herein, is equivalent to $\approx G_T m/r$.

Next, theoretical nuclear force equation (10) pertaining to a portion of the nuclear unified field (which can be related to the conventional residual nuclear force, and the conventional strong and weak forces) is achieved by taking the derivative of the resulting potential from equation (7A) as follows (and is denoted here

as taking the second regular derivative of a first regular derivative):

$$f' \approx K_T(q) * \frac{e^{\left(\frac{\approx -0\pi(mcr)}{h}\right)}}{r} \quad (\text{sum potential which relates to Eq. 7A})$$

$$D_u f' \approx K_r * D_u \frac{1}{\left(\frac{1}{q} \frac{(q_p)}{(m_p)} * r * e^{\frac{\approx 0\pi(mcr)}{h}}\right)}$$

wherein K_r is the remainder of K_T without the charge to mass ratio $\frac{(q_p)}{(m_p)}$, such that

$$f'' \approx K_r * \frac{1}{\left(\frac{1}{q} \frac{(q_p)}{(m_p)} * r * e^{\frac{\approx 0\pi(mcr)}{h}}\right)^2}$$

Here, (q) in the numerator is rewritten and placed in the denominator as $\left(\frac{1}{q}\right)$ along

with (r) , $\left(\frac{(q_p)}{(m_p)}\right)$ (the charge to mass ratio), and $e^{\frac{\approx -0\pi(mcr)}{h}}$ such that $\left(\frac{1}{q} \frac{(q_p)}{(m_p)} * r * e^{\frac{\approx 0\pi(mcr)}{h}}\right) = u$

in the function $f \approx -K_r \frac{1}{u}$. In which case, $D_u^{-K_r} \frac{1}{u} \approx K_r \frac{1}{u^2} \approx K_r \frac{1}{\left(\frac{1}{q} \frac{(q_p)}{(m_p)} * r * e^{\frac{\approx 0\pi(mcr)}{h}} \right)^2}$

such that:

$$f'' \approx -K_C \frac{q^2}{r^2} * e^{2 * \left[\frac{\approx -0\pi(mcr)}{h} \right]}$$

and

$$f'' \approx -K_C (q^2) * \frac{e^{2 * \left[\frac{\approx -0\pi(mcr)}{h} \right]}}{r^2} = N_F \quad \text{Eq. (10)}$$

Wherein, the negative of the resulting derivative was taken for convention.

In this case, $f'' \approx -K_C (q^2) * \frac{e^{\frac{-r}{R}}}{r^2}$ such that $R = \frac{h}{2(\approx 0\pi mc)}$ and is the range, while the resulting

force is in newtons when $h \approx 2\pi mc r$, such that the units of $\frac{2 * \left[\approx -0\pi(mcr) \right]}{h}$ in the exponent cancel. While,

$$R = \frac{h}{2(\approx 2\pi mc)} \text{ when } n_2 \approx 1.$$

Next, a theoretical electromagnetic force equation (11) for the extranuclear field (i.e., a force equation which can be related to the conventional electromagnetic force at weak field and low velocity), and a theoretical

gravitational force equation (12) for the extranuclear field (i.e., a force equation which can be related to the conventional Newtonian gravitational force at weak field and low velocity), is produced by applying a similar second derivative process to each of the two halves of potential which produce the result (sum) of equation (7A)

after substituting $-\frac{1}{2}G_T(m) * \frac{e^{\left[\frac{\approx -0\pi(mcr)}{h}\right]}}{r}$ for $-\frac{1}{2}K_T(q) * \frac{e^{\left[\frac{\approx -0\pi(mcr)}{h}\right]}}{r}$ for one portion as follows:

$$V_{(\text{whole nuclear potential portion})} \approx -\frac{1}{2}K_T(q) * \frac{e^{\left[\frac{\approx -0\pi(mcr)}{h}\right]}}{r} + -\frac{1}{2}G_T(m) * \frac{e^{\left[\frac{\approx -0\pi(mcr)}{h}\right]}}{r} \approx$$

$$-K_T(q) * \frac{e^{\left[\frac{\approx -0\pi(mcr)}{h}\right]}}{r} \approx -1c^2$$

In which case, equation (11) is arrived at upon taking the second derivative of the charge portion

$$D_u -\frac{1}{2}K_r \frac{1}{u} \approx \frac{1}{2}K_r \frac{1}{u^2} \approx \frac{1}{2}K_r \frac{1}{\left(\frac{1}{q(m_p)} * r * e^{\frac{\approx 0\pi(mcr)}{h}}\right)^2}$$

such that

$$f'' \approx -\frac{1}{2} K_C (q^2) * \frac{e^{2 * \left[\frac{\approx -0\pi(mcr)}{h} \right]}}{r^2} = em_F \quad \text{Eq. (11)}$$

and equation (12) is arrived at upon taking the second derivative of the mass portion

$$D_u - \frac{1}{2} G_T \frac{1}{u} \approx \frac{1}{2} G_T \frac{1}{u^2} \approx \frac{1}{2} G_T \frac{1}{\left(\frac{1}{m} * r * e^{\frac{\approx 0\pi(mcr)}{h}} \right)^2}$$

such that

$$f'' \approx -\frac{1}{2} G_T (m^2) * \frac{e^{2 * \left[\frac{\approx -0\pi(mcr)}{h} \right]}}{r^2} = g_F \quad \text{Eq. (12)}$$

Wherein, $1/n_1$, i.e., $\approx 1/2$, is treated as a constant in these cases, and, here also, the negatives of the resulting derivatives were taken for convention.

Note that $K_r \frac{1}{\left(\frac{1}{q} \frac{(q_p)}{(m_p)} * r * e^{\frac{\approx 0\pi(mcr)}{h}} \right)^2} = G_T \frac{1}{\left(\frac{1}{m} * r * e^{\frac{\approx 0\pi(mcr)}{h}} \right)^2}$ in the forgoing

derivatives since $\frac{1}{q} \frac{(q_p)}{(m_p)} = \frac{1}{m}$ when $(q) = (q_p)$ and $(m_p) = (m)$, and note that the additional charge to mass ratio applied in the denominator in (K_C) in figure (2B) is also derived in the forgoing second derivative which pertains to equation (11) along with another charge to mass ratio in the numerator, such that only a value of one is applied, and thus does not affect the respective function (as the first set of charge to mass ratios applied in figure 1A). Moreover, note that when $n_1 \approx 2$ and $n_2 \approx 0$ it is considered that each of two unified fields, e.g., each of two equivalent particles, supplies one half of the force needed to create a whole respective force, i.e., in this case, it takes two equivalent sources of gravitational and electromagnetic potential to create a whole gravitational and a whole electromagnetic force.

Next, consider the following equivalence of the electromagnetic and gravitational forces from the sum of two half portions of each force at Planck scale from equations (11) and (12) when $n_1 \approx 2$ and $n_2 \approx 0$ (weak field and low velocity):

$$\begin{aligned} &\approx K_C \frac{q^2}{r^2} \approx 8.98 \times 10^9 * \frac{(1.87 \times 10^{-18})^2}{(1.61 \times 10^{-35})^2} \approx 1.21 \times 10^{44} \\ &\approx G_T \frac{m^2}{r^2} \approx 6.67 \times 10^{-11} * \frac{(2.17 \times 10^{-8})^2}{(1.61 \times 10^{-35})^2} \approx 1.21 \times 10^{44} \end{aligned}$$

Now, consider the relative force strengths shown below with respect to the following equivalences of $\hbar c$ in Planck units taken from the "fundamental" forces established above:

$$\approx K_C q^2 \approx 8.98 \times 10^9 * (1.87 \times 10^{-18})^2 \approx 3.14 \times 10^{-26} \approx \hbar c$$

$$\approx G_T m^2 \approx 6.67 \times 10^{-11} * (2.17 \times 10^{-8})^2 \approx 3.14 \times 10^{-26} \approx \hbar c$$

For conventional gravitational force strength:

$$\frac{G(\text{proton mass})^2}{\approx K_C(q_P)^2} \approx \frac{6.67 \times 10^{-11} * (1.67 \times 10^{-27})^2}{8.98 \times 10^{+9} * (1.87 \times 10^{-18})^2} \approx 5.92 \times 10^{-39}$$

For conventional electromagnetic force strength:

$$\frac{K_C(\text{electron charge})^2}{\approx K_C(q_P)^2} \approx \frac{8.98 \times 10^{+9} * (1.60 \times 10^{-19})^2}{8.98 \times 10^{+9} * (1.87 \times 10^{-18})^2} \approx 7.32 \times 10^{-3}$$

For conventional weak force strength:

$$\frac{(\text{electron charge})^2}{\approx K_C(q_P)^2} \approx \frac{(1.60 \times 10^{-19})^2}{8.98 \times 10^{+9} * (1.87 \times 10^{-18})^2} \approx 8.15 \times 10^{-13}$$

For conventional strong force strength:

$$\frac{K_C(q_P)^2}{\approx K_C(q_P)^2} \approx \frac{8.98 \times 10^{+9} * (1.87 \times 10^{-18})^2}{8.98 \times 10^{+9} * (1.87 \times 10^{-18})^2} \approx 1$$

when $(q) = (q_P)$

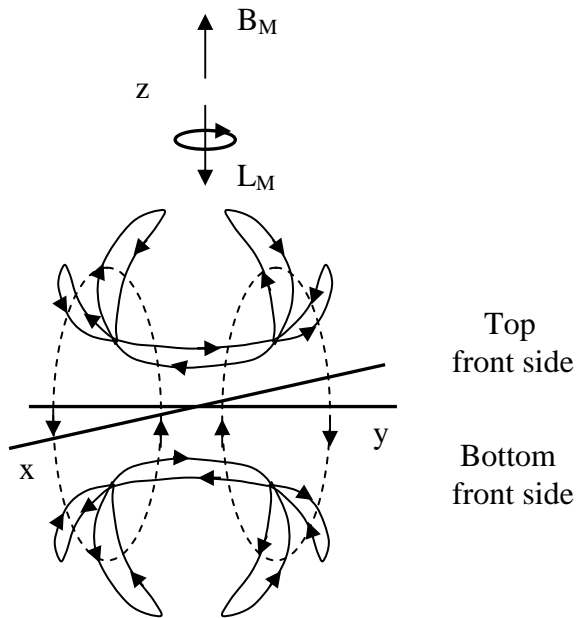
Here, the agreement of these relative force strengths with convention with respect to the terms taken from the fundamental forces at Planck scale above, which are approximately equal to $\hbar c$, support the values and forms of the functions of the present theory of unification, and addresses the problem pertaining to gravitational interactions at the Planck "length scale." Note that the squaring of the potential functions in the process of taking the second derivatives in order to obtain the gravitational and electromagnetic force functions are considered to pertain to the symmetry of the internal structure, and the self interaction of virtual particles (described later), at Planck scale in a unified field.

CONSTRUCTION OF THE UNIFIED FIELD:

Now, "virtual particles" are considered to follow the gradient functions previously presented (with momentum), and are considered to provide substance to the structure and function of the unified field. Accordingly, the unified field theory herein applies a four dimensional gradient vector system which provides for an understanding of the internal structure of the unified field, elementary particles, etc. This greater depth of information proposes to allow for a more detailed understanding of events in physics (e.g., for predictability).

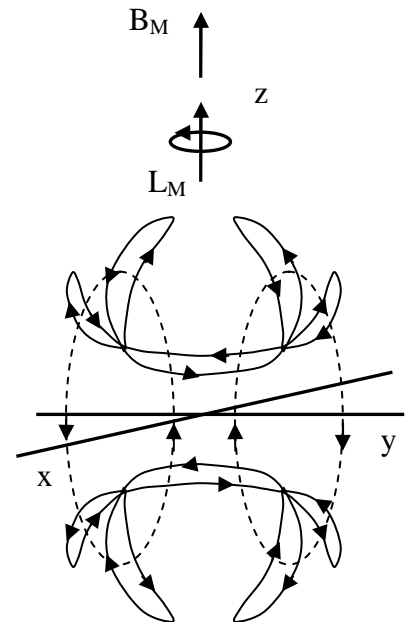
Respectively, virtual particles which follow a gradient function in the respective families of functions are considered to transition through values of potential while having complementary values of n_1 and n_2 , and while having one constant value of $1/N$. Wherein, when $1/N$ is equal to one amongst member functions, the unified field is considered to be in an "elementary" state, while when $1/N$ is an integer number greater than one amongst any member functions, the unified field is considered to experience a macroscopic form of quantization.

The potential of a virtual particle is considered to change as it follows a gradient function due to changes in the values of its parameters as it reflects (screws) in its trajectory during oscillation along its respective virtual particle path (gradient function) as shown in figures (3A) and (3B).



Side view of a negative unified field

FIG. 3A



Side view of a positive unified field

FIG. 3B

Figures (3A) and (3B) show a select few virtual particle paths, which include "more bent" and "less bent" virtual particle paths, in simplified drawings of elementary negative and positive unified fields. Wherein, each virtual particle path is comprised in a respective "band" of virtual particle paths, and each band of virtual particle paths comprises a multitude of virtual particle paths which each comprise respective curvature, dimensions, and alignments; complementary values of n_1 and n_2 ; and a constant value of $1/N$. (Note that the significance of the "more bent" and "less bent" virtual particle paths will be described more so later as, for

example, illustrated in figures 26A and 26B. Also, note that references to the front and back sides are relative references.)

Virtual particles are considered to account for parameters of a unified field including the respective flow of virtual particle "electric" charge (q) as shown directed along the arrows in figures (3A) and (3B). In which case, the virtual particle paths form currents which produce the unified field of, for example, an elementary electrically charged particle with an intrinsic angular momentum (L_M) (i.e., intrinsic spin), and a "macroscopic" magnetic field (B_M) for the electrically charged particle as a whole along a respective (z) axis (also shown in figures 3A and 3B). While, later it will be understood how the magnetic moment of a static electrically charged particle increases in direct proportion to its decrease in mass as the bending of virtual particle paths increase with a respective decrease in mass (as supported by convention by the magnetic moments of a static proton versus a static electron). (Note that the opposite electrically charged unified fields are symmetrical reflections, and are considered to comprise the same density so as to represent matter and antimatter unified fields. However, certain portions of the unified field are not "mirror" symmetrical reflections when spin is added to the unified field, e.g., in terms of angular momentum as shown, and, in terms of microscopic spins which are described later.)

Here, the basic "static" geometry of the unified field is considered to be representative of the basic geometry of a static elementary electrically charged particle, and representative of the operational terms of black holes (which can not be probed) ranging from a theoretical Planck particle (i.e., a theoretical miniature black hole) to a supermassive black hole. Wherein, the internal structure of the unified field provides parameters for describing characteristics of a black hole including the event horizon, accretion disc, jets, etc.

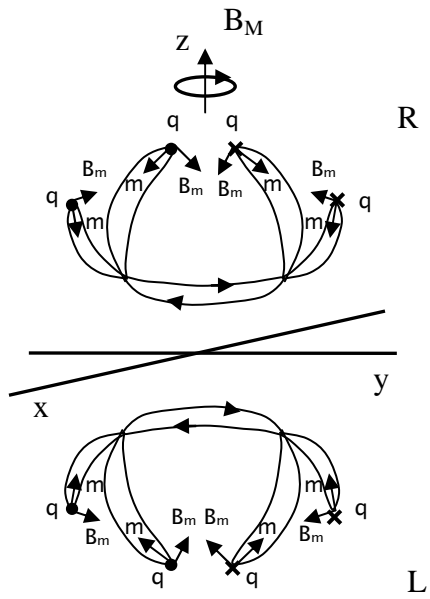
(Note that the nuclear virtual particle paths are shown in figures 3A and 3B as merged in the nuclear region such that the theoretical separation of virtual particle paths is not shown. Also, note that drawings of

unified fields such as those shown in figures 3A and 3B, and other drawings which pertain to them, are only intended to be drawn as rough approximations or also exaggerations of what they represent for viewing purposes.)

Nevertheless, each of the virtual particle paths in the top band of virtual particle paths of a negative electrically charged particle are considered to comprise a right hand screw, and each of the virtual particle paths in the bottom band of virtual particle paths of a negative electrically charged particle are considered to comprise a left hand screw. However, each of the virtual particle paths in the top band of virtual particle paths of a positive electrically charged particle are considered to comprise a left hand screw, and each of the virtual particle paths in the bottom band of virtual particle paths of a positive electrically charged particle are considered to comprise a right hand screw.

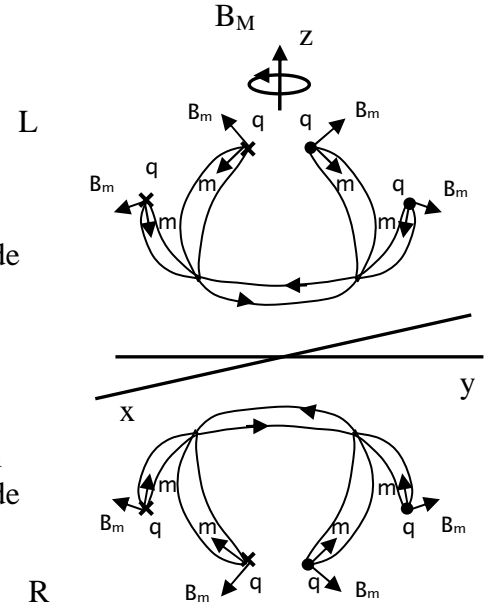
In more detail, the unified field is considered to be constructed with a simple set of orthogonal vectors which provide for the predictable structure and function of the unified field. Accordingly, each virtual particle path is considered to have orthogonal "microscopic spins" comprising microscopic charge (q), mass (m), and magnetic (B_m) spin vectors.

In terms of static negative and positive electrically charged particles, figures (4A) and (4B) show the left and right hand electric (q), mass (m), and magnetic (B_m) microscopic spin vectors of the virtual particles paths on the top and bottom sides of the negative and positive unified fields shown in figures (3A) and (3B), respectively. (Note that the length of a vectors is not a relevant parameter here and elsewhere throughout the present theory.)



Side view of a negative electrically charged particle

FIG. 4A



Side view of a positive electrically charged particle

FIG. 4B

Figures (5A) and (5B) show how the three spin vectors change alignment during portions of oscillation in the extranuclear and nuclear regions in a negative and positive unified field, respectively.

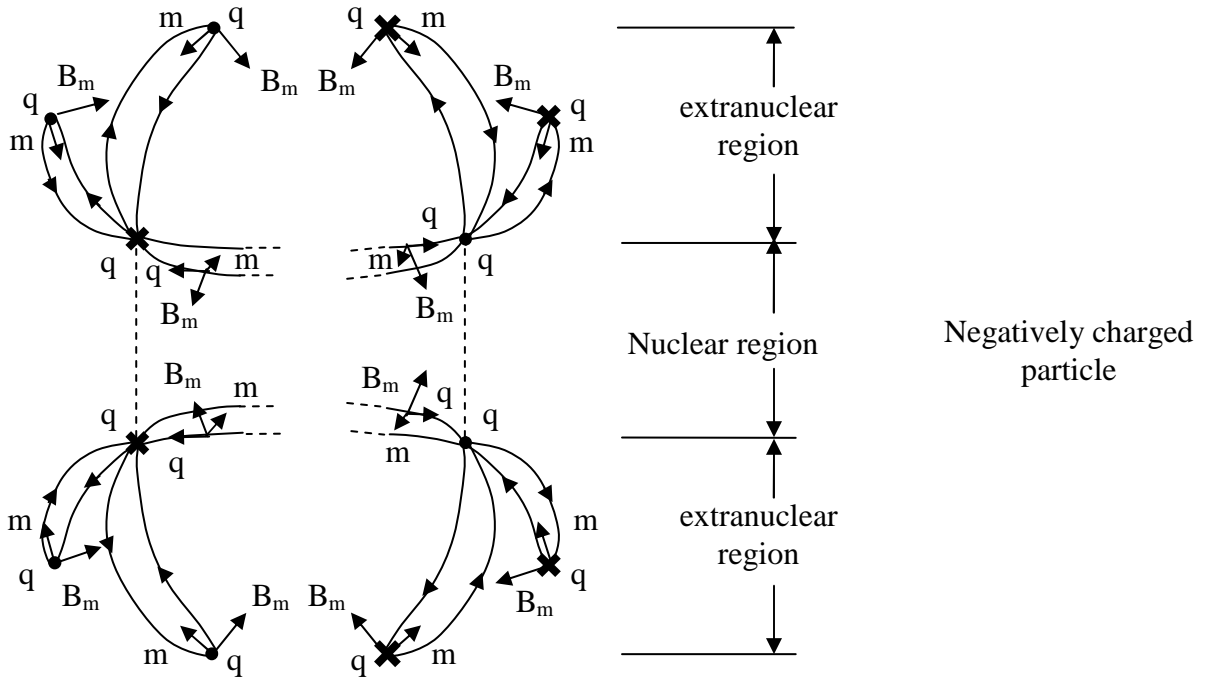


FIG. 5A

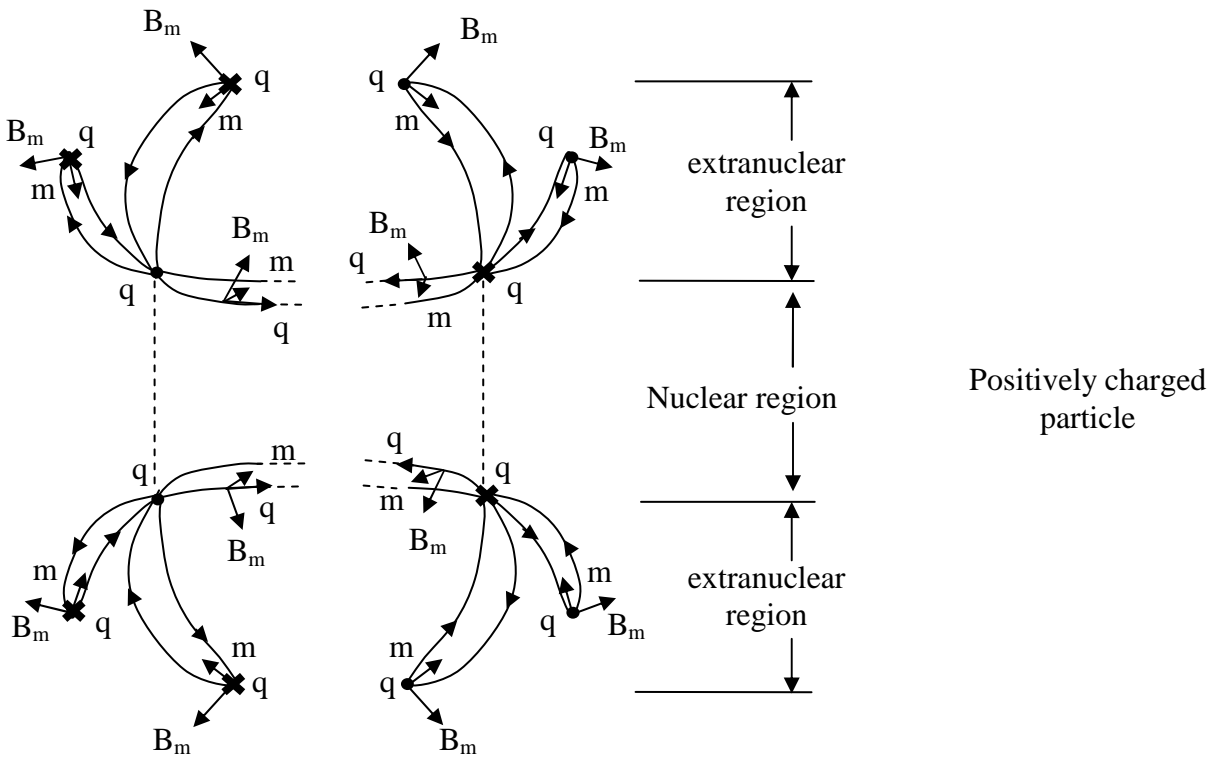


FIG. 5B

Note that virtual particle paths may not be shown with bending hereinafter (for simplification) except, for example, where curvature is emphasized, e.g., in magnetic interactions.

Figure (6A) shows a vector component in the (x-y) plane of a tangent to a select portion of a virtual particle path of a negative electrically charged particle. Wherein, the (x) and (y) axes of the vector component in the (x-y) plane relate to n_1 and n_2 in the respective underlying function, respectively, in which case the (x) and (y) axes, and the respective values of (n_1) and (n_2), are considered to relate to the energy, geometry, etc., of the given virtual particle path. (Note that the arrow on the virtual particle path relates to respective microscopic (q) spin vector direction along the gradient function.)

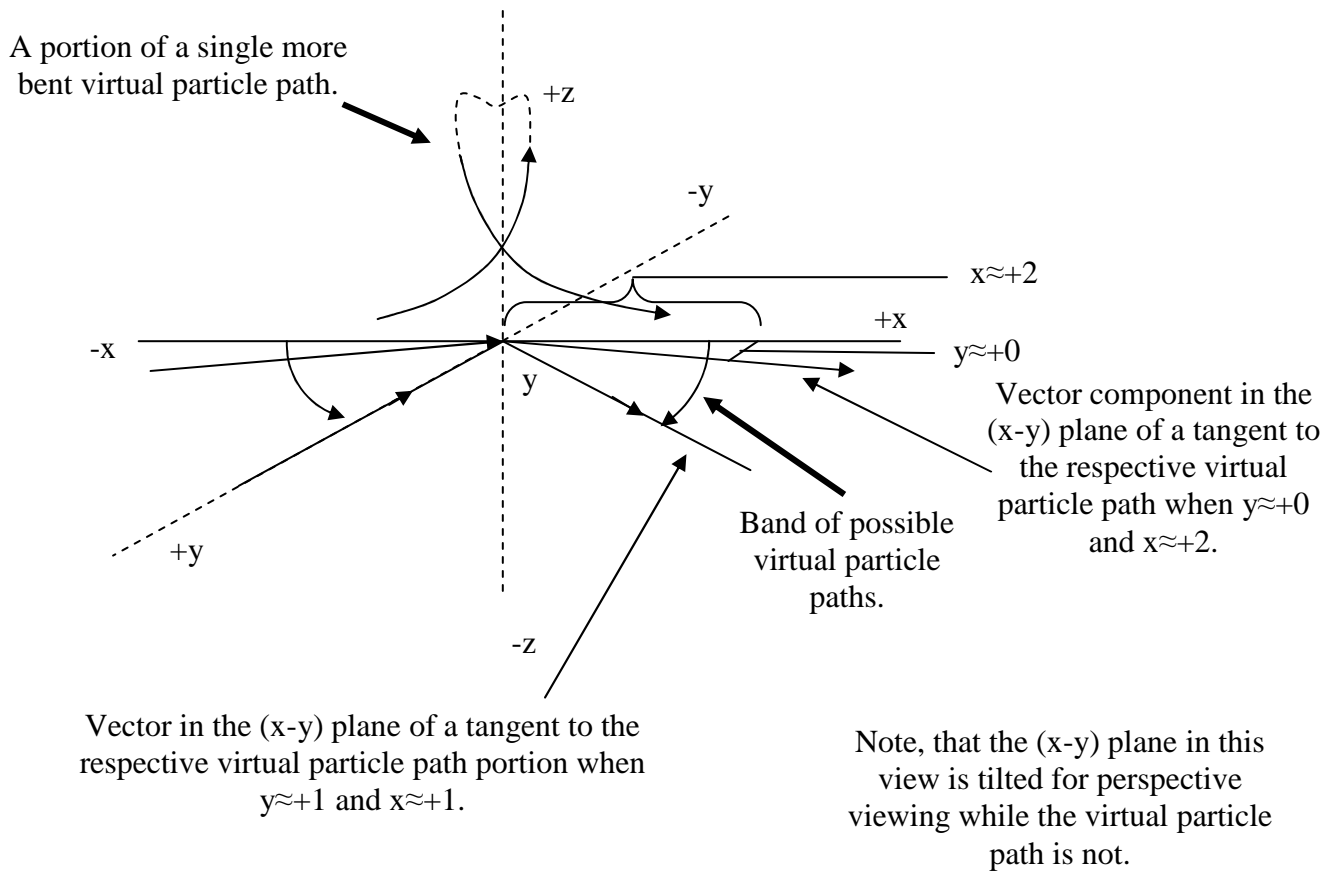


FIG. 6A

Note that when $x \approx +2$ and $y \approx +0$, then the gradient of the virtual particle path is

$\approx -1/2K_T q/r^2 * 1/e^{\approx 0(2\pi mcr)/h}$ for the given one half portion of the theoretical nuclear gradient function (top side),

and is $\approx Kq/r^2 * 1/e^{\approx 0(2\pi mcr)/h}$ for the whole portion (the sum of the top and bottom sides as described more so

later). While, when $x \approx +1$ and $y \approx +1$, then the gradient of the virtual particle path is $\approx K_T q/r^2 * 1/e^{\approx 1(2\pi mcr)/h}$ for

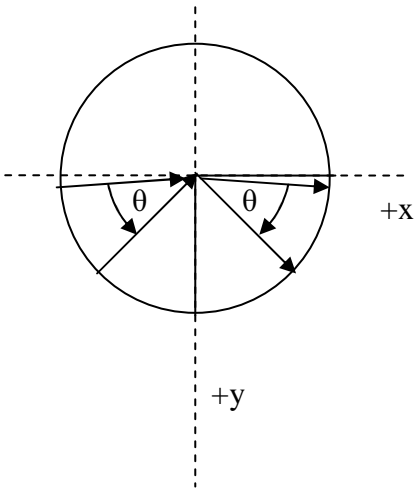
the given one half portion of the theoretical nuclear gradient function (top side), and is $\approx 2Kq/r^2 * 1/e^{\approx 1(2\pi mcr)/h}$

for the whole portion (the sum of the top and bottom sides as also described more so later). Respectively, note

that the inner most radius of the function can represent a theoretical version of the Schwarzschild radius such

that $r_T \approx 2G_T M/c^2 * 1/e^{\approx 1(2\pi mcr)/h}$ when $K_T = G_T$.

Figures (6B) and (6C) describe how certain parameters of the virtual particle paths vary as their angles of trajectory vary. This relates to the (x) and (y) values of the vector component in the (x-y) plane of the tangent to a given virtual particle path, and, correspondingly, (n_1) and (n_2) in the respective gradient function in figure 6A).



Top view

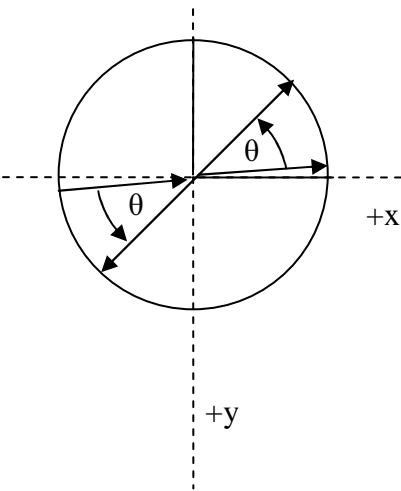
FIG. 6B

Consider the following conditions to be present for virtual particle paths in a band of virtual particle paths as θ increases for a static particle as shown in figure (6B):

- 1) Spin vector alignments rotate according to the change in potential;
- 2) Path length and radius decrease for each elliptically polarized virtual particle path. In which case, the virtual particles in a virtual particle path propagate with an increased frequency and a decreased radius, such that the virtual particle paths can propagate in unison as a wave packet;
- 3) Complementary (n_1) and (n_2) values change, and the elliptically polarized geometry of the virtual particle paths approach a circularly polarized geometry (eccentricity decreases);
- 4) Density of the virtual particle paths increases; and,
- 5) Virtual particles propagate at the same velocity on all virtual particle paths (refer to the description under the heading "virtual particles, self interaction, and superluminal velocity").

When diagram (6B) is applied to an electron in an atomic orbital the following would occur as θ increases along the direction shown:

- 1) KE increases;
- 2) Negative PE increases; and,
- 3) Positional PE decreases.



Top view

FIG. 6C

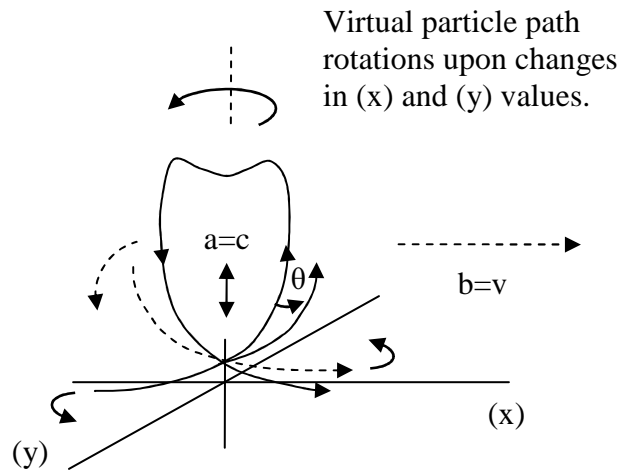
Consider the following conditions when figure (6B) is modified for propagation as in figure (6C), such that theta changes in opposite directions in diagonally positioned quadrants for the leading and trailing edge (for one portion, e.g., the front portion) of a propagating particle as a whole:

1) When this diagram is applied to an accelerated propagating electrically charged particle, "relativistic mass" increases as θ increases along the direction shown for the band of virtual particle paths.

2) When this diagram is applied to an electromagnetic field quantum, virtual particle paths on each the top and bottom sides are comprised in a narrow band with constants approximating $n_1 \approx 1$ and $n_2 \approx 1$, wherein the narrow band of virtual particle paths for different electromagnetic field quanta have virtual particles with higher frequencies and smaller radii on virtual particle paths with corresponding shorter path lengths for electromagnetic field quanta of higher energies.

3) When this diagram is applied to special relativity, length contraction and time dilation increase along the (x) axis as θ increases along the direction shown (as explained more later).

Upon acceleration of an electrically charged particle, the spin vectors of the virtual particles in each of the virtual particle paths are considered to rotate (as referred to in figures 6C and 6D, and more specifically depicted in figures 14A and 14B). Wherein, the rotations of the spin vectors of the virtual particles are considered to affect the parameters of the propagating particle including the radius, amplitude, wavelength, frequency, and relativistic mass (in agreement with electric, magnetic, and mass spin vector interaction between virtual particles as pertains to charged particle propagation and interaction described later). Correspondingly, as θ increases as illustrated for the example virtual particle path shown in figure (6D), each virtual particle path changes its trajectory, and each virtual particle path projects forward such that the eccentricity of each of the virtual particle paths decreases so as to approach a circularly polarized (or helical) geometry to a directly proportional extent. Correspondingly, the velocity of the particle as a whole is considered to increase. (Note that the virtual particle path propagates in agreement with the "interval.")



Changes in the trajectory of a virtual particle path in a propagating particle (excluding size change) as θ increases upon changes in (x) and (y) values, i.e., upon changes in (n_1) and (n_2) values, as described in figure (6A).

FIG. 6D

With respect to relativity, figures (6A-6D), and when working with ellipses, assume $\gamma = \frac{1}{e}$, wherein

(γ) is the Lorentz factor and (e) is eccentricity, such that $\gamma = \frac{1}{e} = \frac{1}{\sqrt{1 - \left(\frac{b}{a}\right)^2}}$. In which case, assuming that

$b=v$ and $a=c$, then $\gamma = \frac{1}{\sqrt{1 - \left(\frac{v}{c}\right)^2}}$. Wherein, when $v \approx 0$, then (γ) is approximately one, and a virtual particle

path approximates its maximum eccentricity, such that the virtual particle path approximates a minimum

Lorentz contraction, a minimum time dilation, and a minimum relativistic mass. While, when $v \approx c$, then (γ) is

approximately infinite, and a virtual particle path approximates a circularly polarized geometry, such that the virtual particle path approximates its minimum eccentricity when $\sqrt{1 - \left(\frac{v}{c}\right)^2}$ is approximately zero, and the virtual particle path approximates a maximum Lorentz contraction, a maximum time dilation, and a maximum relativistic mass.

Accordingly, in particular, changes in (n_2) (mass related changes between $n_2 \approx +0$ and $n_2 \approx +1$) of the potential of a virtual particle path can be interpreted as being especially related to changes in (v) in the conventional Lorentz factor. However, nevertheless, it is considered that each virtual particle path in a band is related to its own Lorentz factor due to their differences in potential, i.e., the basic multiplicative components of a potential are related to, or, for convenience, (n_1) and (n_2) can be correlated with, their own Lorentz factors, such that corresponding Lorentz factors vary amongst virtual particle paths in a band (affecting scale), and such that such Lorentz factors change in a virtual particle path as the potential changes for virtual particles in a virtual particle path as they oscillate, and the virtual particles merge and diverge. Wherein, consequentially, the curvature of a virtual particle path changes as it oscillates due to changes in length contraction, etc. as the potential changes.

Thus, consider relativistically, that the function

$$f = \pm e^{\left[\frac{1}{N} n_1 \frac{\pm 2\pi(qcr)}{h_q} + \frac{1}{N} n_2 \frac{\pm 2\pi(mcr)}{h} \right]} \quad \text{Eq. (3A)}$$

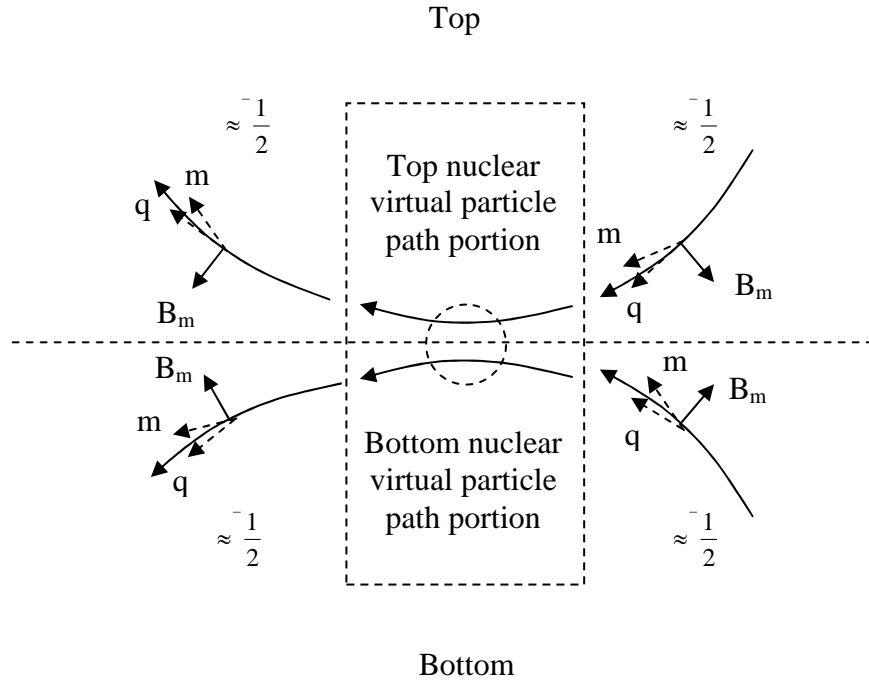
can be reduced to

$f = \pm e^{\gamma_T^2 * \approx 1 + \gamma_T^2 * \approx 1}$ when using the dimensionless values shown in figures (1A) and (1B). Then, upon substitution, reflection of the function, taking the partial derivative, and expanding the function to account for top and sides along the (z) axis the forgoing function becomes:

$$\pm f_x(x, y) = \frac{1}{\gamma_T^2} \frac{1}{N} \frac{h_q c}{n_1 * 2\pi(qr)} * e^{\left[\gamma_T^2 \frac{1}{N} \frac{n_2 * \pm 2\pi(mcr)}{h} \right]} \quad \text{Eq. (13).}$$

This is considered a relativistic version of the unified field function shown in equation (4A) such that the square of the Lorentz factor, i.e., γ_T^2 , in the unified field function accounts for the two indices of the Lorentz factor in general relativity which conventionally relates to energy and volume (or energy density). (Note, refer to equation 15 for the form of the theoretical Lorentz factor applicable in the present theory.)

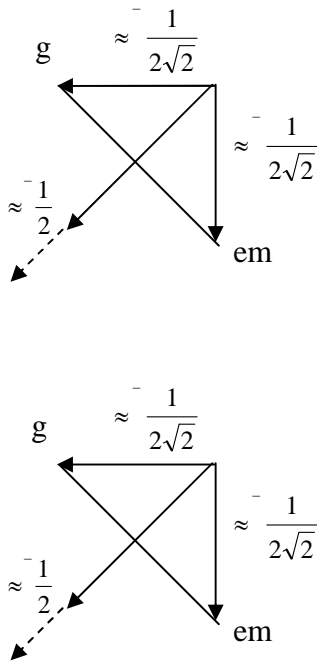
Next, the vector sum of the gradient components of the unified field with respect to equations (8A) and (8B) can be related to the geometry of the unified field as depicted in figures (7A), (7B), and (7C). In which case, only the basic multiplicative factor of the vector summation process is shown (note that a positively charged particle can be presented similarly).



Negatively charged particle

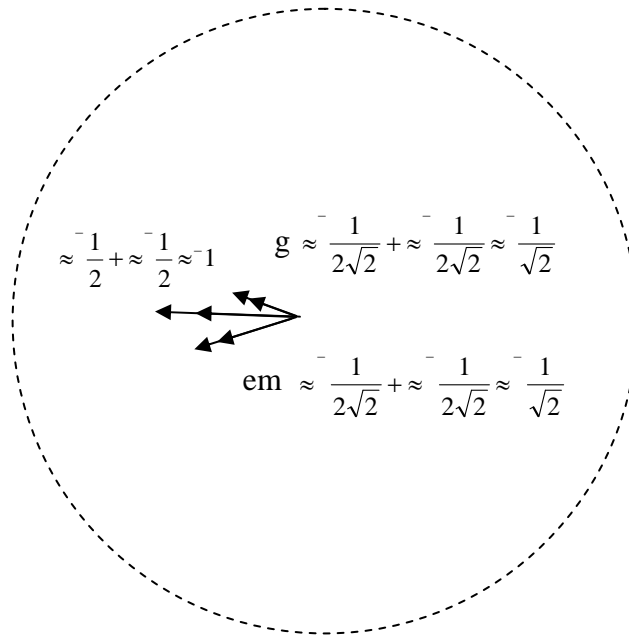
Here, the vector resultant gradients of the top and bottom virtual particle paths can propagate into the nuclear region and add as $\approx \frac{1}{2} + \approx \frac{1}{2} \approx 1$. Alternatively, vector components can propagate into the nuclear region and add as follows so to produce the resultant gradient $(\approx \frac{1}{2}\sqrt{2} + \approx \frac{1}{2}\sqrt{2})^2 + (\approx \frac{1}{2}\sqrt{2} + \approx \frac{1}{2}\sqrt{2})^2 \approx (1)^2$

FIG. 7A



Basic geometry of (em) and (g) gradient vector components of a top or bottom virtual particle path.

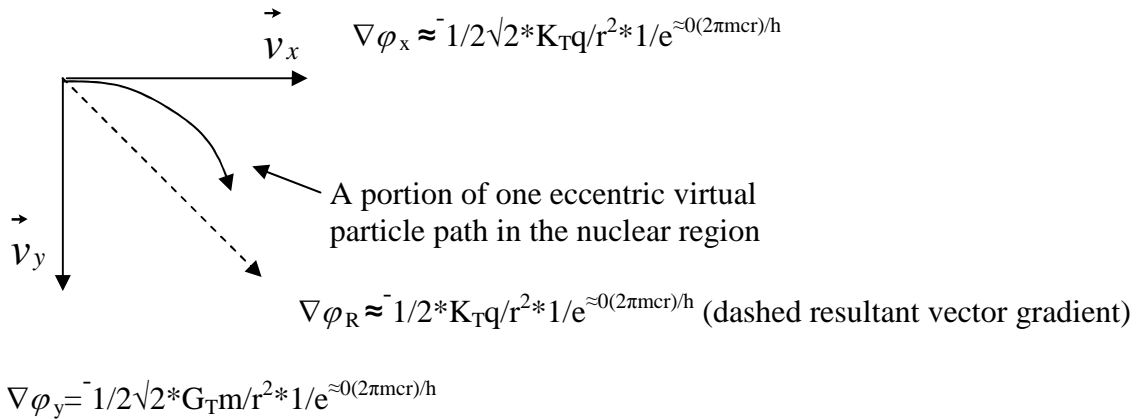
FIG. 7B



An enlarged perspective view of what is occurring in the dashed circle in figure (7A) which shows the basic geometry of the addition of vector components of (em) and (g) of the top and bottom virtual particle paths in the nuclear region.

FIG. 7C

Figure (7D) shows the symmetrical vector components of a portion of one example virtual particle path in terms of electromagnetic and gravitational component gradients.



Top view

$\vec{} \quad \vec{}$
 Here, the vector components (V_x and V_y) of the electromagnetic and gravitational gradient components along the (^+x) and (^+y) axes of the theoretical nuclear gradient $\approx \frac{1}{2}K_{Tq}/r^2 * 1/e^{\approx 0(2\pi mcr)/h} \approx \frac{1}{2}c^2$ are shown in the nuclear region, such that $\sqrt{(\approx \frac{1}{2}\sqrt{2}K_{Tq}/r^2 * 1/e^{\approx 0(2\pi mcr)/h})^2 + (\approx \frac{1}{2}\sqrt{2}G_{Tm}/r^2 * 1/e^{\approx 0(2\pi mcr)/h})^2} \approx \frac{1}{2}K_{Tq}/r^2 * 1/e^{\approx 0(2\pi mcr)/h}$ (dashed line).

FIG. 7D

CHARGED PARTICLE INTERACTION:

It has been a longstanding contentious issue as to how electrically charged particles interact. Wherein, while Newtonian physics suggests that gravitational interactions are based on instantaneous action-at-a-distance, relativity proposes that gravitational interactions are based on the action of the curvature of spacetime on mass over velocity (c).

Herein, electrically charged particles are considered to interact over relatively long distances by the extranuclear virtual particle paths of a particle extending outward to, and interacting with, another particle (or other particles) involved in interaction over a superluminal velocity. Wherein, long range interaction of one particle with another can cause attractive or repulsive effects which included particle acceleration, and the formation of molecules with molecular orbitals (refer to the description under the heading "virtual particles, self interaction, and superluminal velocity").

For example, figure (8) shows a top view of two possible general directions of four possible varieties of virtual particle paths of the extended extranuclear field of a given irregular distribution of static positive electrically charged particles which can interact with a negatively charged particle. (Note that the dashed lines in figure 8 represent virtual particle paths hidden from view.)

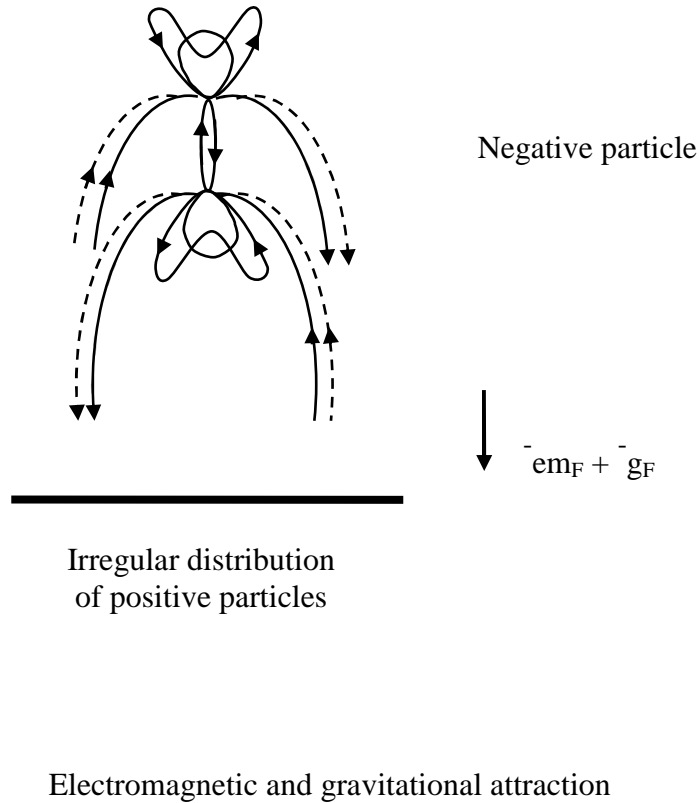
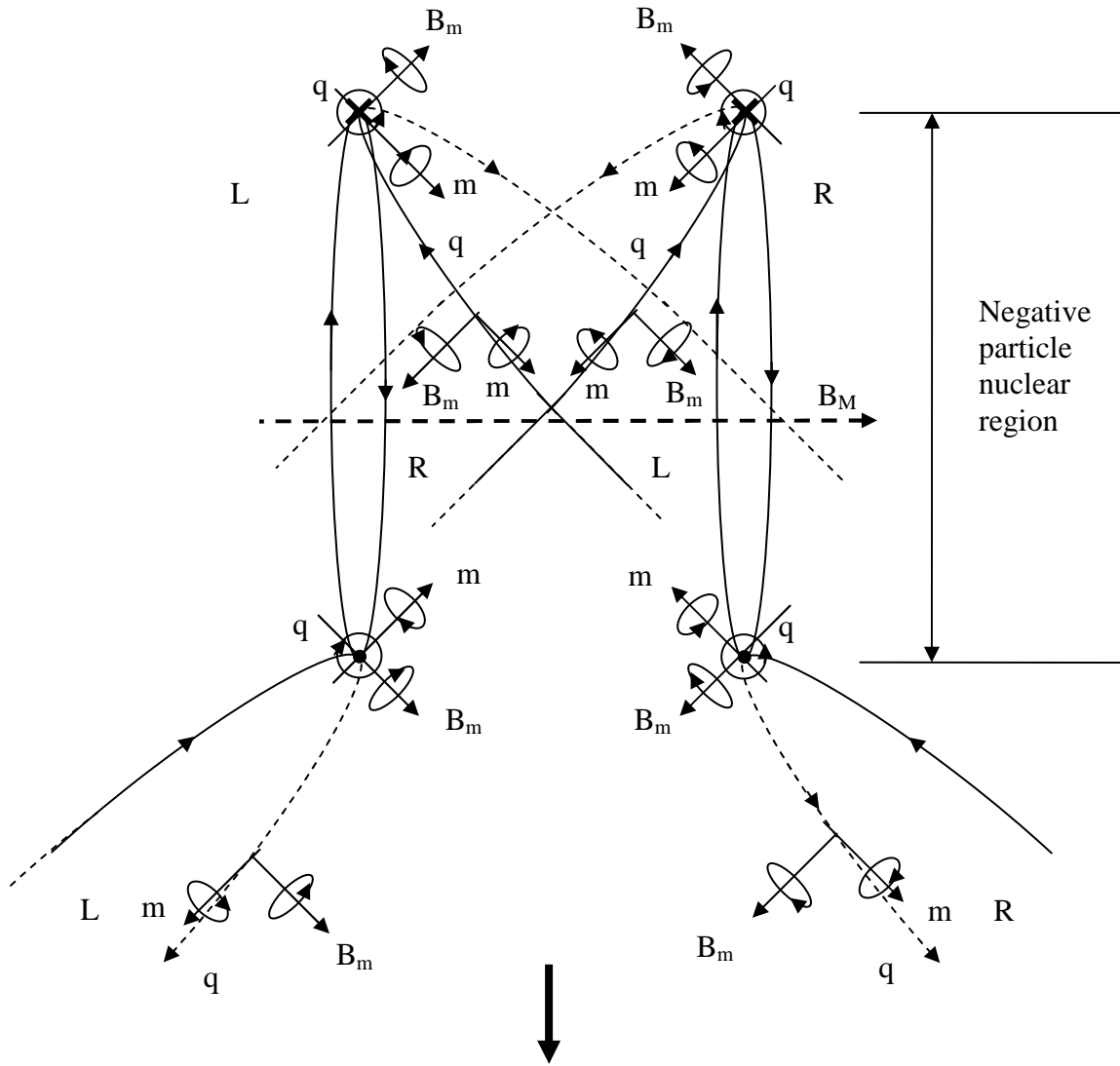


FIG. 8

In this case, the virtual particle paths of the extended extranuclear fields of the irregular distribution of positively charged particles enter, and subsequently exit, along the portion of the nuclear region on respective sides of the negative particle where the virtual particle paths converge and diverge. (Note, the top side where virtual particle paths enter and exit represents the front side of the negative particle with respect to figure 4A, and the bottom side where virtual particle paths enter and exit represents the back side of the negative particle with respect to figure 4A. Also, note that the constituents of the four possible virtual particle paths of an irregular distribution of positively charged particles can be visualized as comprising an irregular distribution of the two varieties of virtual particle paths which extend out going in opposite directions from the top side of each positive electrically charged particle (with respect to figure 4B); and, in addition, comprising an irregular distribution of the two varieties of virtual particle paths which extend out going in opposite directions from the

bottom side of each inverted positive particle (with respect to figure 4B).

Figure (9) shows a perspective view of certain portions of the interacting particles shown in figure (8).



Electromagnetic and
gravitational attraction

Side view

FIG. 9

In figure (9), the four possible varieties of virtual particle paths of the extranuclear fields of the irregular distribution of positive particles which can interact with the negative particle are shown along with their respective microscopic spins. Also, figure (9) shows the virtual particle paths of the nuclear field region of the negative particle which is interacted upon, their respective microscopic spins; and the macroscopic magnetic field alignment of the particle as a whole.

In this case, the virtual particle paths from the irregular distribution of positive particles entering the nuclear region on the top section of the negative particle have microscopic charge (q) and mass (m) spins which are parallel with the microscopic charge (q) and mass (m) spins comprised by the nuclear virtual particle paths in the nuclear region of the negatively charged particle so as to attract. While, the virtual particle paths from the irregular distribution of positive particles entering the nuclear region on the top section of the negative particle have microscopic magnetic spins (B_m) which are antiparallel with the microscopic magnetic spins (B_m) comprised by the nuclear virtual particle paths in the nuclear region of the negatively charged particle so as to also produce attraction. In effect, the virtual particle paths interacting on the top section of the negative particle are considered to attract, such that the respective top section of the unified field of the negative particle shown in figure (9) is considered to increase in mass and accelerate to an extent. Note that in figures (9) and (18) the spins are separated for viewing purposes. Thus, one must conceptually reposition each orthogonal set of virtual particle path spins from the irregular distribution of positive particles while keeping them aligned as they are so that the origins of the spins from the irregular distribution of positive particles are almost abutting with the origins of the orthogonal set of nuclear spins of the interacting charged particle (here, the negatively charged particle) for proper alignments.

Similarly, in figure (9), the microscopic charge spins (q) of the virtual particle paths from the irregular distribution of positive particles which enter the nuclear region on the bottom section of the negative particle are

parallel to the respective microscopic charge spins (q) of the respective virtual particle paths of the nuclear region of the negative particle so as to attract. Yet, the microscopic magnetic spins (B_m) of the virtual particle paths from the irregular distribution of positive particles which enter the nuclear region on the bottom section of the negative particle are parallel to the microscopic magnetic spins (B_m) of the respective virtual particle paths of the nuclear region of the negative particle so as to repel. While, the microscopic mass spins (m) of the virtual particle paths from the irregular distribution of positive particles which enter the nuclear region on the bottom section of the negative particle are antiparallel to the microscopic mass spins (m) of the respective virtual particle paths of the nuclear region of the negative particle so as to also repel, and in effect produce a form of "mass repulsion."

In this case, the virtual particle paths which are interacting on the bottom section of the negative particle are considered to relatively repel due to the repulsion of respective microscopic magnetic and mass spins. Wherein, the bottom section of the unified field of the negative particle shown in figure (9) is considered to decrease in mass and decelerate to an extent.

Consequently, the top side of the negative particle as shown in figures (9) and (10) (starting in the nuclear region where the virtual particle paths begin to converge on the front side of the negative particle) is considered to project forward and downward, and, in effect, establish the leading edge of the particle as indicated in the perspective view of the nuclear region of the negatively charged particle shown in figure (10).

Edge formation of an accelerated
negative particle

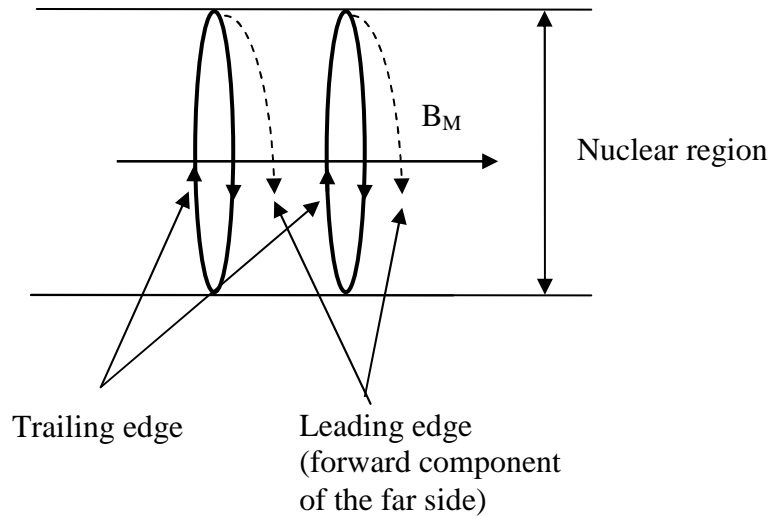


FIG. 10

Correspondingly, the bottom side of the negative particle (starting on the bottom sides in figures 9 and 10, i.e., the opposing nuclear region where the virtual particle paths begin to diverge, is considered to rotate around and follow the leading edge with a different geometrical path (difference not shown), such that, in effect, this portion of the unified field of the particle establishes the trailing edge of the particle.

An attractive, repulsive, or neutral condition of coupling charge and mass spins is considered to occur according to the alignment of the respectively coupled microscopic charge and mass spin vectors (as conventionally with magnetic fields generated by circulating currents of electric charge). Figures (11A) and (11B) show how two right hand and two left hand charge and mass microscopic spin vectors can have totally attractive, totally repulsive, or "neutral" alignment (wherein partial attraction would be situated between neutral and total attraction, and partial repulsion would be situated between neutral and total repulsion). Note that a

forward electric spin (q) alignment is a special requirement for "coupling" of (q) spin vectors in certain interactions including those where the entrance of an interacting virtual particle path from one particle into the nuclear region of another particle is relevant.

Microscopic charge and mass spin vector attraction, repulsion, and neutral alignment

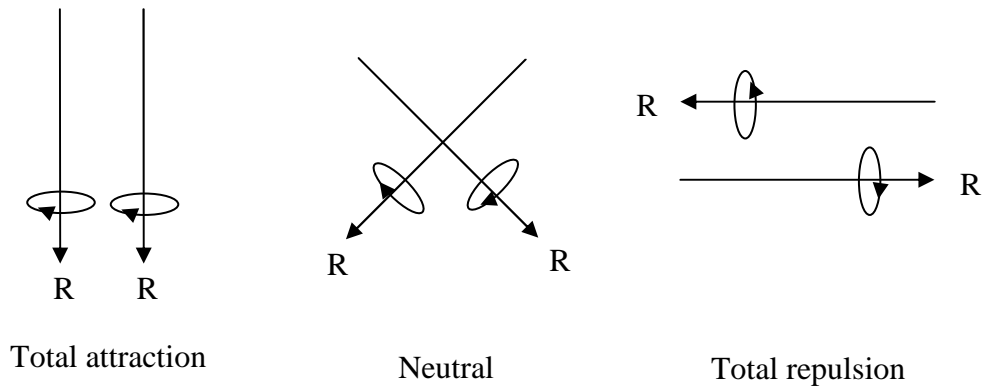


FIG. 11A

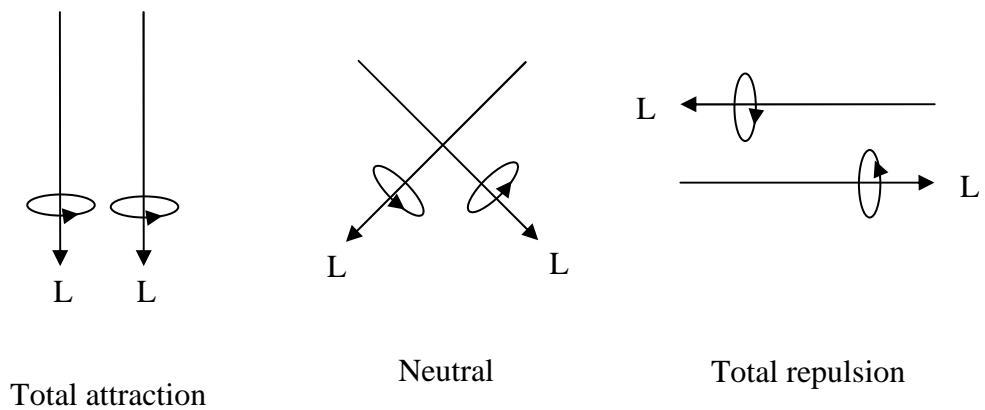


FIG. 11B

However, an attractive, repulsive, or neutral condition of the coupling microscopic magnetic spin is

considered to occur according to the alignment of the respectively coupled microscopic magnetic spin vectors in an effectively different way. Figures (12A) and (12B) show how two right hand and two left hand microscopic magnetic spin vectors can have totally repulsive, totally attractive, or "neutral" alignment (wherein, similarly, partial attraction would be situated between neutral and total attraction, and partial repulsion would be situated between neutral and total repulsion).

Microscopic magnetic spin vector attraction, repulsion, and neutral alignment

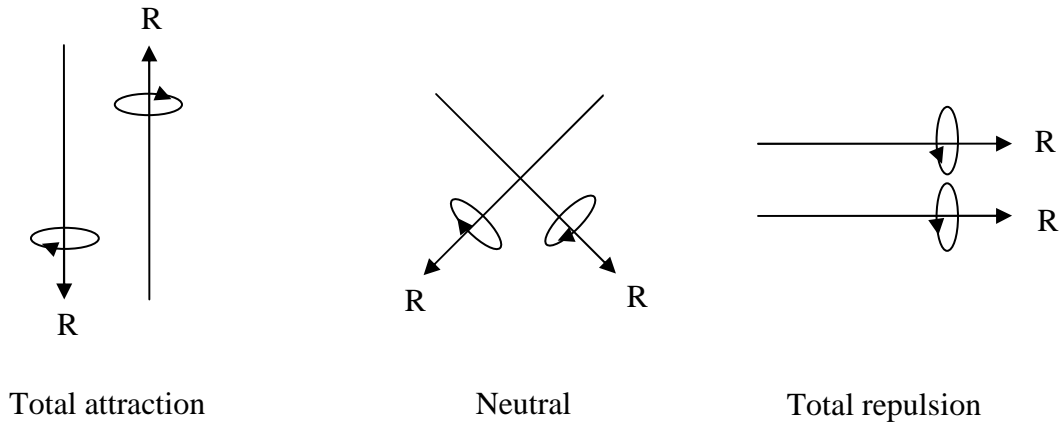


FIG. 12A

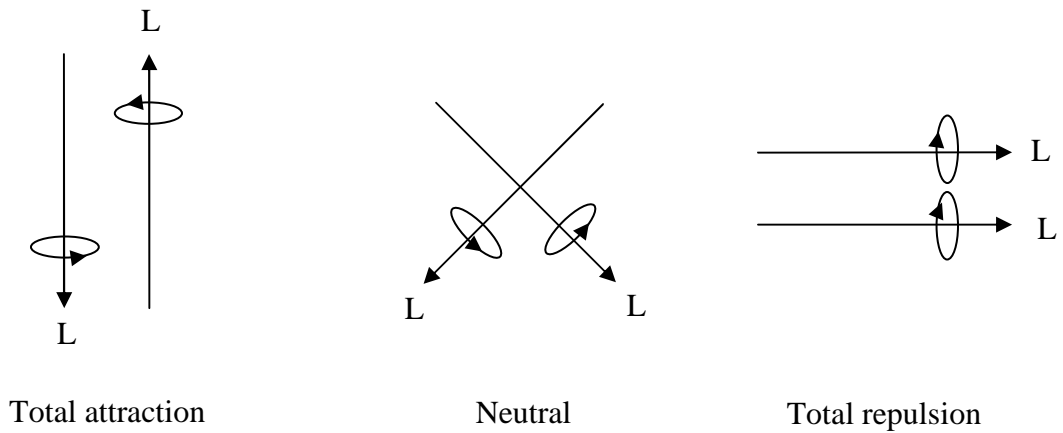


FIG. 12B

Nevertheless, continuing, as the particle rotates around and realigns itself in the interacting extranuclear field extended by the irregular distribution of positive particles, the relatively decelerated trailing edge of the negative particle aligns itself with the field like the leading edge, and establishes the accelerated conditions equivalent to those of the leading edge. Wherein, the negative particle propagates towards the irregular distribution of positive particles as the attractive spin vectors of the extranuclear virtual particle paths of the positive particles continue to accelerate the negative particle, such that the electromagnetic and gravitational attraction of the negative particle by the positive particles results.

Then, the extended extranuclear fields of the positive particles continue to interact with the transformed geometry of the unified field of the propagating negative particle, such that the propagating negatively charged particle moves forward towards the irregular distribution of positive particles according to spin vector interactions, and accelerates according to the increase in the angular rotation of the orthogonal spin vectors of the extranuclear virtual particle paths from the positive particles in accordance with the increase in the density of the extranuclear virtual particle paths from the positive particles as the negative particle approaches the positive particles. While, the virtual particle paths of the top and bottom sides of the accelerated negative particle propagate side-by-side with respective elliptical polarizations and relative orientations.

Figures (13A) and (13B) show how the leading edge of example top and bottom virtual particle paths of an accelerated positively and negatively electrically charged particle effectively reflect around certain lines (including lines which are aligned along the vertical dashed lines shown, and the horizontal dashed line which is in the plane of symmetry separating the top and bottom sides), and project forward in order to establish the respectively combined right and left hand elliptically polarized virtual particle paths of the top and bottom sides of a propagating electrically charged particle.

Reflections of an accelerated negative
particle

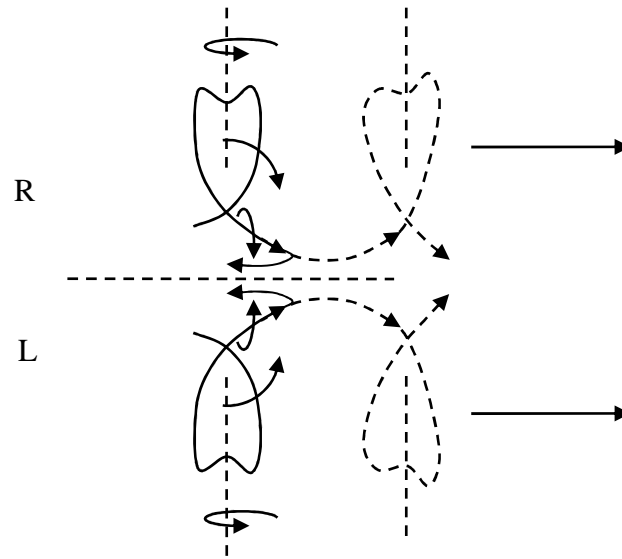


FIG. 13A

Reflections of an accelerated positive
particle

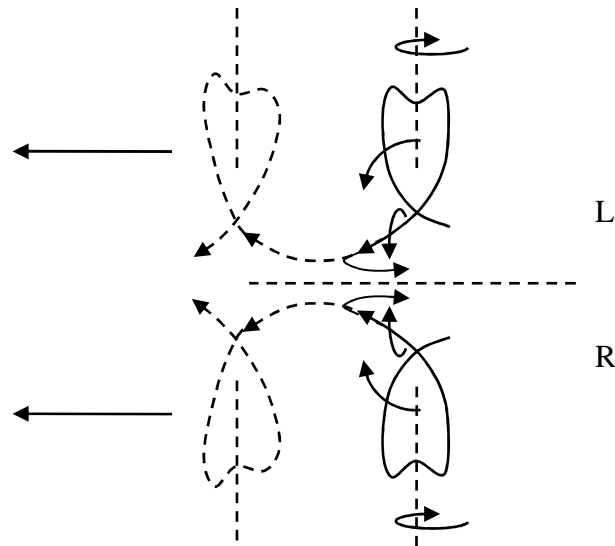
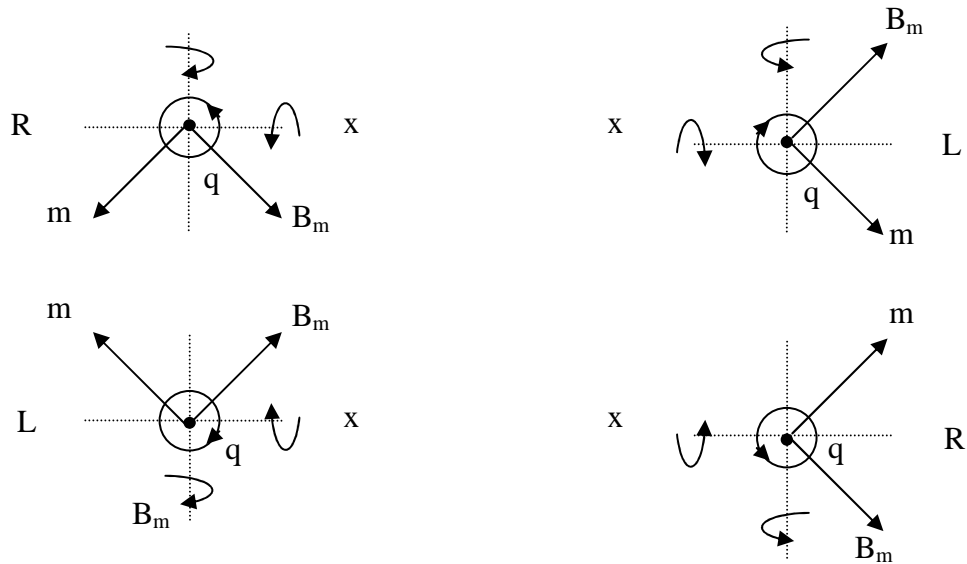


FIG. 13B

Figures (14A) and (14B) show a front view (with respect to the direction of propagation) of the respective rotations of the microscopic spin vectors (at the leading edge) of some example nuclear virtual particle paths of a negatively charged particle and a positively charged particle which are each accelerated and propagating out of the page. It is considered that the spin vectors rotate around orthogonal rotational axes using the intersecting point of the spin vectors at a tangent point along a respective virtual particle path as a pivot point. (Note that these rotations are considered equivalent to the rotations experienced by virtual particle paths going from the extranuclear region into the nuclear region in electrically charged particles as pertains to figures

5A and 5B; and are considered equivalent to the rotations experienced by the virtual particle paths of accelerated electrically charged particles as pertains to figure 6D, and figures 13A and 13B).



Rotations of nuclear virtual particle paths (at the leading edge) of the front side of a negative particle in the nuclear region due to acceleration.

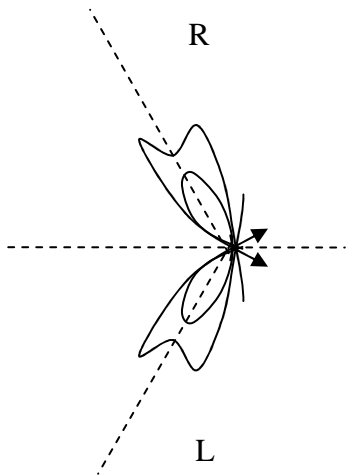
Rotations of nuclear virtual particle paths (at the leading edge) of the front side of a positive particle in the nuclear region due to acceleration.

Note that the directions of rotation invert as the orthogonal spins invert.

FIG. 14A

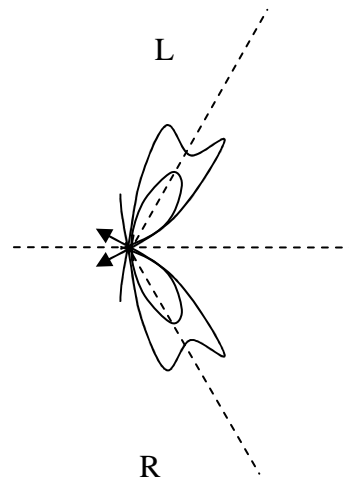
FIG. 14B

Figures (15A) and (15B) show front views of the top and bottom more bent and less bent virtual particle paths of the front portion of propagating negative and positive electrically charged particles.



Front view of more and less bent virtual particle paths of a negatively charged particle propagating out of the page.

FIG. 15A



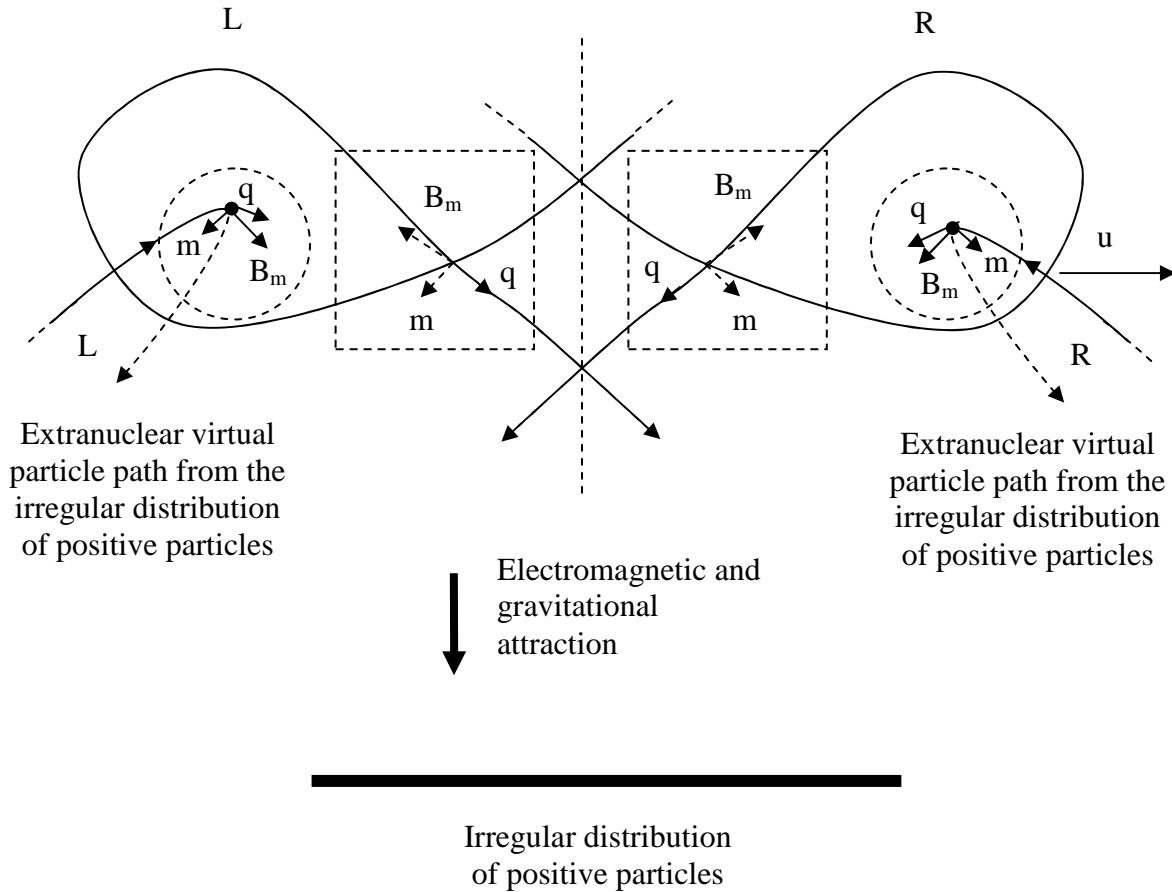
Front view of more and less bent virtual particle paths of a positively charged particle propagating out of the page.

FIG. 15B

Figure (16) shows a side view of the two possible varieties of virtual particle paths of the irregular distribution positively charged particles which interact with the virtual particle paths of the propagating negatively charged particle as it propagates down the page. Wherein, it is consider that interaction occurs as if a "dense nuclear region" of sorts has been preserved on the top and bottom sides of the propagating electrically charged particle. As shown in figure (16), the respective spin vector components are aligned such that the propagating negatively charged particle is accelerated downward towards the positively charged particles. Note that only the front portion of the negatively charged particle is shown. Furthermore, note that the spin vectors in the dashed squares include spin vectors which are aligned in a somewhat tilted manner in and out of the page such that the respective components of them align accordingly. Moreover, note that in figure (16) (and in

similar drawings) the interacting spins are separated for viewing purposes. Thus, one must conceptually reposition each orthogonal set of extranuclear spins shown in a dashed circle while keeping them aligned as they are so that the origins of the orthogonal set of extranuclear spins are almost abutting with the origins of the orthogonal set of nuclear spins shown in a corresponding dashed square for proper alignments.)

Negative particle propagating down the page interacting with two of the varieties of virtual particle paths from an irregular distribution of positive particles



Virtual particle paths (with spins in dashed circles) extending out from the positively charged particles (thick solid line) and interact with the "nuclear region" of the propagating negative particle (with spins in dashed squares), such that the charge (q) and mass (m) spins of respectively interacting right and left hand screw sides are parallel and respectively attract, and such that the magnetic spins (B_m) of respectively interacting right and left hand screw sides are antiparallel and attract. Note that the top and bottom sides of the propagating negative particle tilt out of the page.

FIG. 16

Similarly, consider that the positive particles are accelerated towards the negative particle due to the changes in the potentials of their interacting virtual particle paths upon passing through the nuclear region of the negative particle, and then returning to their respective positive particles.

As shown in figures (15A) and (15B), it is considered that the virtual particle paths of an electrically charged particle only partially reflect around the horizontal dashed line in the plane of symmetry which separates the top and bottom sides while helically propagating around respective axes and one common central axis, such that the top and bottom virtual particle paths of an electrically charged particle do not completely come together. Respectively, it is considered that the virtual particle paths in a band of virtual particle paths comprised in a particle have relatively different angular alignments (in a graduated way), and are rotated to respectively different extents upon acceleration. Wherein, in effect, each virtual particle path in a particle as a whole has a respectively different energy attributable to it before and during propagation. While, as the degree of rotation around the respective rotational axes changes for all of the virtual particle paths in the respective bands of virtual particle paths in an accelerated particle, the energy (including a change in relativistic mass) for an accelerated particle as a whole changes.

Inertia has been a curious issue over the centuries particularly since Galileo. Respectively, it is considered that the virtual particle paths in a band of virtual particle paths in an electrically charged particle are considered to interact and resist acceleration while having "inertia" (i.e., requiring potential or force to change their respective alignments). However, the bands of virtual particle paths in the electromagnetic field quantum (which is described more so later) are considered to be relatively converged due to the absence of a significant extent of their eccentricities, such that they collectively occupy a relatively narrow band compared to the band of virtual particle paths in a propagating electrically charged particle, and such that the virtual particles on the

top side and the virtual particles on the bottom side of the quantum propagate in a more aligned manner while also having inertia (i.e., also requiring force to change their respective alignments).

Conventionally, an electron has arguably been considered to be a point particle with no internal structure. However, the structure and function of the present unified field has shown how the virtual particle paths of an electrically charged particle can statically oscillate, and then open upon acceleration such that the internal structure of the static field can transmute into the propagating field of an electrically charged particle such as a propagating electron or proton. While, the resulting propagating particle comprises top and bottom bands of virtual particle paths which can be considered to comprise a wave packet, which, expounding upon further, can be described in terms of families of complex exponential functions representing polarized virtual particle paths.

Consider here how the form of the function for a time dependent particle in quantum mechanics corresponds to the unified field presented herein:

$$\psi(x) = Ae^{-ikx-\omega t} = Ae^{\frac{-i2\pi mcr}{h} - (kc)t} = Ae^{\frac{-i2\pi mcr}{h} - \frac{2\pi mc^2 t}{h}} = Ae^{\frac{-i2\pi mcr}{h} - \frac{2\pi mcr}{h}}$$

(when $k=2\pi mc/h$ and $x=r$)

Wherein, quantum mechanically, (A) can be a scalar amplitude, such that, for example, $A=1/2kx^2 \equiv mgh$ which pertains to $\approx G_T m/r$ (when the other mass is positioned at infinity) which, herein, is equivalent to $\approx K_T q/r$; or (A) can be a vector amplitude, e.g., E (electric vector strength), i.e., $K_C q/r^2$, which is the gradient of the potential $K_C q/r$ which herein relates to $\approx K_T q/r$ which again, herein, is equivalent to $\approx G_T m/r$.

Now, continuing, if the irregular distribution of particles creating the extended extranuclear fields and the static particle located a distance away have the same charge, then electromagnetic repulsion will be produced along with the respective gravitational attraction as shown in figures (17), (18), and (19) for an irregular distribution of positively charged particles interacting with a positively charged particle (wherein, in this case, electromagnetic repulsion would dominate over gravitational attraction).

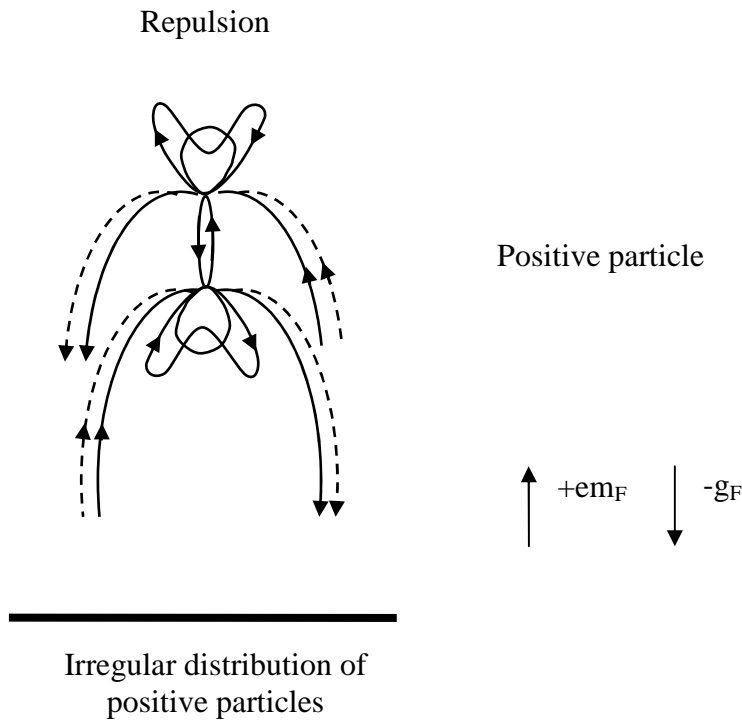


FIG. 17

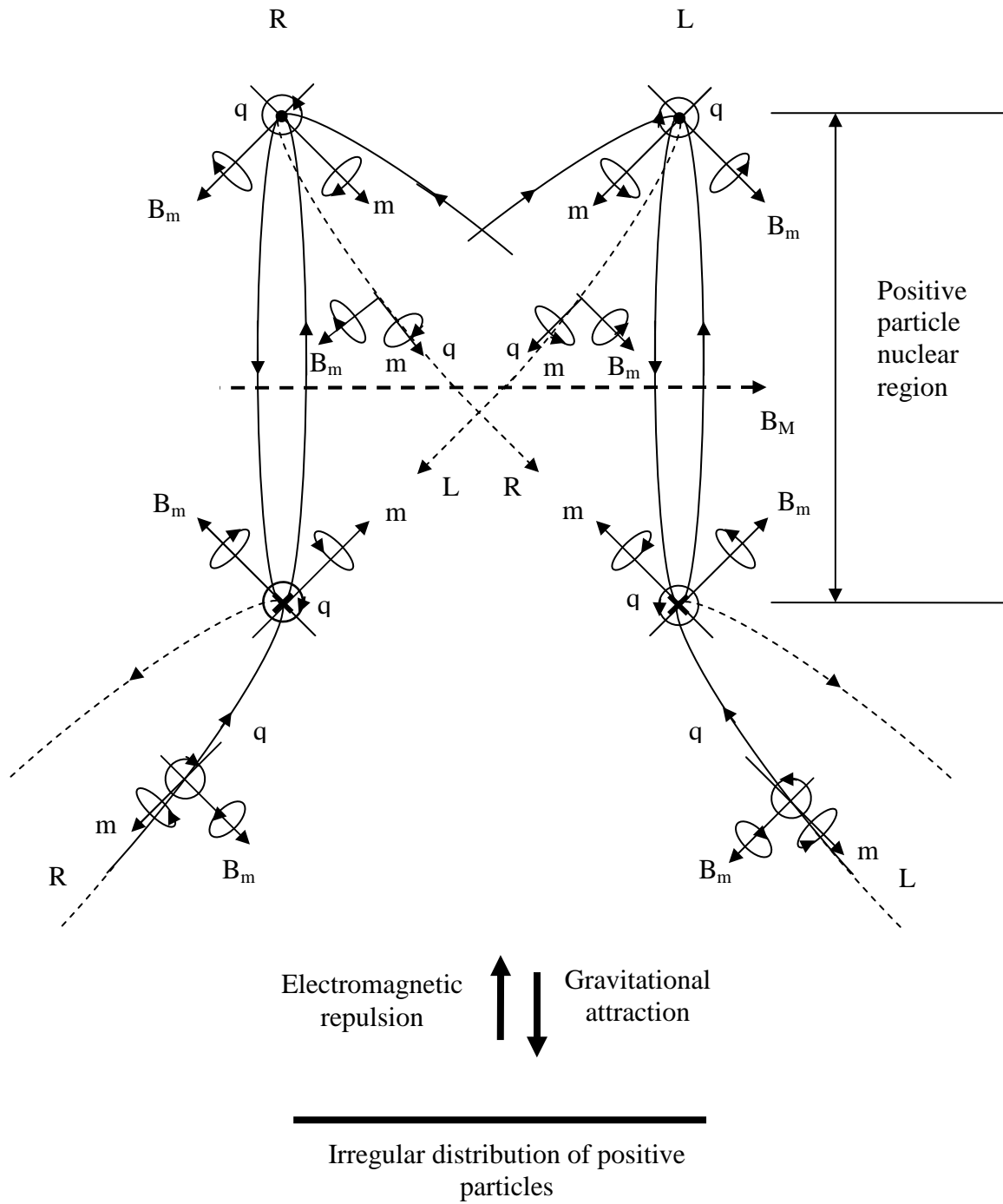


FIG. 18

Edge formation of an accelerated positive particle

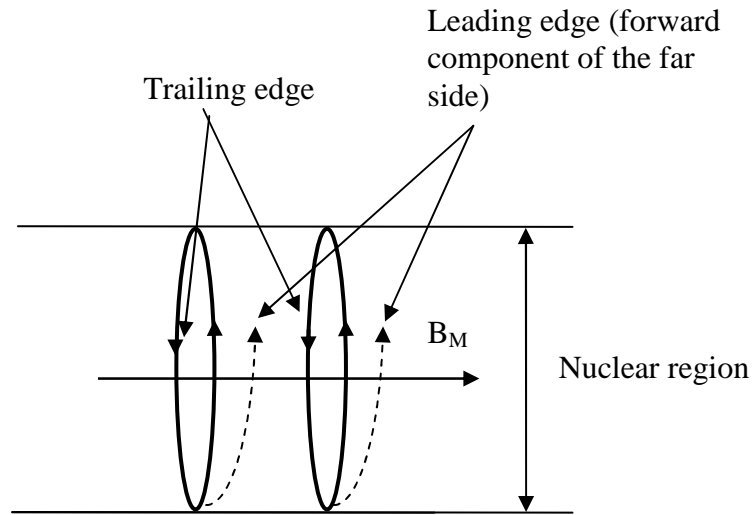
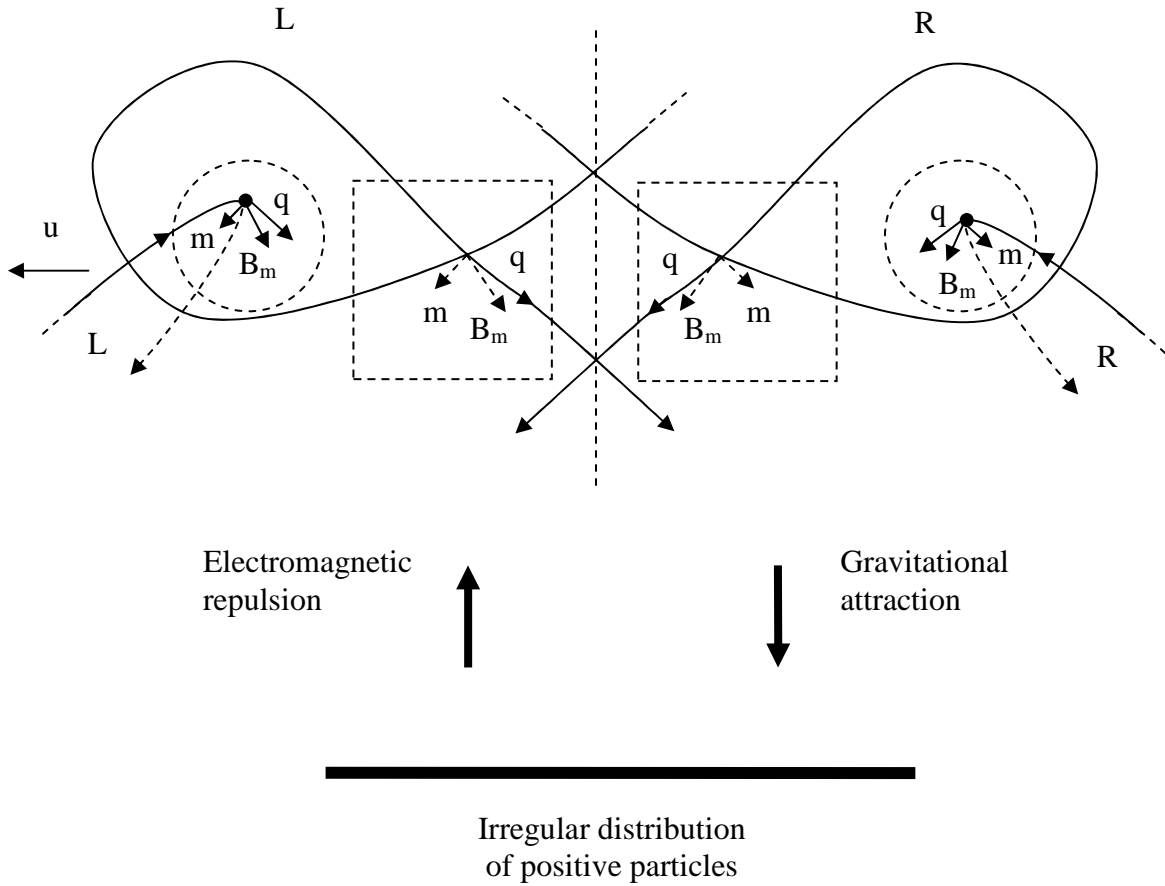


FIG. 19

Figure (20) shows the two possible varieties of virtual particle paths of the irregular distribution of positively charged particles which would interact with the virtual particle paths of a positively charged particle if it were initially propagating down the page, such that the positively charged particle is decelerated as it approaches the positively charged particles. Note that the spin vectors in the dashed squares include spin vectors which are aligned in a somewhat tilted manner in and out of the page such that the respective components of them align accordingly.

Positive particle propagating down the page interacting with two varieties of virtual particle paths from an irregular distribution of positive particles



Virtual particle paths (with spins in dashed circles) extending out from the positively charged particles (thick solid line) interact with the "nuclear region" of the propagating positive particle (with spins in dashed squares), such that the charge (q) and mass (m) spins of respectively interacting right and left hand screw sides are parallel and respectively attract, and such that the magnetic spins (B_m) of respectively interacting right and left hand screw sides are parallel and repel. (Note that the top and bottom sides of the propagating positive particle tilt out of the page.)

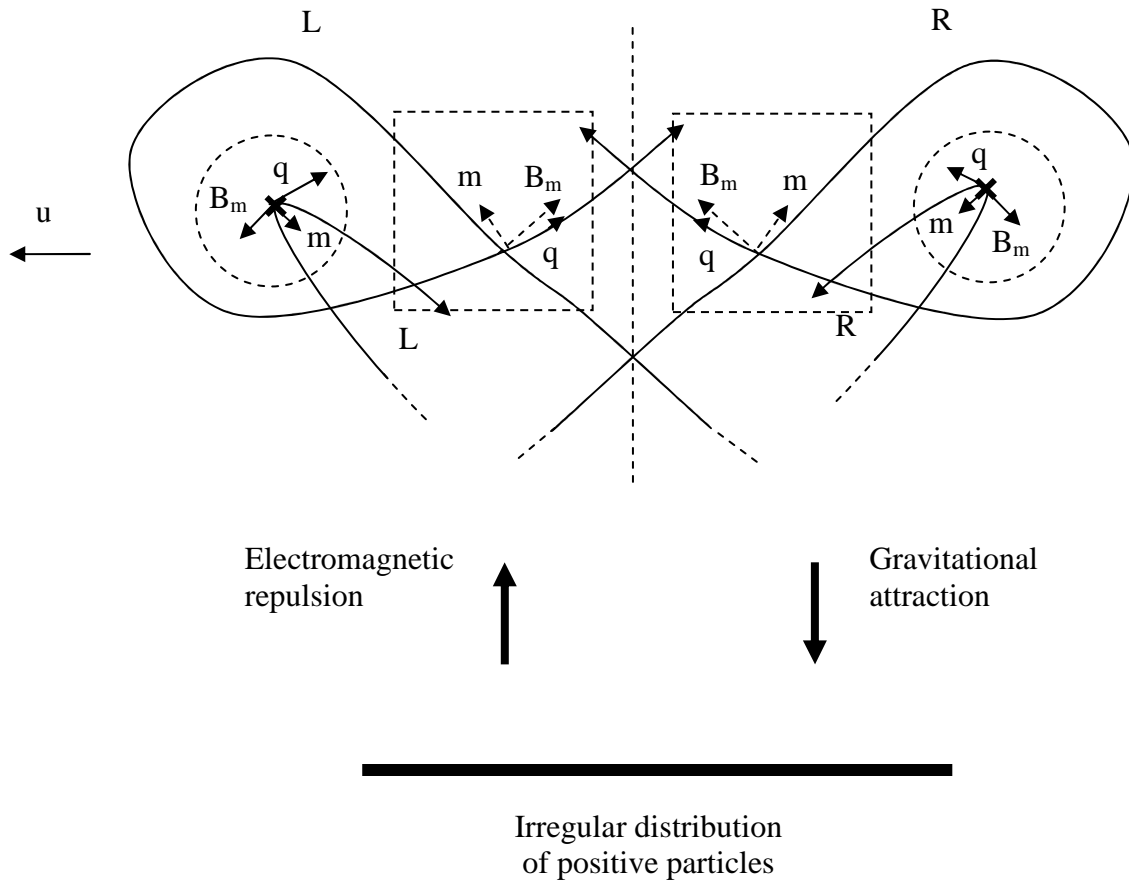
FIG. 20

Here, the virtual particle paths of the irregular distribution of positively charged particles, in effect, would electromagnetically repel the virtual particle paths of the positive particle, and cause the virtual particle paths of the propagating positive particle to change geometry such that the positive particle would decelerate and turn away from the positively charged particles.

In this case, the positive particle would turn away from the irregular distribution of positively charged particles against the affect of the gravitational attraction of the virtual particle paths of the irregular distribution of positively charged particles. Wherein, the gravitational attraction would cancel an extent of the electromagnetic repulsion while attempting to cause (to a respective extent) the opposite turning effect on the positive particle in order that the positive particle "accelerate" toward the positively charged particles (or "decelerate" in terms of its propagation away from the positively charged particles). In effect, the positive particle would be accelerated in the opposite direction away from the irregular distribution of positive particles by the electromagnetic repulsion of the irregular distribution of positive particles which, in this example, would dominate over gravitational attraction.

Figure (21) shows the two possible varieties of virtual particle paths of the irregular distribution of positively charged particles which interact with the virtual particle paths of the propagating positively charged particle which is turned around and accelerated up the page away from the irregular distribution of positively charged particles. Note that the spin vectors in the dashed squares include spin vectors which are aligned in a somewhat tilted manner in and out of the page such that the respective components of them align accordingly.

Positive particle propagating up the page
 interacting with two varieties of virtual
 particle paths from an irregular
 distribution of positive particles



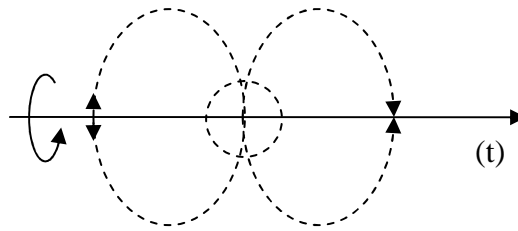
Virtual particle paths (with spins in dashed circles) extending out from the positively charged particles (thick solid line) interact with the "nuclear region" of the propagating positive particle (with spins in dashed squares), such that the charge (q) spins of respectively interacting right and left hand screw sides are parallel and respectively attract, and such that the mass spins (m) of respectively interacting right and left hand screw sides are antiparallel and repel (attempting to turn the positive particle around), and furthermore such that the magnetic spins (B_m) of respectively interacting right and left hand screw sides are antiparallel and attract (and propel the positive particle away from the irregular distribution of positive particles). (Note that the top and bottom sides of the propagating positive particle tilt into the page.)

FIG. 21

It is considered that the virtual particle paths of oppositely electrically charged particles can produce electrically neutral effects. Wherein, if a uniform irregular distribution of both positive and negative electrically charged particles (with respective mass) interact with an electrically charged particle, then the microscopic magnetic spins of the four varieties of extranuclear virtual particle paths (from eight possible virtual particle paths altogether) from the given positive and negative electrically charged particles would "symmetrically" neutralize so as to neutralize the electromagnetic effects, while the same mass spins would continue to be affective and maintain gravitational attraction. (Note that gravitational attraction occurs with both electromagnetic attraction and electromagnetic repulsion, and thus gravity is perceived as only causing acceleration towards a massive particle.)

As further examples of the symmetrically neutral affects of the virtual particle paths of one or more electrically charged particles, it is considered that a neutron comprises the virtual particle paths of a positive electrically charged proton and a negative electrically charged electron (as elaborated upon later) which can effectively interact together in a symmetrical manner so as to produce an electrically neutral effect. While, an electromagnetic field quantum is considered to comprise top and bottom sides which propagate side-by-side, and interact electromagnetically in an electrically neutral manner upon being "symmetrically" absorbed into a particle (such as an electron) along the nuclear field region. While, outside of this sort of interaction, it is considered that an electromagnetic field quantum can not be significantly electrically interacted upon by electrically charged particles due to the particular alignment of the microscopic spin vectors of the virtual particle paths on the top and bottom sides in its internal structure.

Figure (22A) shows a rotated view of the top and bottom virtual particle paths of a quantum with respect to an interacting irregular distribution of positive and negative electrically charged particles (e.g., a star of significant mass).

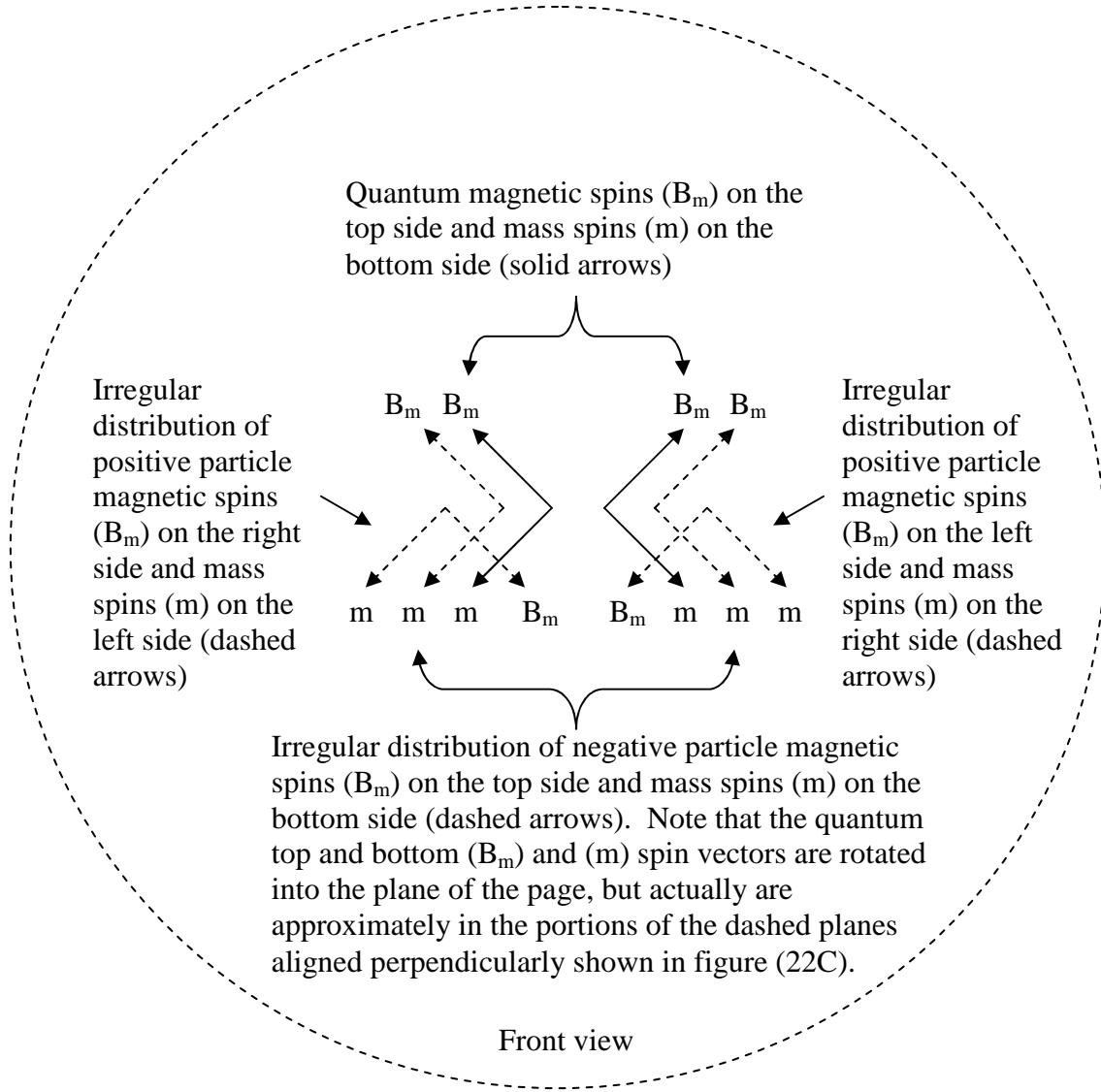


Top view

Arrangement of a propagating matter quantum with respect to an interacting irregular distribution of positive and negative electrically charged particles (solid line). Here, the top and bottom virtual particle paths of the quantum are rotated 90 degrees around the (t) axis in order to show the top view of the quantum.

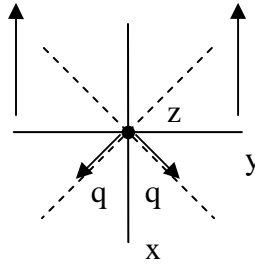
FIG. 22A

Figure (22B) is an enlarged view of what is occurring in the dashed sphere in figure (22A) with the spin vectors rotated back 90 degrees around the (t) axis (back to its proper alignment), and then viewed as would be seen from the front (also 90 degrees rotated).



Here, figure (22B) is an enlarged view of what is occurring in the dashed sphere in figure (22A) with the spin vectors rotated 90 degrees around the (t) axis, and as would be seen from the front view (also rotated 90 degrees). Wherein, in figure (22B), on the top portion of the quantum, the mass spins (m) from the irregular distribution of positive and negative particles are aligned parallel with the matter quantum mass spins (m), and thus all attract so as to produce gravitational attraction. While, the magnetic spins (B_m) of the irregular distribution positive particles are all aligned antiparallel and thus attract, and the magnetic spins (B_m) of the irregular distribution of negative particles are all aligned parallel and thus repel, such that antiparallel and parallel magnetic spins cancel and produce charge neutralization.

FIG. 22B



When viewed from the top, the quantum top and bottom (B_m) and (m) microscopic spin vectors are aligned approximately in the dashed planes aligned perpendicularly in the portions indicated by the arrows. While, the (q) spin vectors are aligned respectively perpendicular and the quantum as a whole would be propagating along the (x) axis.

FIG. 22C

Accordingly, equation (14) shows the theoretical form of the function for the gravitational lensing effect for an irregular distribution of positive and negative particles interacting with a quantum (the result of which is similar to that of general relativity):

$$V_{(\text{large mass total potential})} \approx 4 * \sum \left(\frac{-1}{2}c^2 + \frac{-1}{2}c^2 \right) + \dots \approx 4 * \sum (-c^2) + \dots \approx -4G_T \frac{M}{r} * e^{\approx -0\pi(mcr)/h} \approx -4G_T \frac{M}{r}$$

Eq. (14)

when $e^{\approx -0\pi(mcr)/h}$ is approximately equal to one.

Wherein, the net charge of the interacting large mass is equal to zero so that only the potential

$\approx \sim 1/2G_{TM}/r * 1/e^{\approx 0(2\pi mcr)/h} \approx \sim 1/2c^2$ (which is the virtual particle path mass associated potential for each of the top and bottom sides of the particles in the large mass) is effective for the respectively coupled quantum virtual particle paths. Note that when a static electron is applied instead of a quantum that the internal spin vectors of the electron are rotated so that the potential of the larger mass is effectively half the effective potential on a quantum, i.e., $\approx \sim 2G_{TM}/r * 1/e^{\approx 0(2\pi mcr)/h} \approx \sim 2G_{TM}/r$, as would be measured at weak field and low velocity (when $1/e^{\approx 0(2\pi mcr)/h}$ is equal to one). Nevertheless, also note that according to the present unified field theory, and contrary to convention, a quantum can be electrically interacted upon by an electrically charged particle to an infinitesimally small extent, i.e., in particular, a large amount of electrically charged particles comprising the same electrical charge could electrically interact in an observable way with a quantum according to the spins of the charged particles and the spins of the quantum.

Now, it is considered that when the virtual particle paths which extend out from a particle interact with another particle that they do so such that the potentials of the virtual particle paths summate (i.e., add and subtract) in agreement with their respective spin alignments, so as to effectively attract or repel, and consequently cause a respective extent of electromagnetic and gravitational attraction or repulsion. As with respect to figure (6D) and the reasoning which follows immediately thereafter, the Lorentz factor can be related to the geometry of the propagation of the mass-energy of the unified field (or of a particle). Wherein, in order to unify "spacetime" (as considered with respect to the unified field herein) with the mass-energy of the unified field, it is considered that γ_T (theoretical gamma) is proportional to a change in potential as shown in equation (15) upon redefining the Lorentz factor as follows:

$$\gamma_T = \frac{1}{\sqrt{1 - \frac{v^2}{c^2}}} = \frac{1}{\sqrt{\frac{c^2}{c^2} - \frac{v^2}{c^2}}} = \frac{1}{\sqrt{\frac{c^2 - v^2}{c^2}}} =$$

$$\frac{1}{1 - \frac{\frac{1}{N} \frac{1}{n_2} G_T(m) * e^{\left[\frac{1}{N} \frac{1}{h} 2\pi(mcr) \right]} - \frac{1}{N} \frac{1}{n_2} G_T(m) * e^{\left[\frac{1}{N} \frac{1}{h} 2\pi(mcr) \right]}}{\frac{1}{N} \frac{1}{n_2} G_T(m) * e^{\left[\frac{1}{N} \frac{1}{h} 2\pi(mcr) \right]}}}$$

$$\frac{1}{1 - \frac{\Delta \frac{1}{N} \frac{1}{n_2} G_T(m) * e^{\left[\frac{1}{N} \frac{1}{h} 2\pi(mcr) \right]}}{\frac{1}{N} \frac{1}{n_2} G_T(m) * e^{\left[\frac{1}{N} \frac{1}{h} 2\pi(mcr) \right]}}}$$

such that

$$\gamma_T = \frac{1}{1 - \frac{\Delta \frac{1}{N} \frac{1}{n_2} G_T(m) * e^{\left[\frac{1}{N} \frac{1}{h} 2\pi(mcr) \right]}}{\frac{1}{N} \frac{1}{n_2} G_T(m) * e^{\left[\frac{1}{N} \frac{1}{h} 2\pi(mcr) \right]}}}$$

Eq. 15

Wherein, the charge form of potential could be converted to the mass form of potential and included when electric charge is relevant.

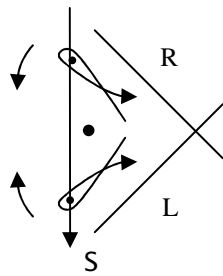
In which case, the Lorentz factor is considered to be "carried" by the virtual particle paths (mass-energy) and the respective volume subtended by the virtual particles (virtual particle paths) of the unified field, such that the parameters of Lorentz transformations are inherent in the unified field (providing background independence). Thus, the gradient of a single virtual particle path (or a four dimensional array of virtual particle paths) provides the gravitational (and electromagnetic) energy of interaction, and effectively supplies the Lorentz factor. While, the path along which the respective body interacted upon travels is effectively produced by the respectively interacting virtual particle path (or paths) and the body interacted upon according to such terms which include the potentials and corresponding alignments of the spin vectors of the interacting fields before, and as a consequence of, interaction.

In result, the mass-energy and the "spacetime" of "gravity" are both comprised by the virtual particle paths of the unified field, and are applied together in a more direct manner than in general relativity. Yet, the unified field described herein unifies "spacetime" with not only mass, but also electric charge. In which case, for example, at weak field and low velocity, a virtual particle path of the unified field (which, again, carries the Lorentz factor of "spacetime,") comprises both a gravitational component which accounts for conventional gravitational interaction, and an electromagnetic component which accounts for conventional electromagnetic interaction, and in the present theory, also accounts for nuclear proton-proton attraction (in nucleonic interaction) while gravity includes repulsive spins as will be described later (wherein gravity is considered negligible in conventional terms in this latter case).

Accordingly, the theory as presented thus far neither supports gravitons as independent mediators of the gravitational interaction nor gravitational waves as existing independent of electromagnetic waves. In response, the unification herein proposes that the gravitational and electromagnetic components of the unified field together mediate gravitational and electromagnetic interactions as described before and more so later.

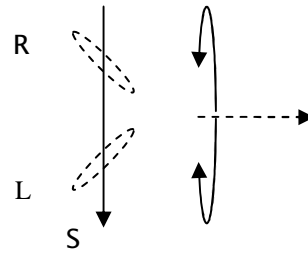
CHARGED PARTICLE PROPAGATION AND INTERACTION:

Now, consider that a propagating electrically charged particle has an intrinsic spin (S) which is aligned through the virtual particle path loops which only partially reflect around the axis in the plane of symmetry which separates the top and bottom sides as shown for a propagating negatively charged particle in figures (23A), (23B), and (23C), and for a positively charged propagating particle in figures (24A), (24B) and (24C). (Note that only the front portion of each propagating particle is shown.)



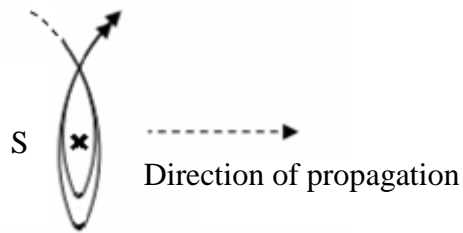
Front view

FIG. 23A



Side view

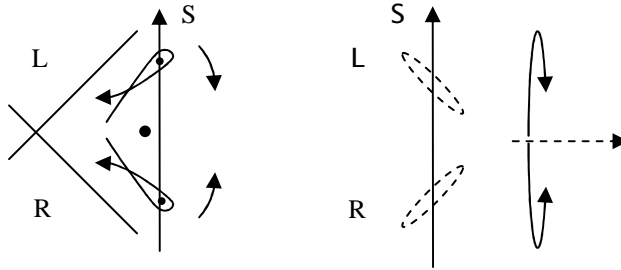
FIG. 23B



Top view

Intrinsic spin for a propagating negatively charged particle. Note that (S) is into the page using the right hand rule.

FIG. 23C

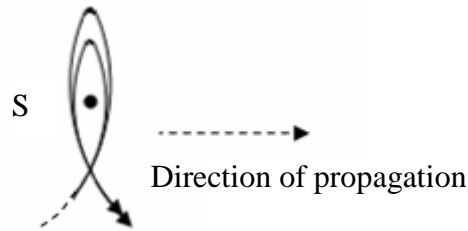


Front view

Side view

FIG. 24A

FIG. 24B



Top view

Intrinsic spin for a propagating positively charged particle. Note that (S) is out of the page using the right hand rule.

FIG. 24C

Next, consider that propagating negatively charged particles prefer to be relatively upright during interaction while propagating in parallel or antiparallel, and similarly for propagating positively charged particles as shown in figure (25A) for juxtaposed parallel propagating negatively and positively charged particles. While, similar alignment is shown in figure (25C) for vertically aligned parallel propagating

negatively and positively charged particles. On the other hand, propagating positively and negatively charged particles prefer to be relatively inverted during interaction while propagating in parallel or antiparallel as shown in figure (25B) for juxtaposed parallel propagating positively and negatively charged particles, and as shown in figure (25D) for vertically aligned parallel propagating positively and negatively charged particles. Wherein, in all of the case, the intrinsic spins are aligned parallel.

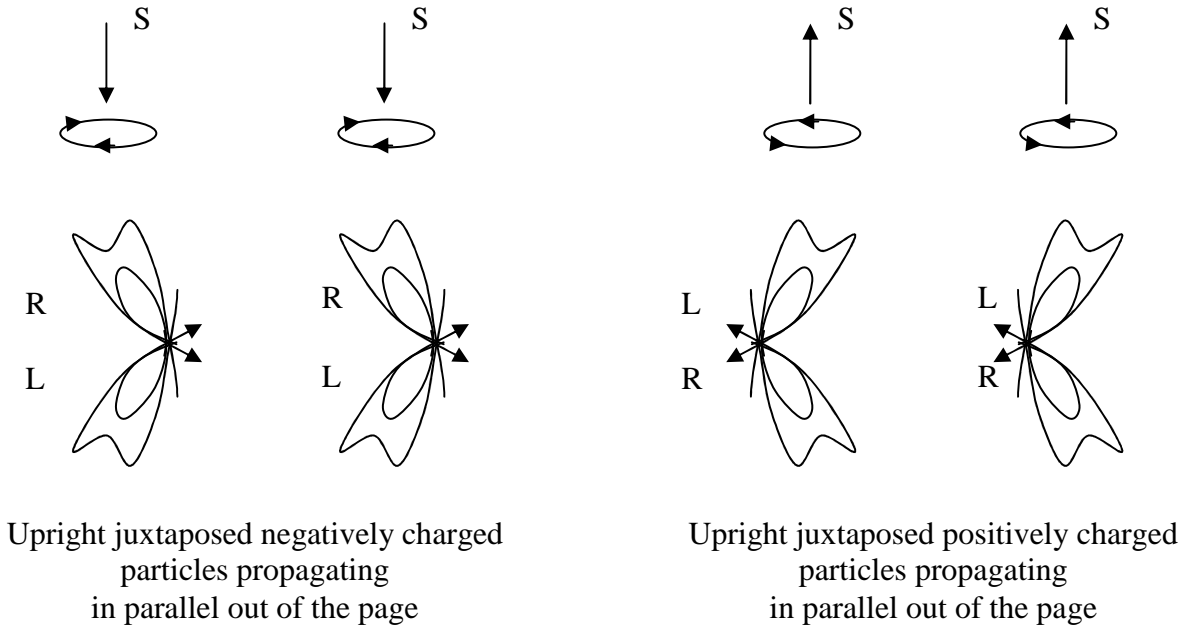


FIG. 25A

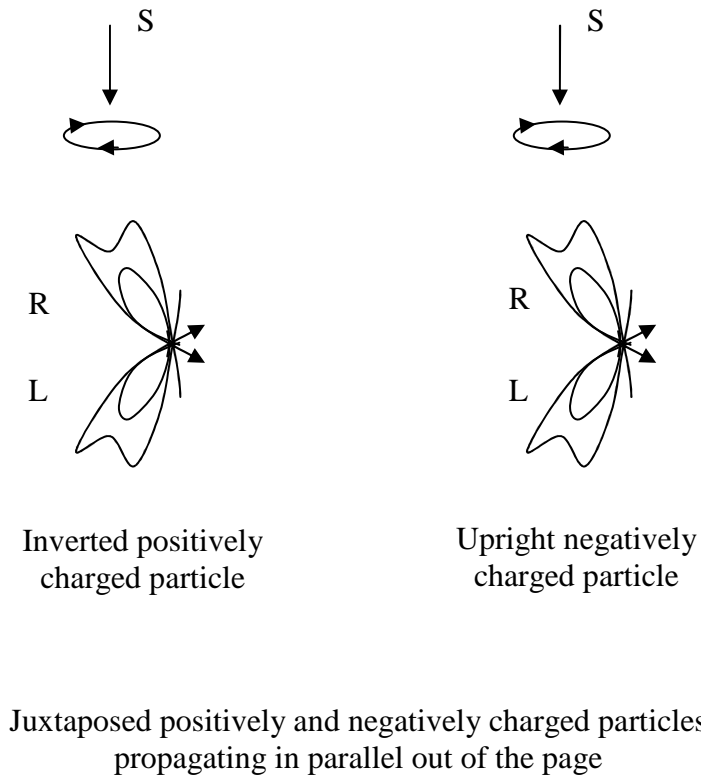


FIG. 25B

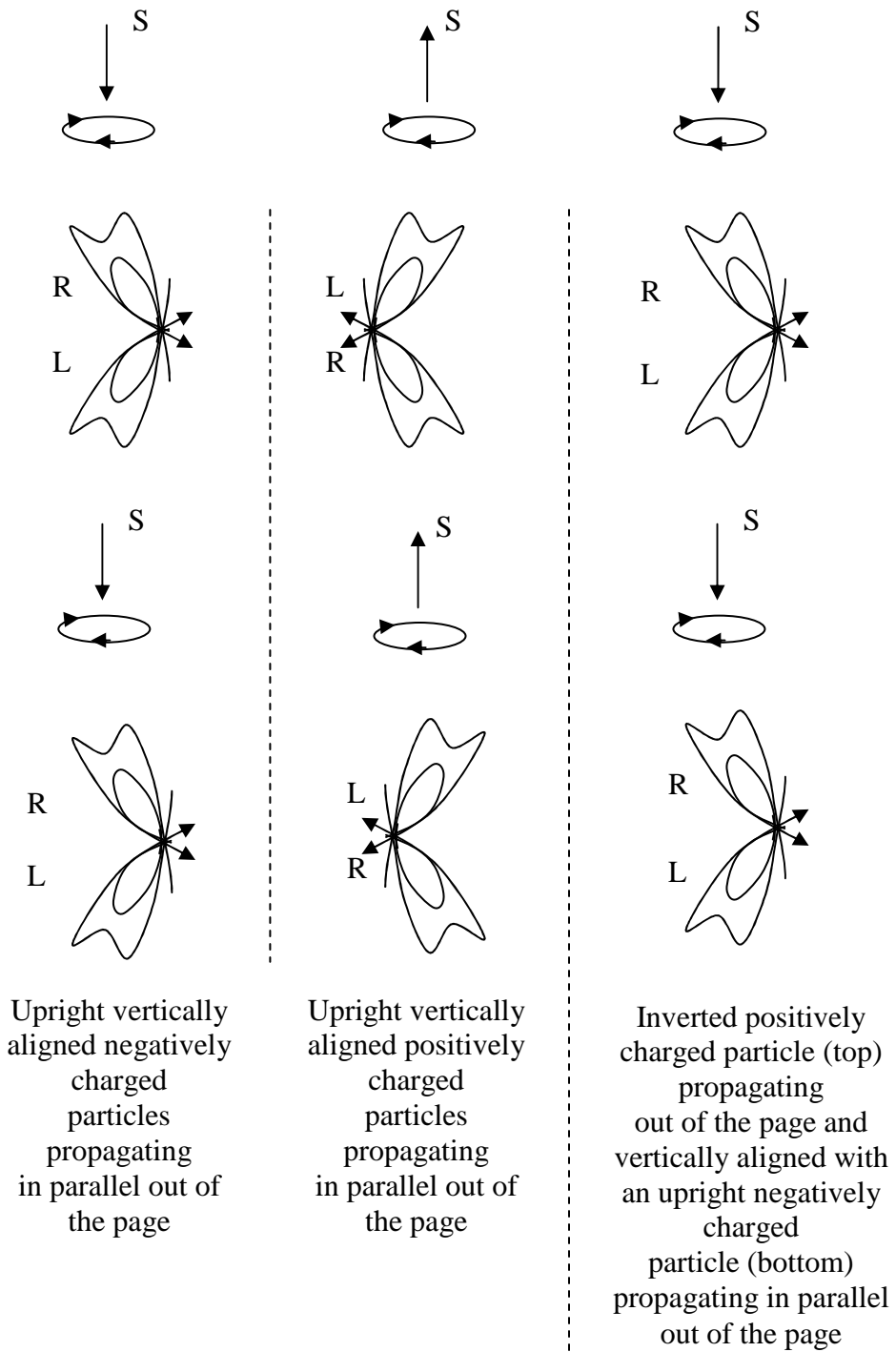


FIG. 25C

FIG. 25D

Consider especially important for certain interactions (e.g., for interactions of electrically charged particles which are in a orderly aligned distribution as in the case of the interaction of spin aligned propagating electrically charged particles, the interaction of magnets, and molecular interactions), that the microscopic spin vectors of more bent extended virtual particle paths are relatively inverted due to "bending" compared to less bent virtual particle paths, such that, for example, the microscopic electric spin vector (q) rotation around the respective (z) axis is reversed, and, importantly, the magnetic (B_m) and mass (m) spin vectors are inverted as shown in figures (26A) and (26B), for example, for the extranuclear field region on the front top right hand screw side of a negatively charged particle. Wherein, this inversion characteristic, or the lack thereof, affects the alignment and rotational directions of the spin vectors of interacting virtual particle paths, and thus affects the respective attraction or repulsion of spin vectors during certain interactions.

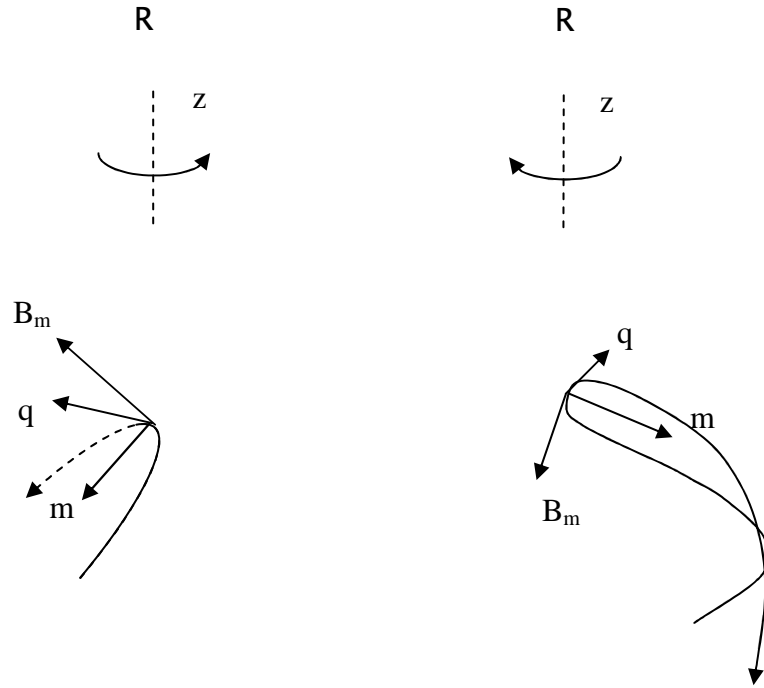


FIG. 26A

FIG. 26B

Spin rotation reversal around the (z) axis depicted for electric spin vector (q) such that the direction of the rotation is relatively inverted in the less bent virtual particle path shown in figure (26A) compared to the electric spin vector (q) in the more bent virtual particle path shown in figure (26B) in the extranuclear field region on the front top right hand screw side of a negatively charged particle. While also, the microscopic magnetic and mass spin vectors are inverted along respective axes accordingly.

Also, consider important for interaction during propagation, that the acceleration of the unified field causes relatively different rotations in different portions of a virtual particle path. Wherein, the rotations shown by dashed curved arrows in figure (27A) for an increase in mass for the microscopic mass spin vectors (m) are in relatively different directions for different portions of a virtual particle path. Then, when considered together as shown by the dashed curved arrows in figure (27B), the bent condition of a more bent virtual particle path is maintained as the different portions of the virtual particle path rotate in opposite directions, and as the relativistic mass of the electrically charged particle increases.

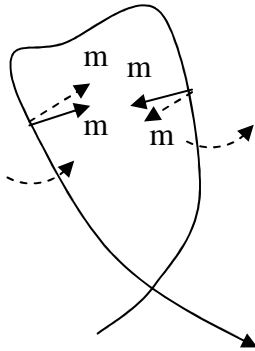


FIG. 27A

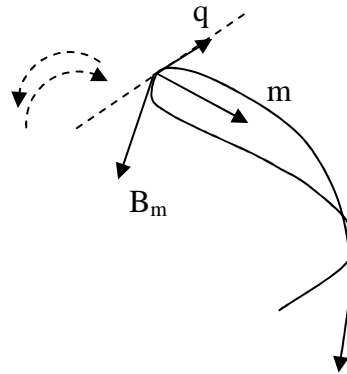
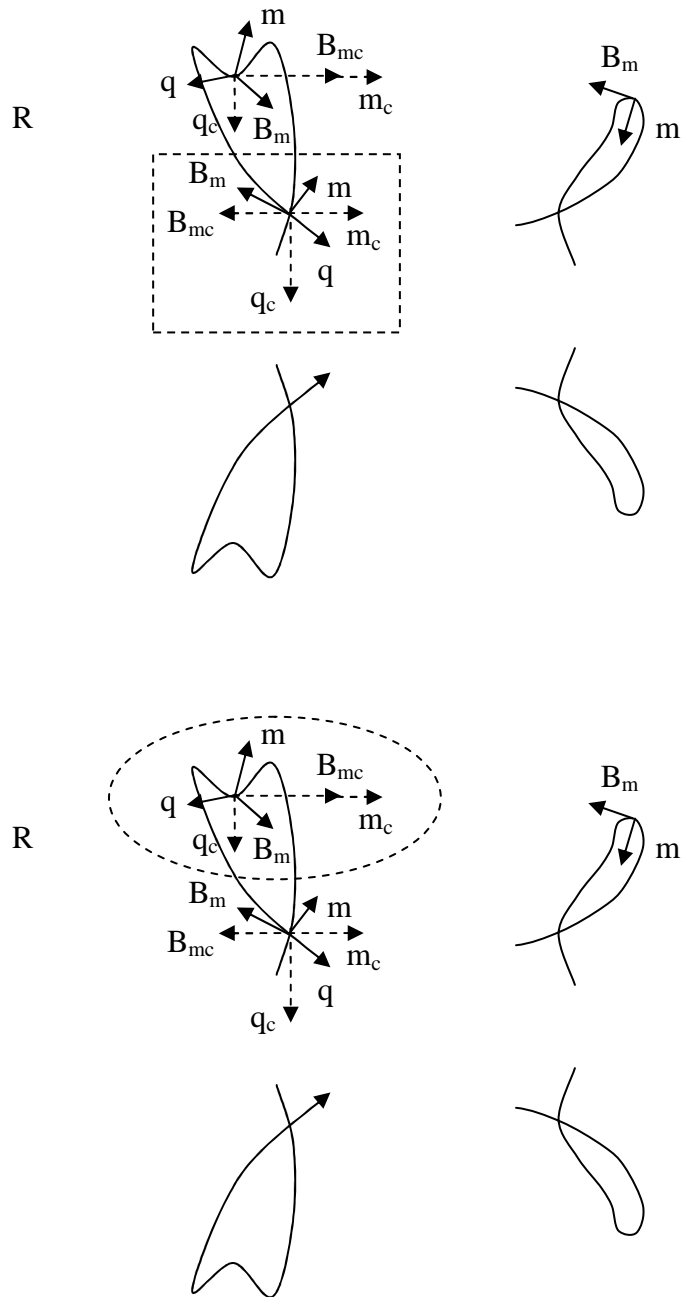


FIG. 27B

Now, figure (28) shows how the microscopic magnetic spin vector component (B_{mc}) of a more bent virtual particle path (dashed oval) of the right hand screw side of the upright negatively charged particle propagating on the bottom is aligned antiparallel (in a horizontal plane) to the microscopic magnetic spin vector component (B_{mc}) of the coupling virtual particle path of the right hand screw side in the “nuclear region” (dashed rectangle) of the upright negatively charged particle propagating in parallel on the top, thus causing magnetic attraction. Note, the particles in figures 28-31 are shown separated. Thus, one must conceptually reposition each orthogonal set of extranuclear spins shown in a dashed oval while keeping them aligned as they are so that the origins of the spin vectors in an oval are almost abutting with the origins of the orthogonal set of nuclear spins shown in the dashed rectangle of the other relevant charged particle for proper alignments. Also, note that the vertical component of (q) is effective in both parallel and antiparallel propagating cases in which a significant plurality of electrically charged particles is applied. Furthermore, note that the following examples of propagating electrically charged particle interaction also include attraction or repulsion according to the microscopic charge, mass, and magnetic spin vectors of the respectively less bent virtual particle paths of the extranuclear field of a propagating electrically charged particles with the nuclear region of the opposing

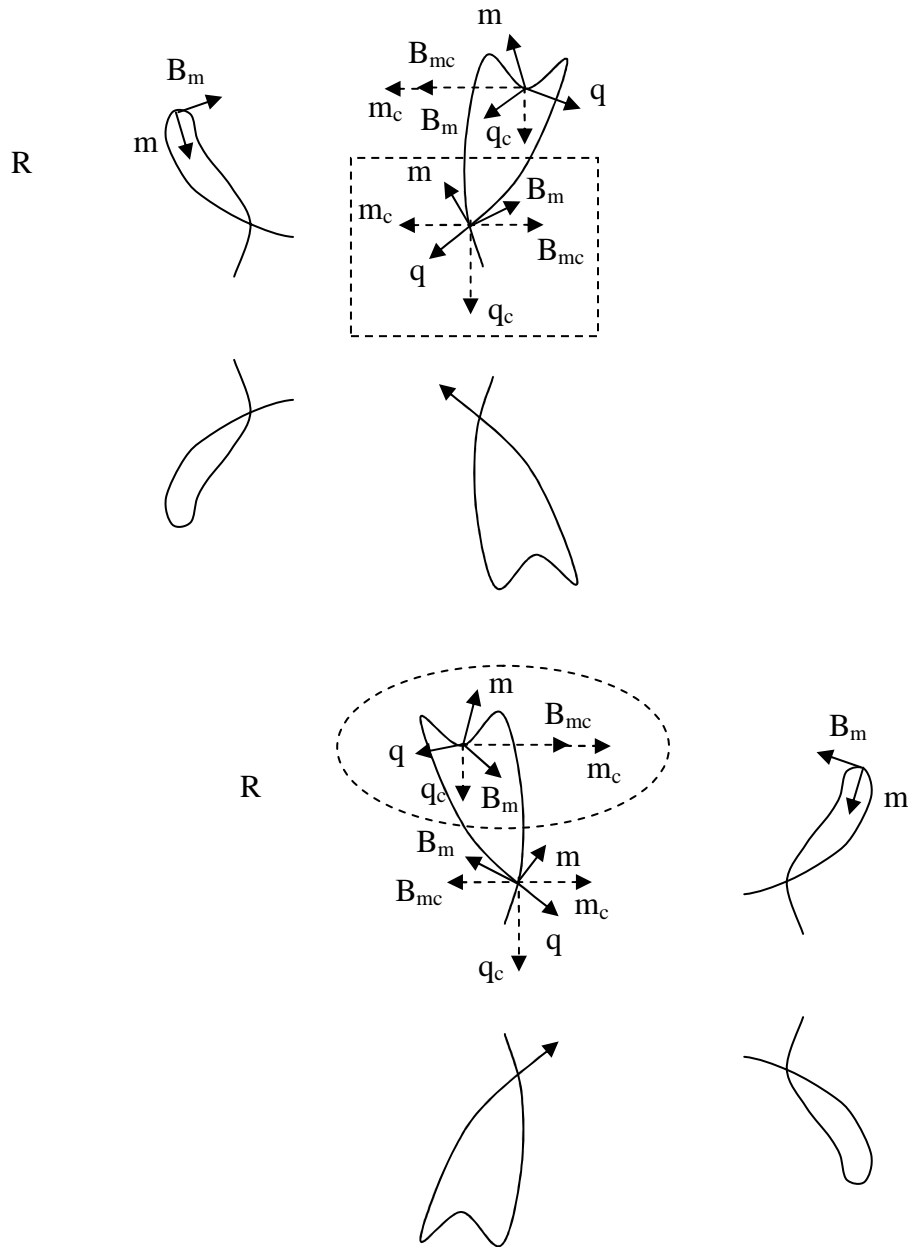
propagating charged particle, i.e., in particular, during juxtaposed propagating charged particle interaction, so as to account for electric and respective gravitational interaction accordingly.



Here, the magnetic spin vector component (B_{mc}) of the more bent virtual particle path (dashed oval) of an upright negative particle propagating out of the page on the bottom is aligned antiparallel in the horizontal plane to the microscopic magnetic spin vector component (B_{mc}) of the “nuclear region” (dashed rectangle) of an upright negative particle propagating in parallel out of the page on the top, thus causing magnetic attraction.

FIG. 28

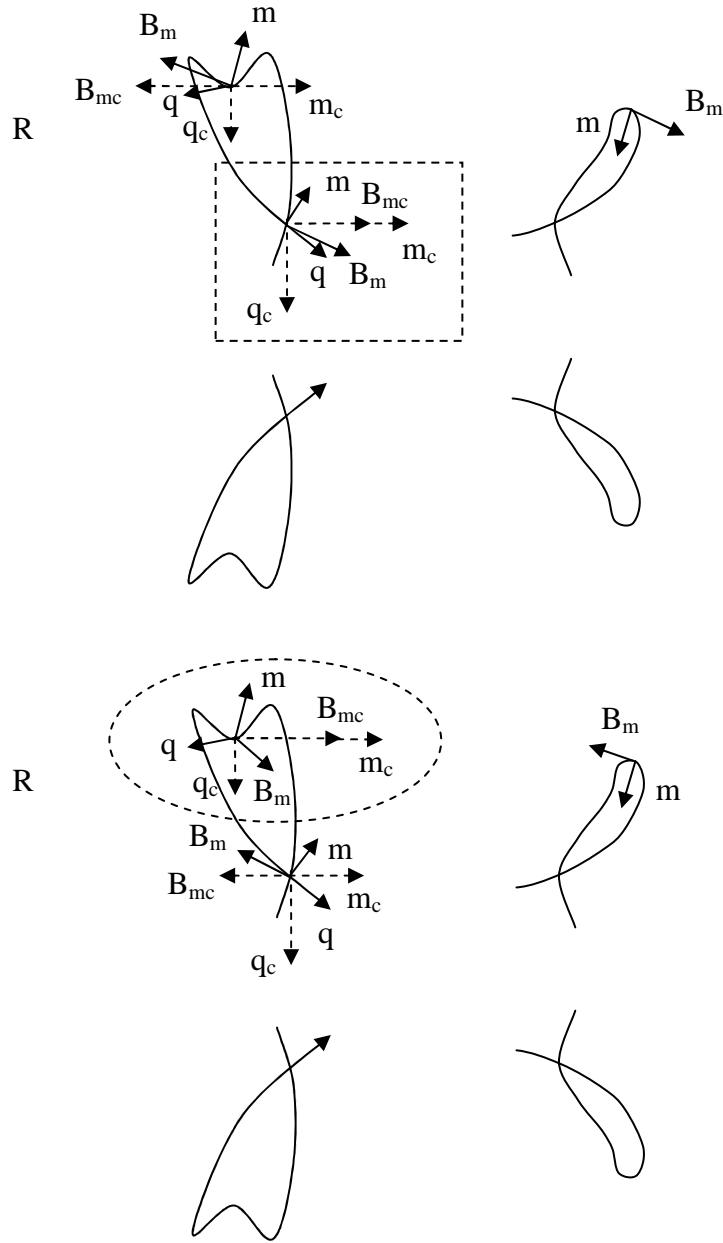
Here, the two negatively charged particles are thus considered to magnetically attract. (Note that two equivalently arranged positively charged propagating particles are considered to interact similarly.) Figure (29) shows how the microscopic magnetic spin vector component (B_{mc}) of a more bent virtual particle path (dashed oval) of the right hand screw side of the upright negatively charged particle propagating on the bottom is aligned parallel to the microscopic magnetic spin vector component (B_{mc}) of the coupling virtual particle path of the right hand screw side in the “nuclear region” (dashed rectangle) of the upright negatively charged particle propagating antiparallel on the top, thus causing magnetic repulsion.



Here, the magnetic spin vector component (B_{mc}) of the more bent virtual particle path (dashed oval) of an upright negative particle propagating out of the page on the bottom is aligned parallel in the horizontal plane to the microscopic magnetic spin vector component (B_{mc}) of the “nuclear region” (dashed rectangle) of an upright negative particle propagating antiparallel into the page on the top, thus causing magnetic repulsion.

FIG. 29

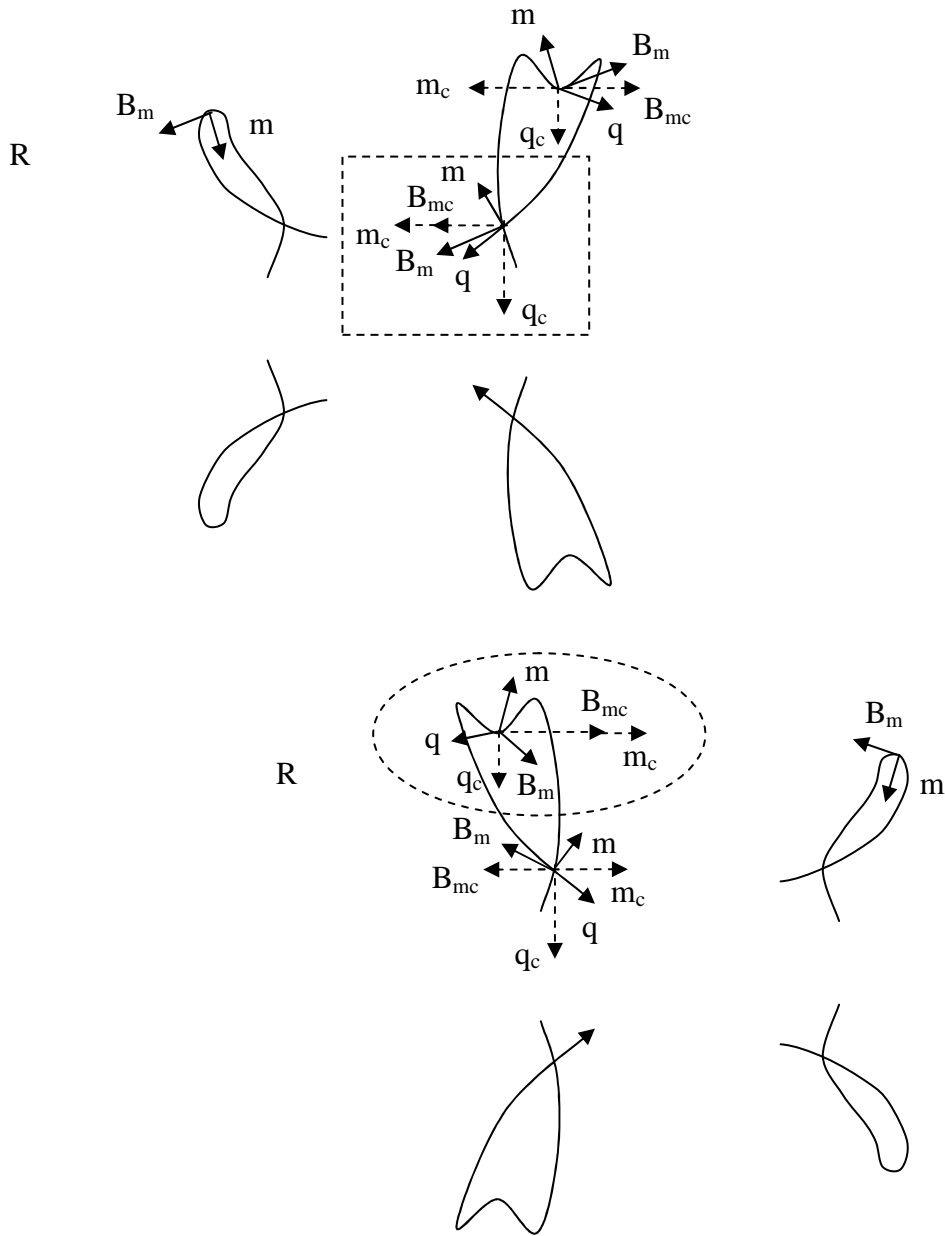
Figure (30) shows how the microscopic magnetic spin vector component (B_{mc}) of the more bent virtual particle path (dashed oval) of the right hand screw side of the negatively charged particle propagating on the bottom is aligned parallel to the microscopic magnetic spin vector component (B_{mc}) of the coupling virtual particle path of the right hand screw side in the “nuclear region” (dashed rectangle) of the inverted positively electrically charged particle which is propagating in parallel on the top, thus causing magnetic repulsion. (Note that the spins of the propagating charged particles shown in figures (29) and (31) including the antiparallel mass components, which attempt to turn the particles around, are considered to especially disclose the role they could play in the formation of a two-body system.)



Here, the magnetic spin vector component (B_{mc}) of the more bent virtual particle path (dashed oval) of an upright negative particle propagating out of the page on the bottom is aligned parallel in the horizontal plane to the microscopic magnetic spin vector component (B_{mc}) of the “nuclear region” (dashed rectangle) of an inverted positive particle propagating in parallel out of the page on the top, thus causing magnetic repulsion.

FIG. 30

Figure (31) shows how the microscopic magnetic spin vector component (B_{mc}) of the more bent virtual particle path (dashed oval) of the right hand screw side of the negatively charged particle propagating on the bottom is aligned antiparallel to the microscopic magnetic spin vector component (B_{mc}) of the coupling virtual particle path of the right hand screw side in the “nuclear region” (dashed rectangle) of the inverted positively electrically charged particle which is propagating antiparallel on the top, thus causing magnetic attraction.



Here, the magnetic spin vector component (B_{mc}) of the more bent virtual particle path (dashed oval) of an upright negative particle propagating out of the page on the bottom is aligned antiparallel in the horizontal plane to the microscopic magnetic spin vector component (B_{mc}) of the “nuclear region” (dashed rectangle) of an inverted positive particle propagating antiparallel into the page on the top, thus causing magnetic attraction.

FIG. 31

VIRTUAL PARTICLES, SELF INTERACTION, AND SUPERLUMINAL VELOCITY:

Conventionally it has been difficult to detect and measure parameters of particles which are thought to constitute the internal structure of matter, e.g., due to the confinement of "quarks (the existence of which the present theory does not support)," etc. Herein, the theory of unification reuses the same parameters for "everything" for structure, function, and simplicity, such that virtual particles constitute the internal structure of mass-energy, and have an internal structure and function which is analogous to propagating electrically charged particles (wherein virtual particles comprise "virtual-virtual particles," etc.).

Accordingly, "self interacting" virtual particle paths (which account for internal bonding) align in agreement with their respectively interacting spin vectors so as to effectively produce the shape of the virtual particle paths, and consequentially the shape of a static or propagating particle as a whole. In which case, virtual particles on the top and bottom sides of a negatively and positively charged particle are considered to self interact with virtual particles on the same side by way of the respective right-right and left-left hand spin vector interactions, such that parallel microscopic charge and mass spin vector interactions are attractive, and antiparallel microscopic magnetic spin vector interactions are attractive, etc. This is because virtual particles are also considered, in their own way, to comprise top and bottom sides which are either right or left hand screw. Similarly, it is considered that virtual particles on the top and bottom sides interact with virtual particles on the respectively opposing side in self interaction by way of respective right-right and left-left hand spin vector interactions. Figure (32A) shows the virtual particles posited for the front side of an example virtual particle path on the top and bottom sides in the nuclear region of a negative and positive electrically charged particle.

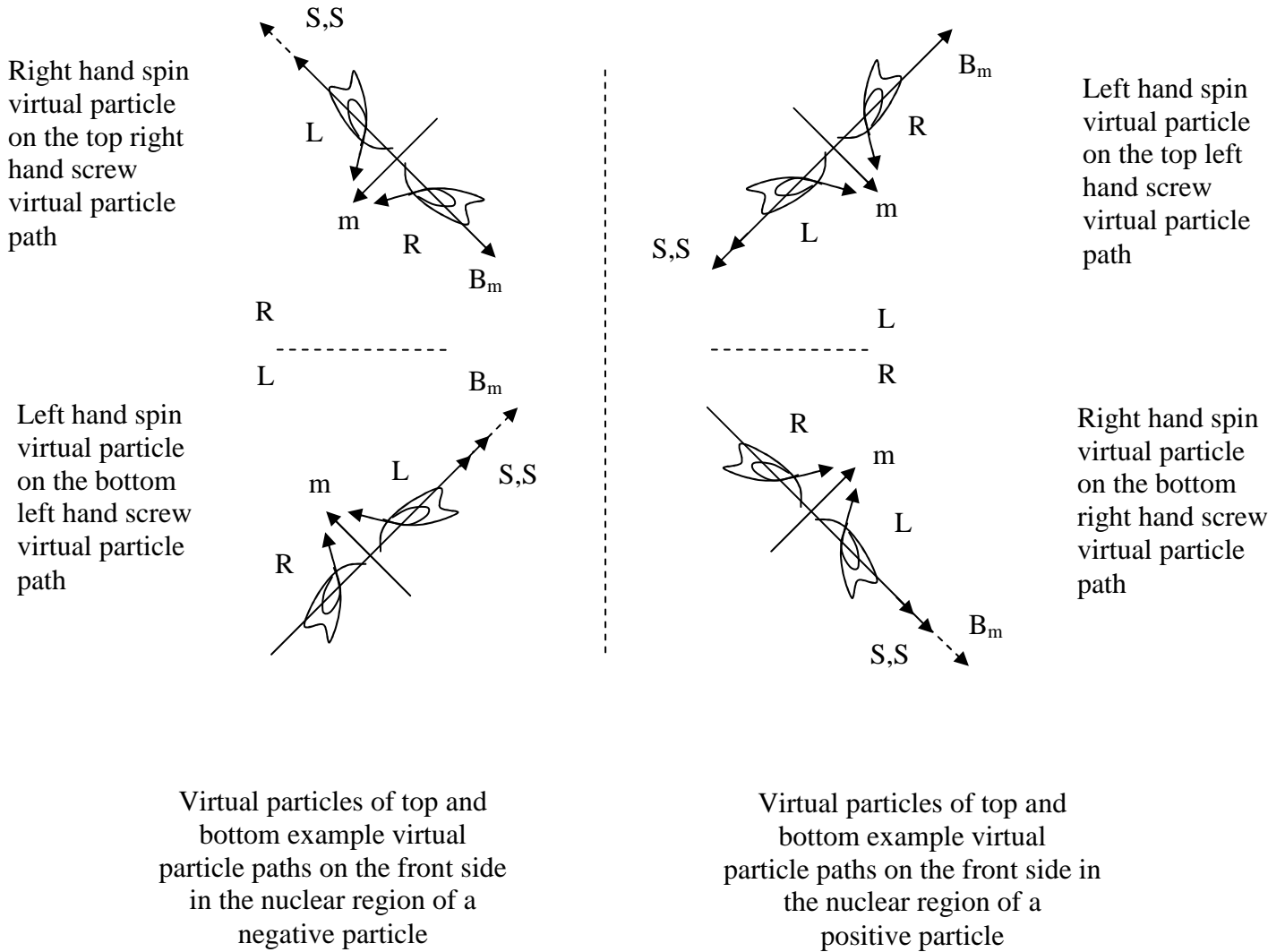
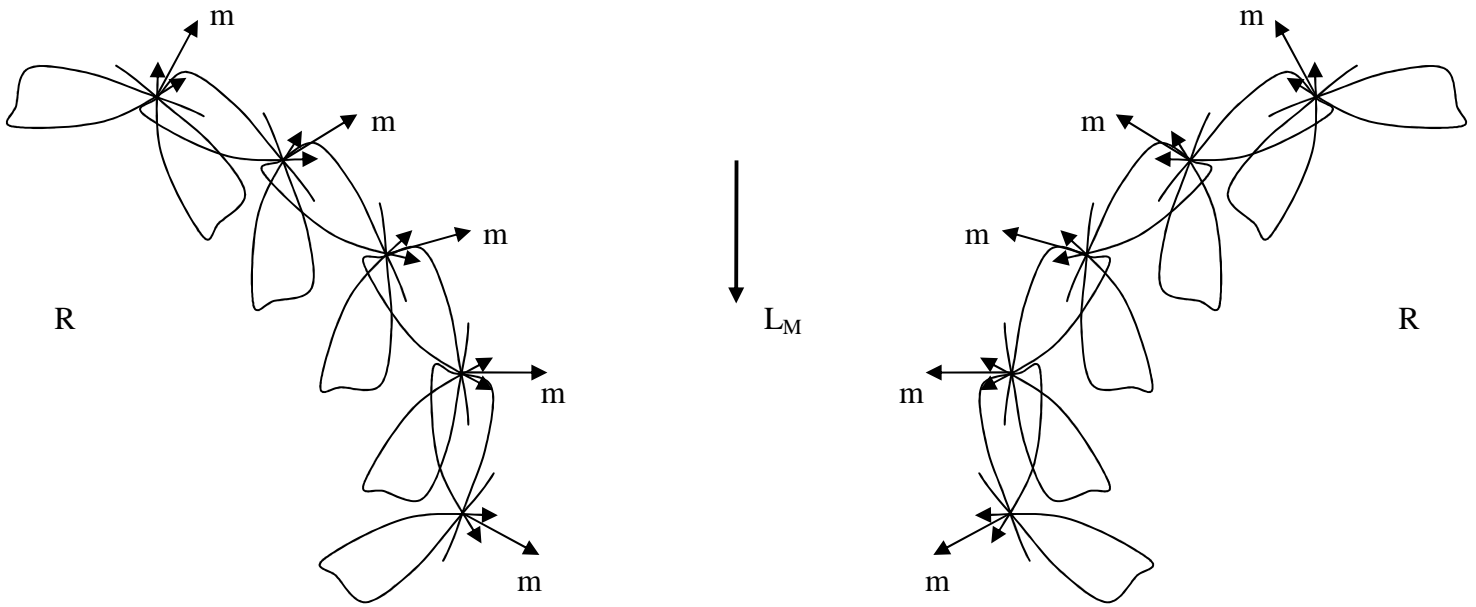


FIG. 32A

However, as shown in figure (32A), virtual particles have microscopic magnetic spin vectors (B_m) which are aligned according to the screw (charge) of the particle in which they are comprised by switching hand rules. Wherein, a right hand spin virtual particle in a negatively charged particle and a right hand spin virtual particle in a positively charged particle have oppositely aligned microscopic magnetic spin vectors (B_m) when their

intrinsic spins are aligned parallel, and similarly for the left hand spin virtual particles. In which case, as described for propagating charged particle interaction before, "real" propagating electrically charged particles of, for example, opposite electric charge which are propagating in parallel with parallel intrinsic spins would have electric attraction based on virtual particles on less bent virtual particle paths which are propagating with "antiparallel" microscopic magnetic spins. Yet, conversely, the virtual particles would also magnetically repel because of the more bent virtual particle paths on which the virtual particles are propagating in the extranuclear region of one of the real propagating particles relative to the virtual particle paths in the nuclear region of the other real propagating particle during interaction, thus producing parallel microscopic magnetic spins and accounting for the differences in the microscopic magnetic spins of the virtual particles of the same spin in opposite screw particles (i.e., here, in oppositely electrically charged propagating particles).

Still, virtual particles from charged particles which mediate electromagnetic and gravitational interaction (as described before) attract or repel analogous to the way propagating electrically charged particles attract or repel during interaction (as also described before). While, virtual particles bonded in a band in a particle, e.g., bonded in a band of virtual particles in a system of opposing sides as in the nuclear region of a static electrically charged particle, also interact analogous to the way propagating electrically charged particles interact, but in a way in which they change in spacing (increasing vertically and horizontally in an outward manner from the center) and rotate (increasing in the less massive, or more decelerated, rotational direction in an outward manner from the center) as shown in figure (32B). Wherein, such bonding occurs in order to maximize attraction and minimize repulsion in conjunction with the bends in their "virtual-virtual" particle paths (which function analogous to the more and less bent virtual particle paths of interacting propagating electrically charged particles described before), thus effectively contributing to the shape of the unified field.



Example virtual particles in virtual particle paths propagating out of the page (right portion) and propagating into the page (left portion) on the top front and back sides, respectively, of the nuclear region of a negative particle.

FIG. 32B

Now, as pertains to the geometry of virtual particle paths and velocity, it is considered in the present

theory that $h \approx 2\pi mcr = 2\pi(2.1764 \times 10^{-8}) \left(\frac{1.6162 \times 10^{-35}}{5.3912 \times 10^{-44}} \right) (1.6162 \times 10^{-35}) \approx 6.6253 \times 10^{-34}$

so that $2\pi mcr/2\pi \approx \hbar/2\pi$, i.e., reduced Planck constant (\hbar); and

Planck length (1.6162×10^{-35})/Planck time (5.3912×10^{-44}) = speed (c) which represents a translational velocity.

In which case, (\hbar), i.e., unreduced Planck constant ($\approx 2\pi mcr$), is applied herein in a context in which it relates to

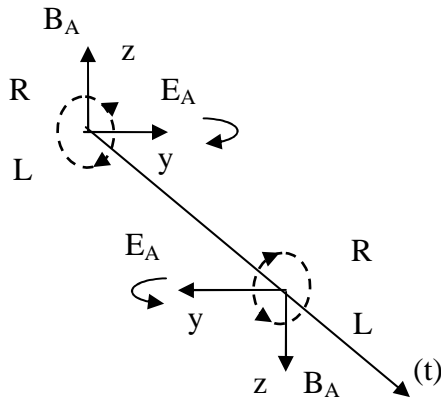
the geometry of the virtual particle paths of the unified field, such that $2\pi * 1.6162 \times 10^{-35}$ (i.e., $2\pi r$) is

"unreduced" Planck length when $r=1.6162 \times 10^{-35}$, and is applied such that $2\pi * 1.6162 \times 10^{-35}$ (unreduced Planck

length)/ 5.3912×10^{-44} (Planck time)= $1.8835 \times 10^{+9}$ m/s which is the superluminal velocity of virtual particles propagating over virtual particle paths.

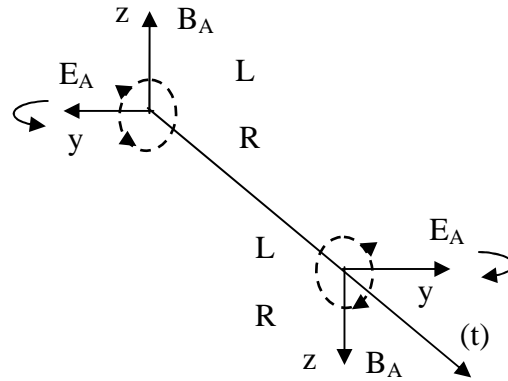
ELECTROMAGNETIC FIELD QUANTUM ("MASSLESS" PARTICLES):

Consider that an "electromagnetic field quantum" produces a conventional alternating electromagnetic field comprising an alternating electric field (E_A) aligned along the (y) axis which is perpendicular to the axis around which the top and bottom sides reflect in the plane of symmetry which separates the top and bottom sides, and perpendicular to the direction of propagation as shown in the perspective views in figures (33A) and (33B). Furthermore, consider that an electromagnetic field quantum also produces a conventional alternating magnetic field (B_A) which is generated as the virtual particle paths helically propagate left and right, and which is aligned along the (z) axis perpendicular to the axis around which the top and bottom sides reflect in the plane of symmetry which separates the top and bottom sides, and perpendicular to the direction of propagation as also shown in figures (33A) and (33B).



Matter
electromagnetic field
quantum

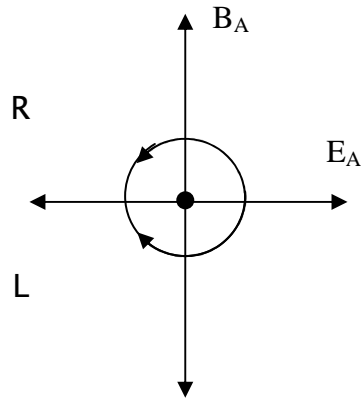
FIG. 33A



Antimatter
electromagnetic field
quantum

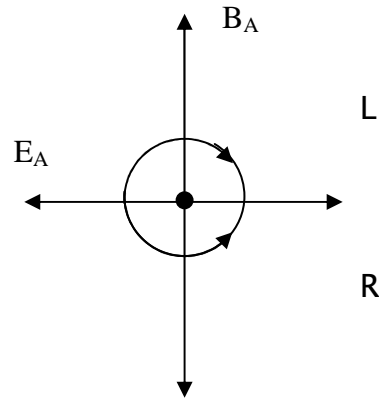
FIG. 33B

The electric field (E_A) and magnetic field (B_A) axes are considered to be aligned as shown in the front views for matter and antimatter electromagnetic field quanta in figures (34A) and (34B), and as also shown in perspective views in figures (35A) and (35B) (as they would also be aligned in a similar manner, and for similar reasons, for a negatively and positively electrically charged particle, respectively). Note that the top and bottom sides shown in figures (34A) and (34B) are propagating around a common central axis, such that the infinitesimally small separation of the top and bottom sides is not shown. Nevertheless, the spin of an electromagnetic field quantum is almost entirely eliminated when considered in the same context as that of the spin of an electrically charged particle in the theory hererin. Also, note that the configuration of the electromagnetic field quantum in the present theory is supported by conventional theory in which a photon is considered to comprise right and left helical components.



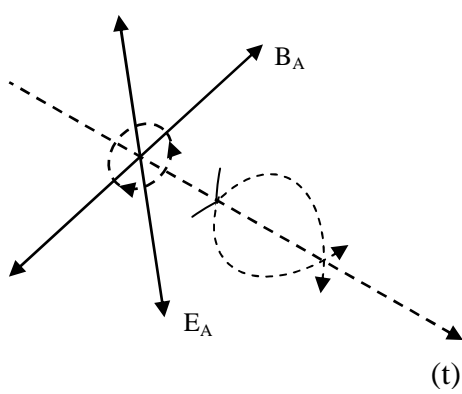
Matter quantum

FIG. 34A



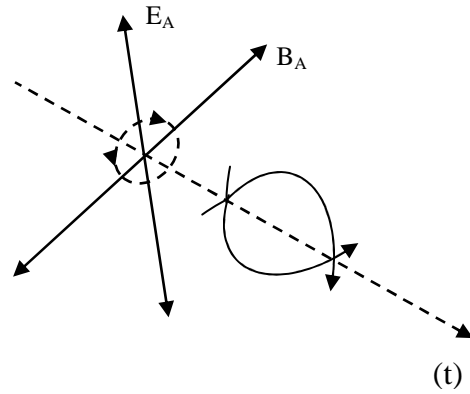
Antimatter quantum

FIG. 34B



Matter quantum

FIG. 35A

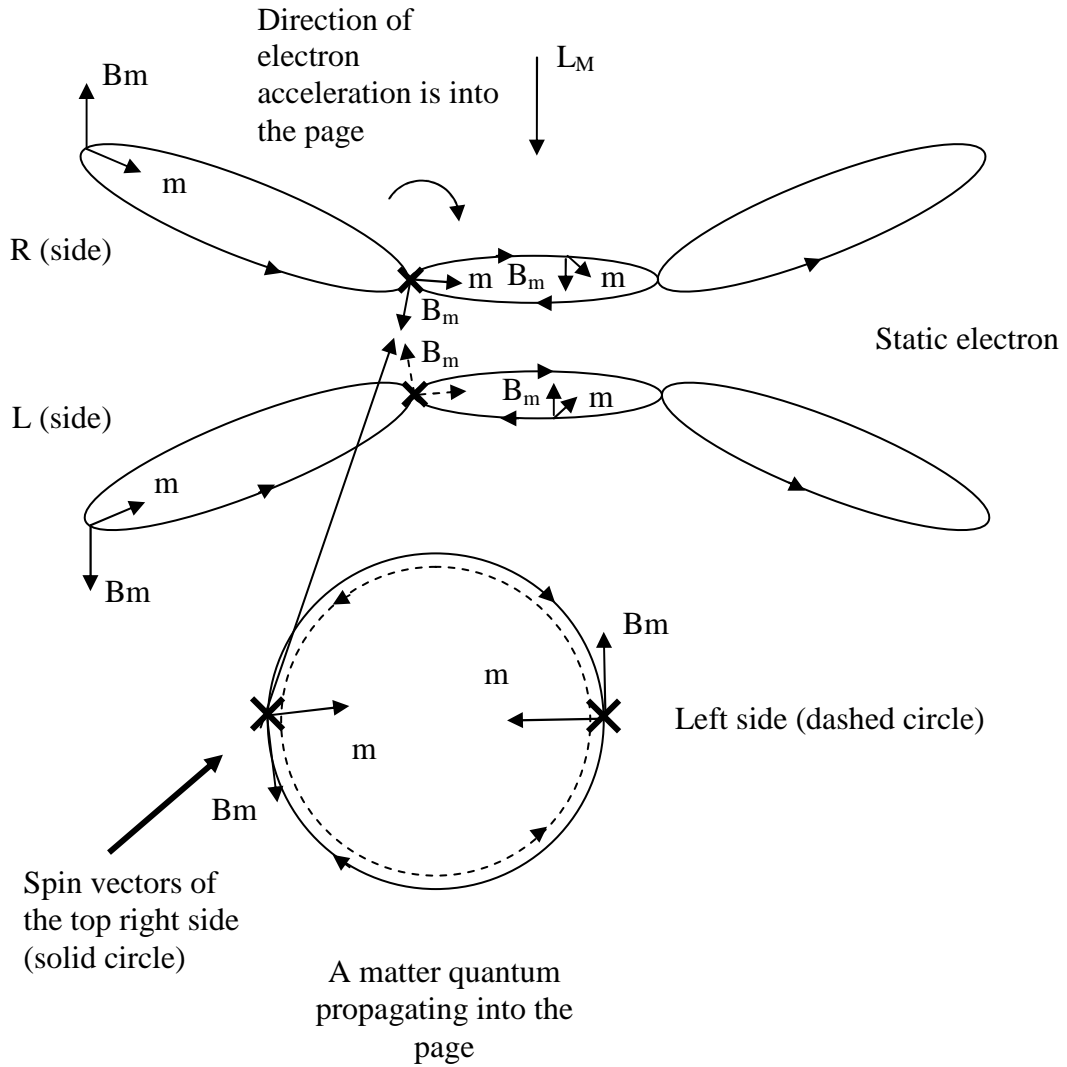


Antimatter quantum

FIG. 35B

Note that a matter quantum is considered to be emitted, for example, by an electron, and an antimatter quantum is considered to be emitted, for example, by a positron, and it will be shown later how an antimatter quantum can interact in a manner which is equivalent to a matter quantum, and vice versa.

The electric and magnetic fields of an electromagnetic field quantum (or an electrically charged particle) are considered to be detected during measurement as a consequence of the affect that the virtual particle paths of the propagating electromagnetic field quantum (or an electrically charged particle) have on another particle upon interaction. In figure (36), for example, consider that the right and left hand spin virtual particle paths of the matter quantum would align, and be respectively absorbed by, the top and bottom sides of the electron shown, such that the virtual particle paths of the quantum interact with the virtual particle paths of the electron, and thus cause the nuclear virtual particle paths of the electron to accelerate and project forward so as to establish the combined right and left elliptically polarized top and bottom sides of a propagating electron along the direction of the propagating quantum (which is propagating into the page). Here, consider that the quantum is absorbed due to a lack of repulsion because of its field geometry (comprising a lack of eccentricity) thus allowing the quantum's field to merge with the electron's field, and then become eccentric with the eccentric geometry of the electron's field upon deceleration (refer to the description later herein regarding the quantum's unified field spin vector geometry with respect to annihilation and pair production under the heading "particle transmutation and generation").

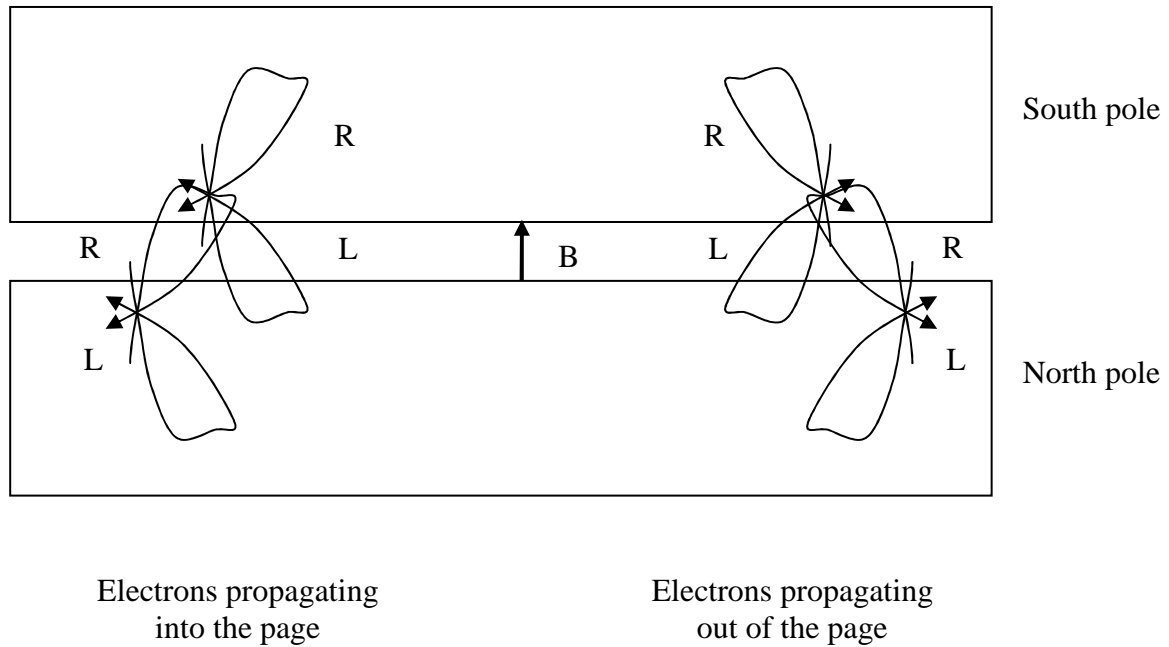


Static electron acceleration during absorption of the energy of an electromagnetic field matter quantum (only details of the absorption of top right side are shown)

FIG. 36

MAGNETIC INTERACTION:

Now, certain longstanding questions about magnetic fields can be addressed by examining the internal structure of static electrically charged particles, e.g., the conclusion that the existence of magnetic monopoles is not supported by the present theory can be made. Wherein, in a description of a magnetic field produced by magnets according to the unified field theory herein, consider that the more bent virtual particle paths from the top side of each of a number of electrons propagating in the north pole of one magnet, and the more bent virtual particle paths from the bottom side of each of a number of electrons propagating in the south pole of an opposing magnet, respectively extend out to produce the virtual particle paths of the static magnetic field between the north and south poles of two magnets as shown in figure (38A). In which case, the more bent virtual particle paths of electrons which are propagating in parallel with parallel intrinsic spins in orbitals magnetically interact attractively with electrons which are propagating in parallel with parallel intrinsic spins in orbitals in the opposing magnet as shown in figure (37). Consequentially, in two such magnets, electrons in orbitals of protons in one magnet would be magnetically accelerated in an attractive manner towards parallel propagating electrons in orbitals of protons in the opposing magnet, such that the atoms in the opposing magnetic materials would accelerate towards each other.



Here, example virtual particle paths extend out from parallel propagating electrons in one magnetic (e.g., the north pole here) into the opposing magnetic and interact in a magnetically attractive manner with the nuclear regions of parallel propagating electrons in the opposing magnet (as for propagating electrically charged particle interaction described previously).

FIG. 37

Figure (38A) shows the right and left spins of certain more bent virtual particle paths extending out from electrons which are comprised in opposing magnets so as to produce a magnetic field. While, figure (38A) also shows how the virtual particle paths of the magnetic field would interact with the top and bottom sides of negatively and positively charged particles which are propagating out of the page while propagating in, and perpendicular to, the magnetic field such that the top and bottom sides are accelerated in a respectively curved path. Wherein, the negatively and positively charged particles turn to the right and left (as shown looking into the page at figure 38A) for a negatively and positively charged propagating particle, respectively, due to the repulsion and attraction, respectively, of, in particular, the microscopic magnetic spin vector

components (B_{mc}) of the curved portions of the more bent extranuclear virtual particle paths of the opposing magnets on the nuclear microscopic magnetic spin vector components (B_{mc}) of the negatively and positively charged propagating particles (i.e., the propagating negatively and positively electrically charged particles would be accelerated in a direction which is perpendicular to the direction of the magnetic field (B) according to conventional left and right hand rules, respectively).

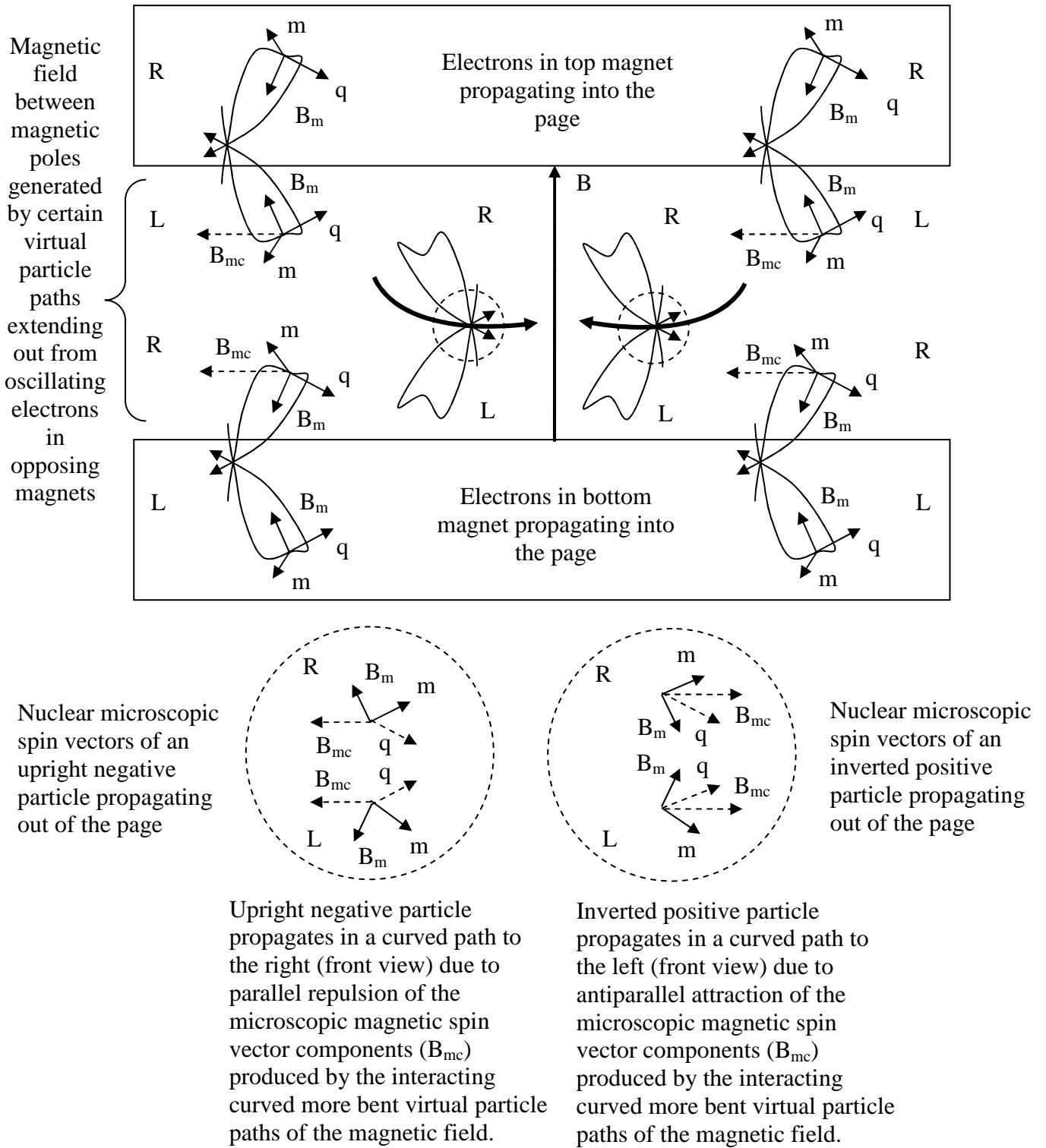
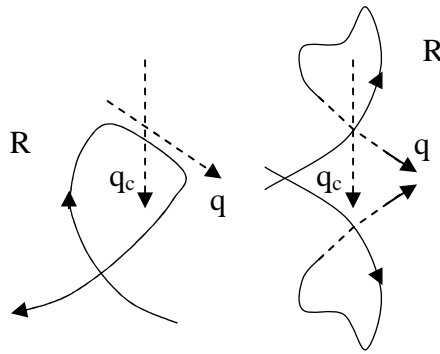


FIG. 38A

Figure (38B) shows the microscopic charge spin vector (q) and vertical component (q_c) of a right hand screw more bent virtual particle path of a portion of the magnetic field depicted in figure (38A) aligned with the charge spin vector (q) and vertical component (q_c) in the nuclear region of the right hand screw side of a negatively charged particle propagating in, and perpendicular to, a portion of the magnetic field.



The microscopic charge spin vector (q) and vertical component (q_c) of a portion of the magnetic field shown aligned with the charge spin vector (q) and vertical component (q_c) in the nuclear region of a negatively charged particle propagating to the right in, and perpendicular to, the magnetic field.

FIG. 38B

In application, for example, the spiral courses of negative and positive electrically charged propagating particles (and the undeflected course of neutral propagating particles) in a bubble chamber can be more clearly understood.

NUCLEAR INTERACTION:

Figure (39) shows some orthogonal charge, mass, and magnetic microscopic spin vectors of example virtual particle paths in the nuclear region of a static proton (static positively charged particle).

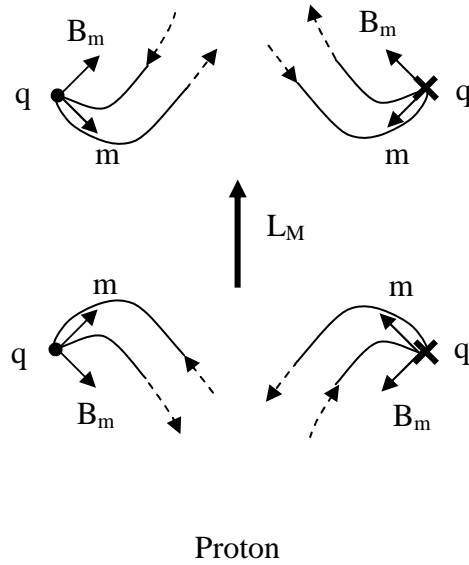


FIG. 39

Figure (40) shows some orthogonal charge, mass, and magnetic microscopic spin vectors of example virtual particle paths in the nuclear region of a static electron (static negatively charged particle).

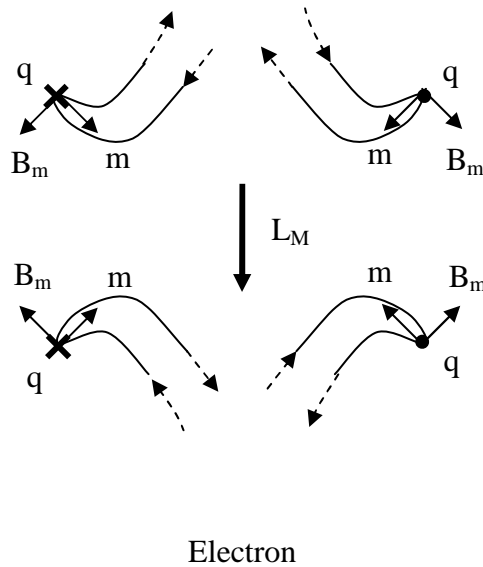


FIG. 40

Again, consider that the virtual particle paths on the top, bottom, and top and bottom sides self interact as propagating electrically charged particles interact by way of the respective right-right and left-left hand (q), (m), and (B_m) spin vector interactions, and consequentially experience a respective attractive, repulsive, or neutral alignment (internal bonding).

It is considered that a proton can bond with an electron to form a neutron as has been long argued by some in conventional physics. Figure (41A) shows the spin vectors which could exist for certain virtual particle paths of one side of an entirely isolated proton and electron before a possible "nuclear" interaction, and figure (41B) shows the alignment of the spin vectors of the virtual particle paths of one side of the proton and electron which could exist after forming a "nuclear bond" in the formation of a neutron. Wherein, the microscopic spin vectors of respective virtual particle paths are considered to rotate around respective orthogonal rotational axes upon interaction for a proton-electron bond in the formation of a neutron as shown by the arrows in figure

However, microscopic spin vectors of the virtual particle paths of a proton are considered to rotate around the orthogonal rotation axes upon interaction in the formation a proton-neutron bond as shown in figures (42A) and (42B).

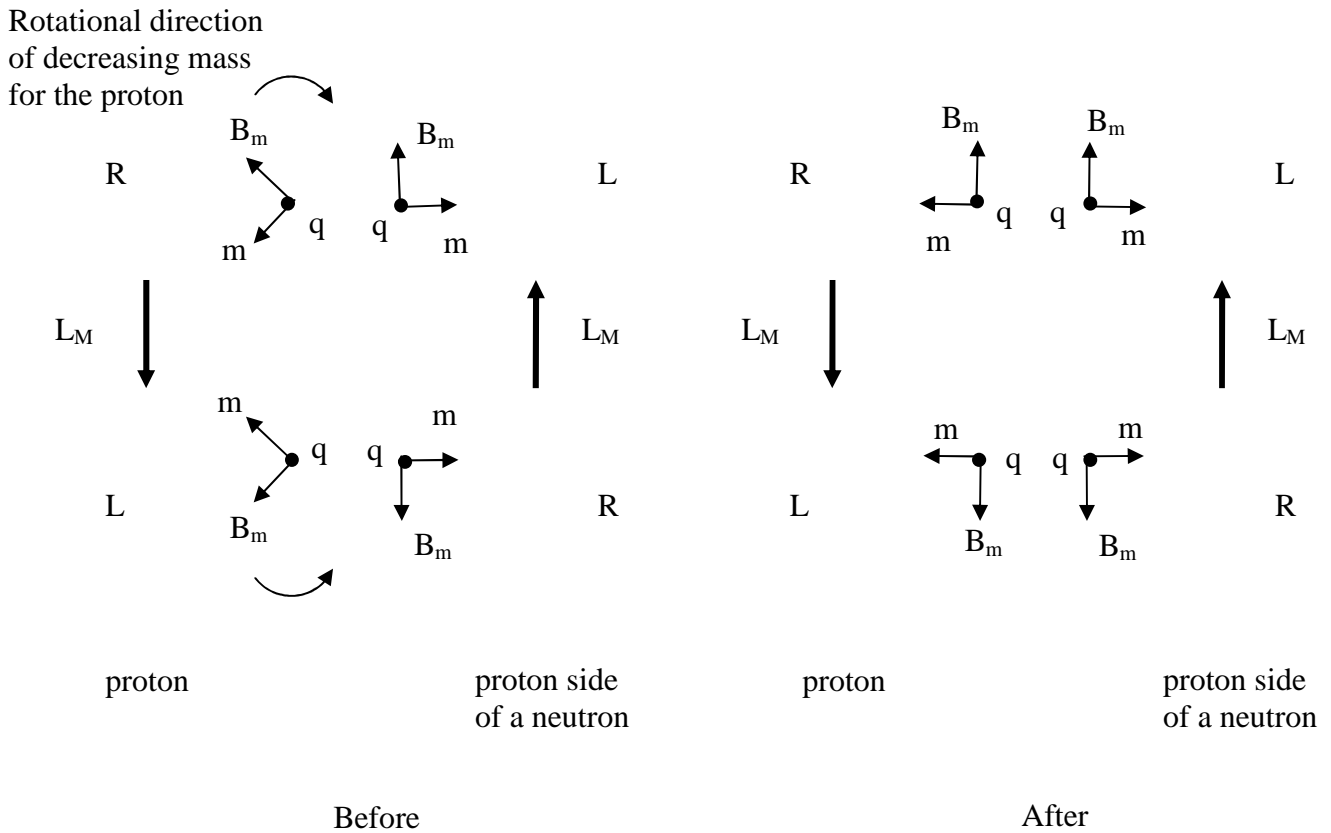


FIG. 42A

FIG. 42B

In the case of the proton-neutron bond, the spin vectors of the newly bonded proton are considered to rotate to a less massive alignment such that, in effect, the total mass of the nuclearily bonded proton and neutron decreases so as to produce a mass defect. Wherein, in respectively interacting virtual particle paths positioned diagonally, the microscopic electric spin vectors (q) align parallel and thus attract, the mass spin vectors (m) align antiparallel and thus repel, and the microscopic magnetic spin vector (B_m) align antiparallel and thus attract.

Thus, the unified theory herein depicts the physical meaning of mass defect and binding energy. (Note that for the proton-neutron bond, microscopic spin vector alignments are equivalent to the alignments of the microscopic spin vectors in extranuclear interaction for electromagnetic repulsion and gravitational "attraction" (which, in the latter case, attempts to turn the particle around) for particles of the same electric charge when the repelled particle is propagating away from the repulsive source. This is considered the preferred alignment of such particles in both cases, such that in the case of nuclear bonding, this alignment of the microscopic spin vectors represents the electromagnetic attraction and the gravitational "repulsion" of nucleons, i.e., in the latter case, a form of mass repulsion or "antigravity" which, along with the other cases of mass repulsion described herein, addresses the essence of the longstanding issue in physics questioning the existence of the property of antigravity.)

In this train of thought, the properties of the unified field, which include the attractive and repulsive aspects, need to be considered when accounting for dark energy and dark matter. Accordingly, consider a supermassive black hole in which a significant amount of the less bent virtual particle paths of the top and bottom sides are concentrated along the event horizon, accretion disc, and beyond (because of the mass of the black hole). In this case, the electromagnetic and gravitational components of the virtual particle paths of the top and bottom sides of the black hole would present an electromagnetic force on ordinary matter (comprising positively and negatively charged matter) by virtue of the electromagnetic component of the unified field, and would also present a gravitational force on ordinary matter by virtue of the gravitational component as well, thus enabling a supermassive black hole, for example, to maintain a galaxy. While still, however, it is considered that a black hole can have both gravitational and electromagnetic attraction and repulsion on another black hole depending upon the spin vectors of their respective virtual particle paths. Wherein, the repulsive interaction between black holes as such needs to be considered when accounting for the expansion of the universe, etc.

Nevertheless, continuing, the proton and electron in the neutron attract, and the sum of their masses is more than their resulting mass due to the respective rotations and realignments of their spin vectors. In which case, the electron is considered to “accelerate” (increase in mass) to a greater extent than the proton is considered to "decelerate" (decrease in mass) due to the disproportionate affect of the proton on the electron. While, the nuclearly bonded proton and neutron each attract, and yet, nevertheless, the sum of their masses is less than their resulting mass according to the rotations and realignments of the spin vectors of the decelerated proton.

As the spin vectors in a particle change alignment upon bonding, the virtual particle paths are redistributed in a denser manner for acceleration (resulting in an increase in mass), and are distributed in a less dense manner for deceleration (resulting in a decrease in mass). In which case, the extranuclear virtual particle paths in a nuclearly bonded proton in an atom comprising two or more nucleons has a certain amount of sideways bend due to the changes in the trajectories of its respective virtual particle paths, i.e., in particular, the extranuclear virtual particle paths, as a consequence of the rotations of the respective spin vectors, and, in result, produces the proper alignment for a respective orbital portion (as described more so later).

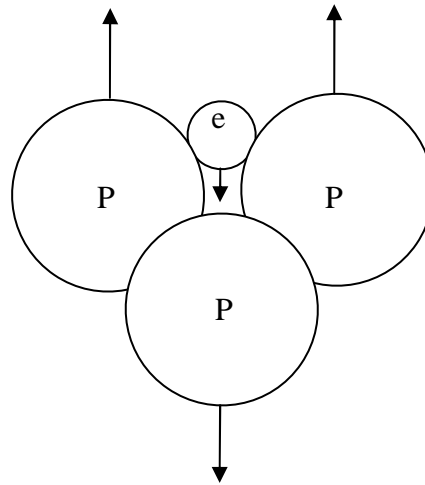
Now, the energy of an electron antineutrino which is associated with the formation of a neutron can be related to the acceleration ("compression") of the unified field of the bonded electron, and to an overall more massive condition which is created due to changes in spin vector alignments and the redistribution of its respective virtual particle paths to an overall more dense condition. Wherein, when a neutron decays in the process of beta decay, the proton and electron would separate, and the compressed unified field of the electron would recover to a respectively less compressed condition. In which case, it is considered that the energy of the electron antineutrino which is associated with beta decay corresponds to the release of the energy stored in the compressed unified field of the electron upon separation of the proton and electron. Then, the antineutrino would be produced from the resulting accelerated (i.e., decelerated) beta particle due to such changes (refer to

the description of particle generation by acceleration later herein under the heading "particle transmutation and generation").

ATOMS AND MOLECULES

In conventional physics, the Pauli exclusion principle is considered to play a significant role in the structure and function of matter (or mass-energy) (e.g., in the stability of atoms). The present unified field theory shows how this is the case.

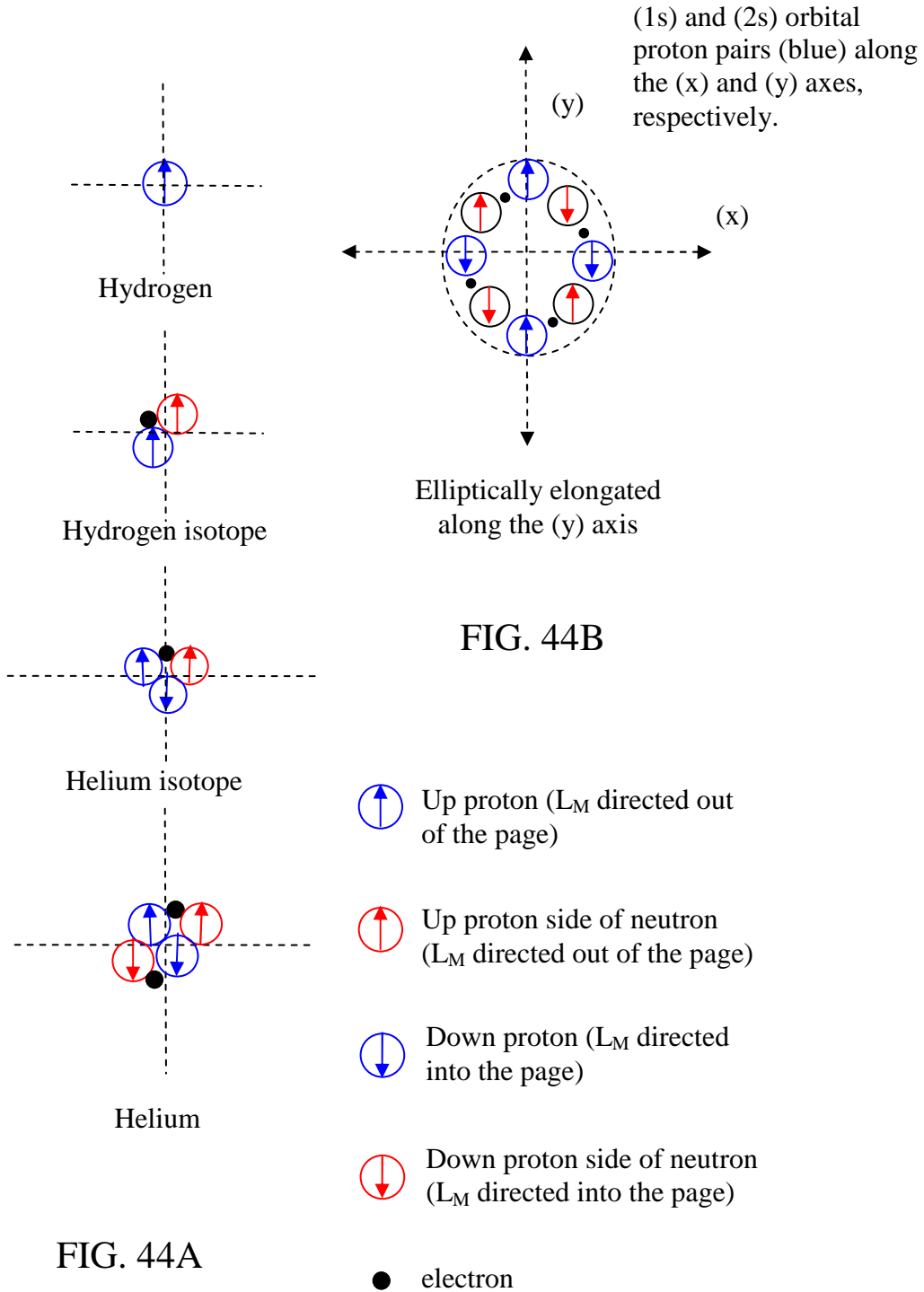
First, consider that the neutron assists in the bonding of protons according to the Pauli exclusion principle which includes assisting in the manner of nuclear bonding described hereinbefore. In the example shown in figure (43), three protons can be bonded by the placement of an electron between the two protons which have the same alignments of angular momenta. Wherein, one proton and a respectively bonded electron act as a neutron. (Note that the relative sizes of a proton and an electron relate to mass not radius, and is for pictorial purposes.)



Bonding of protons with an electron according to the Pauli exclusion principle (showing respective angular momenta).

FIG. (43)

Figures (44A) and (44B) show the nucleonic bonding in the (x-y) plane of a few nuclei in agreement with the Pauli exclusion principle. Notice how, according to up and down alignments, there is no net spin in terms of protons or electrons, and there is no net magnetic moment in terms of protons or electrons, in particular, in figure (44B), and also notice the respective quadrupole configuration of the protons.



Orbital proton and neutron positions are considered not only to be influenced by bond alignments, but are also considered to be influenced by nucleon proximity in which case the repulsion of a proton or protons, and the neutral presence of a neutron (or neutrons) are considered to affect proton positioning in the nucleus, and thus affect orbital positional potential energy. For example, in figure (44B) it is considered that the (1s) orbital is formed first with the (1s) protons along the (x) axis, and that, subsequently, repulsion by the (1s) protons affect the potential (and respective spin vector angles) of the protons which attempt to form the (2s) orbital. In which case, repulsion rotates the spin vectors of the approaching protons and they bond with neutrons at a slightly greater distance from the center than the (1s) protons (here, recall that spin alignment of a nuclearly bonded proton and neutron can be equivalent to the spin alignment, and the rotational directions thereof, of electromagnetic repulsion, such that, here, electromagnetic repulsion and nuclear bonding can work together). Consequentially, an elliptically shaped octet of nucleons is formed. In result, the (2s) protons along the (y) axis have slightly greater positional potential energy than the (1s) orbital protons (as relates to their spin vector angles, virtual particle path distributions, position relative to the center of the nucleus, etc.). Then, certain (p) orbital protons and neutrons form the next octet in the (x-y) plane, etc.

Orbital portions are considered to be affected asymmetrically by the repulsion of protons as shown in figure (45).

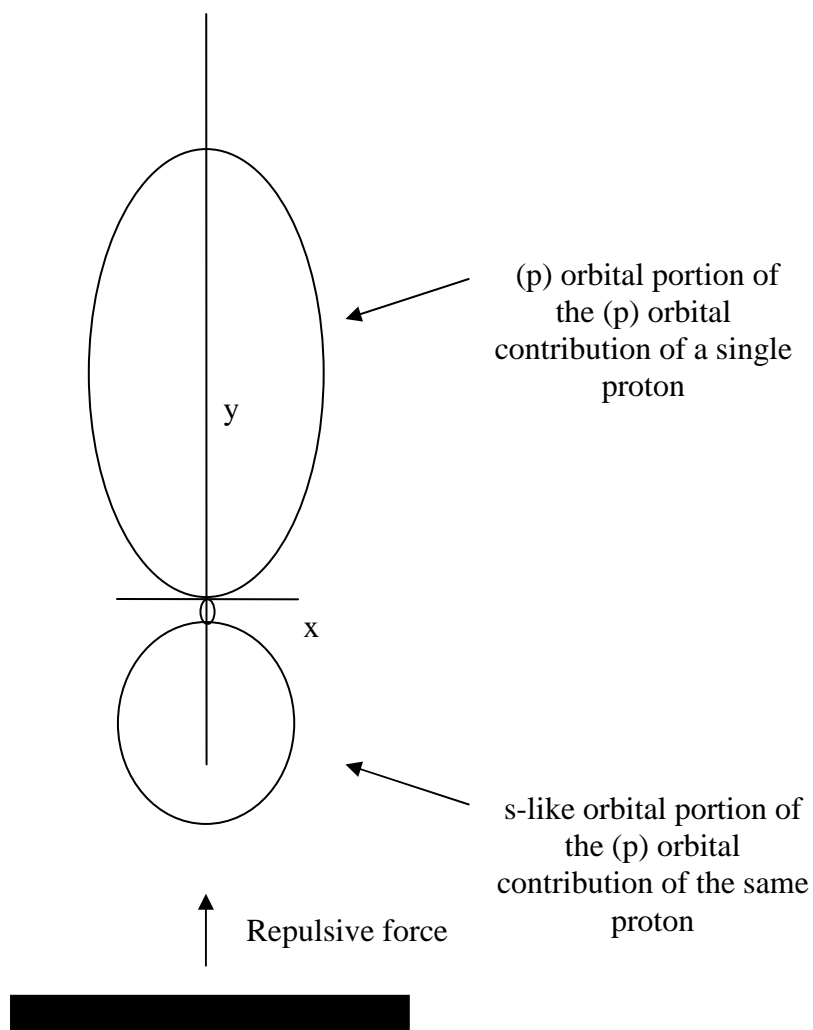
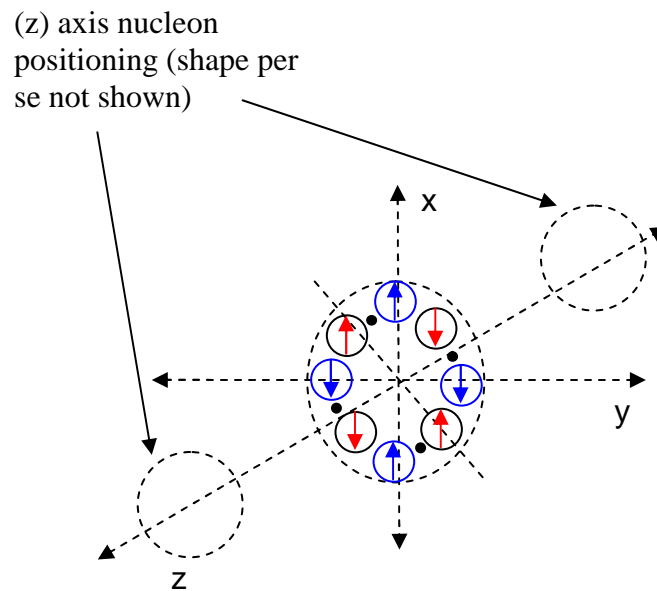


FIG. 45

With respect to figure (45), recall, still again, that spin alignment of a nucleary bonded proton and neutron can be equivalent to the spin alignment (and rotational directions thereof) of electromagnetic repulsion. In this case, initially present protons (solid black rectangle) repel new protons, and thus a new proton bonds in an

asymmetric elliptical configuration such that the virtual particle paths of each of the newly bonded protons experiences acceleration and deceleration rotations on opposite sides due to repulsion which corresponds to a decrease in mass on one side (top side here) and an increase in mass on the other (bottom side here) as exemplified by the more eccentric (p) orbital virtual particle paths on one side (less massive side) of the proton in contrast to those of the less eccentric (s-like) orbital virtual particle paths on the other side (more massive side) of the proton, respectively.

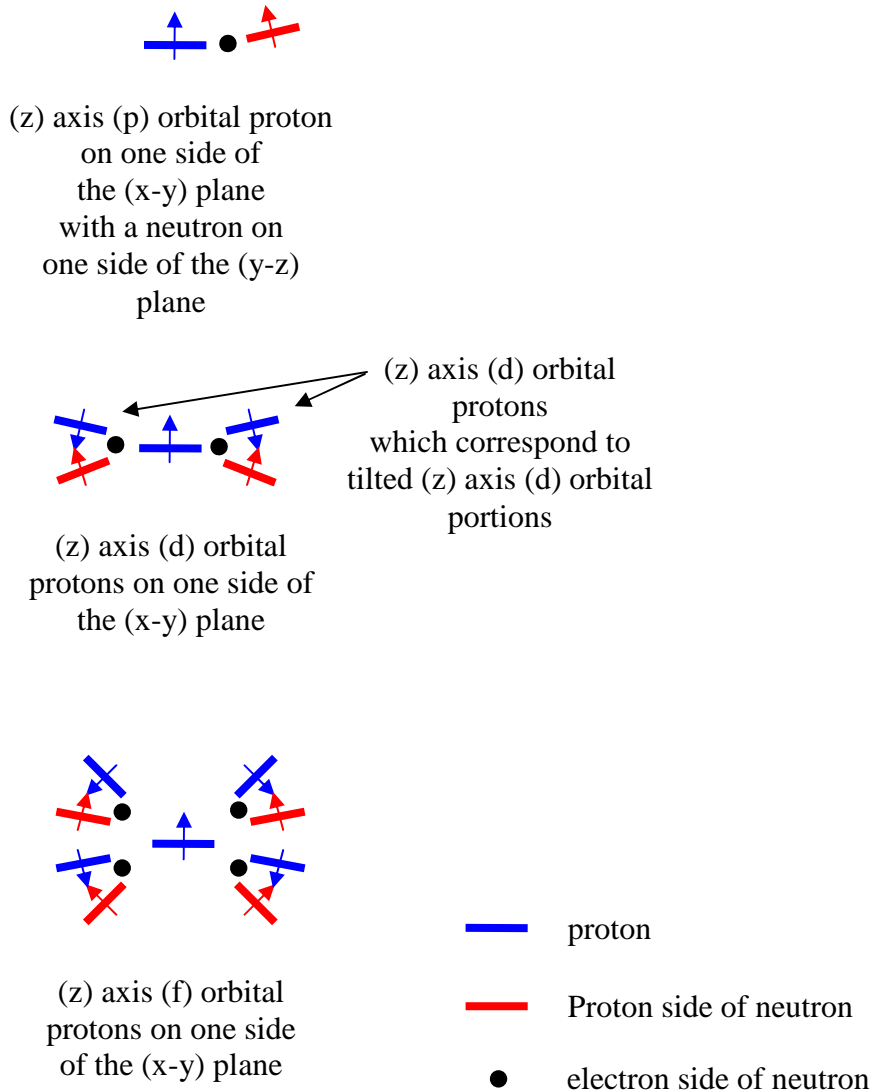
Figure (46) shows (z) axis nucleon positioning.



It is considered that in atoms with (z) axis nucleons, that nucleons along the (z) axis establish certain terms which affect nucleon positioning in the nucleus, such that, for example, certain (d) orbital bonding in the (x-y) plane occurs along certain axes due to proton repulsion and neutral neutron positioning of (d) orbital nucleons along the (z) axis.

FIG. 46

Figure (47), shows the (z) axis nucleon bonding of (p), (d), and (f) orbital nucleons on one side of the (x-y) plane, and the configuration of the (z) axis orbital protons on the two sides of the (x-y) plane are considered to symmetrically complement each other upon completion of a sub-shell. Wherein, as (s) and (p) orbital portions are constructed from the interacting extranuclear virtual particle paths of two protons in the (x-y) plane, certain (d), (f), etc. orbital portions are constructed from tilted versions of the same configuration (with respect to the z-axis). In which case, the nucleonic bonding of (z) axis nucleons also occurs in agreement with the Pauli exclusion principle. (Note that the “nesting” of orbital portions is considered to pertain to the ability of an electron to propagate in any orbital portion by switching virtual particle paths where virtual particle paths combine.)



Here, the (z) nucleon bonding of (p), (d), and (f) orbital nucleons is shown. As for the octets, the (z) orbital proton and neutron positions as shown are considered not only to be influenced by bond alignments but are also considered to be influenced by the protons and neutrons along the (z) axis, and influenced by the protons and neutrons in the octets in the (x-y) plane.

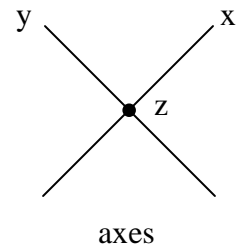


FIG. 47

Figure (48) shows two (d) orbital nucleon configurations in the (x-y) plane which are considered to establish the $d_{x^2-y^2}$ and d_{xy} (d) orbitals.



FIG. 48

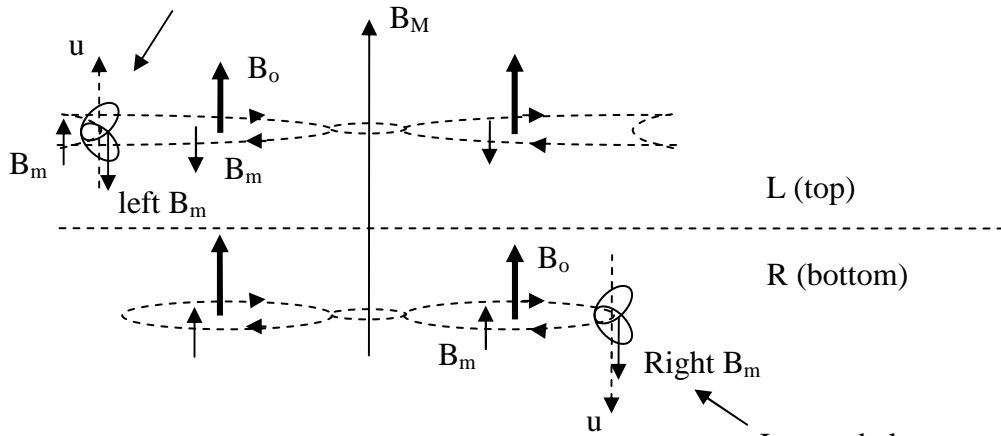
It is considered that as atomic number increases so to does the repulsion and respective orbital eccentricity increase in general for newly bonded protons, and as the number of related nucleonic bonds (azimuthal quantum number related orbital nucleons) increases so to increases the eccentricity of the resulting orbitals. While, in general, the size of an orbital is considered to increase as the positional potential energy of an orbital increases according to its spin vector rotations (in the less massive direction) due to field repulsion and the number of related nucleonic bonds.

The (s) orbitals are considered to be bonded in nucleonic octets which are separate from the (p), (d), (f), etc. sub-shell protons bonded in nucleonic octets in the (x-y) plane which are considered to have bonds with nucleons which are also situated along the (z) axis (e.g., via the tilted alignment of the z-axis d-orbital protons of a d-sub-shell extending out to respective nucleons of other d-orbital sub-shell portions in octets in the x-y plane). Wherein, in the example given, the (d) orbital nucleons bond while aligned so as to pass over the

relevant (s) orbital protons to some extent, i.e., (s) orbital protons are situated in field "pockets" absent of some repulsion. Thus, the (s) orbitals are considered to be less elliptical in shape, less asymmetric, and are considered to have less positional potential energy than, for example, (d) orbitals due to less field repulsion and a lesser number of related nuclear bonds, and, are considered to fill first since they are produced by inner positioned nucleons.

Next, the unified field theory shows in figure (49A) how the Pauli exclusion principle is involved in fine and hyperfine structure in a hydrogen atom. Figure (49A) shows a side view of one electron at any given time in the horizontal plane on the top or bottom side of the (s) orbital formed by a single non-nuclearly bonded proton (hydrogen atom). It is considered, for example, as shown in figure (49A), that the top side right hand spin virtual particle paths of a first inverted low energy electron could couple with (and be accelerated by) the less bent bottom side right hand spin virtual particle paths of the (s) orbital proton, such that the right hand (top side) microscopic magnetic spins (B_m) of the electron are antiparallel with microscopic magnetic spins of the right hand spin virtual particle paths (bottom side) of the of the proton, and such that the electron would oscillate with its magnetic moment (μ) antiparallel with the magnetic field (B_o) which it generates while orbiting (fine structure), and antiparallel with the macroscopic magnetic field (B_M) of the proton (hyperfine structure). While, as shown in figure (49A) at another time, an effectively upright high energy electron in the same (s) orbital could oscillate with its left hand (bottom side) microscopic magnetic spins (B_m) antiparallel with microscopic magnetic spins of the more bent left hand spins (top side) virtual particle paths of the proton, and oscillate with its magnetic moment (μ) parallel with the magnetic field (B_o) which it generates while orbiting (fine structure), and parallel with the macroscopic magnetic field (B_M) of the proton (hyperfine structure). Wherein, the more bent top sides of the proton are considered to comprise higher positional potential energy.

Upright electron propagating into the page on a more bent orbital portion on the top left side of an (s) orbital (shown in a plane in a horizontally sectioned view). Note that the direction of the electron is aligned by factors including the bending of the virtual particle paths of the proton.



Electron at different times in more and less bent orbital portions in the (s) orbital of a hydrogen atom (shown in planes in a horizontally sectioned view).

Inverted electron (lower energy) propagating out of the page on a less bent orbital portion on the bottom right side of an (s) orbital (shown in a plane in a horizontally sectioned view).

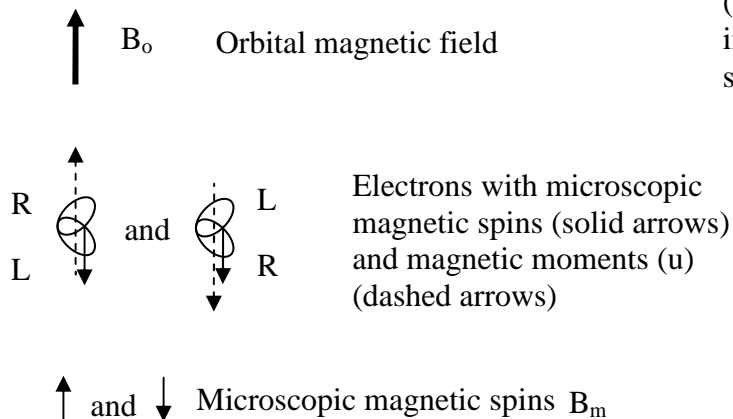
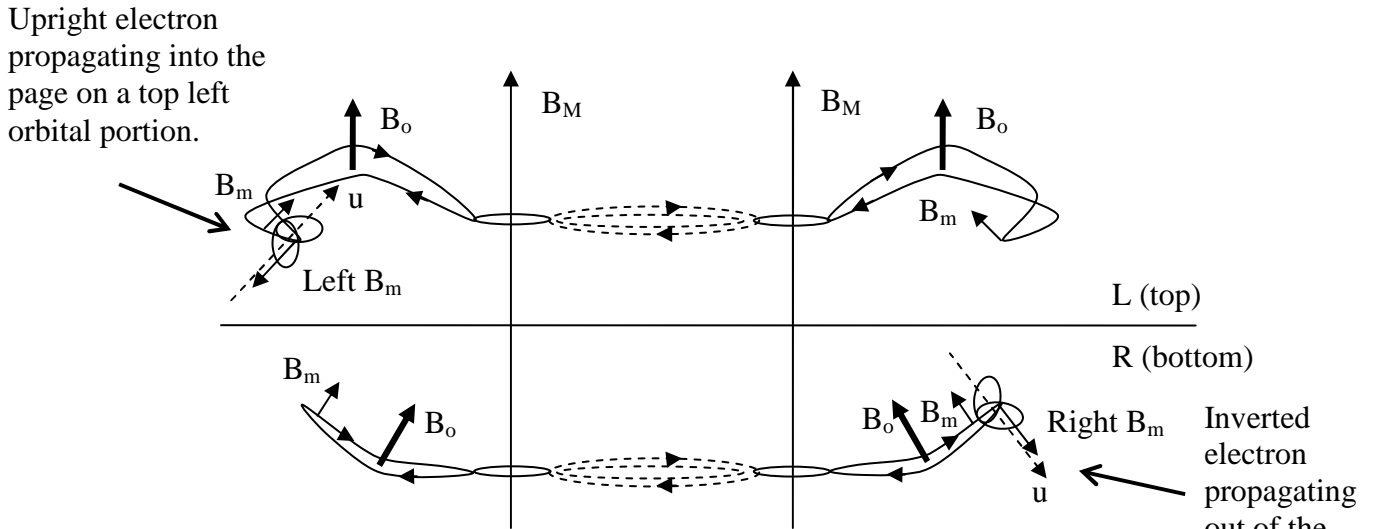


FIG. 49A

A similar example of the role of the Pauli exclusion principle in the fine and hyperfine structure in the unified field is shown in an (s) orbital of an atom formed by two nuclearily bonded protons in figure (49B).



Electrons in orbital portions in an (s) orbital produced from the combining of orbital virtual particle path portions from two protons. Wherein the combined portions, as in terms of "phase," extend out over the orbitals of both protons, in which case the combined center portions are shown in dashed line format. Note that the microscopic magnetic spins of the more bent virtual particle paths on the top left orbital portion invert the electron so that it is effectively upright, while the alignments of microscopic magnetic spins of the less bent virtual particle paths on the bottom right orbital portion effectively produce an inverted electron.

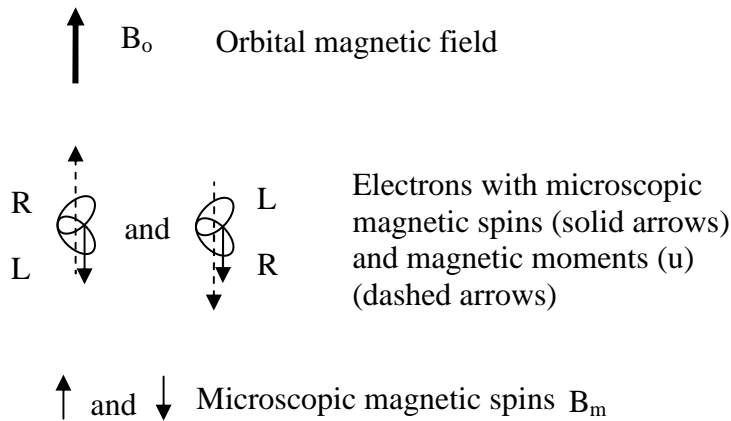
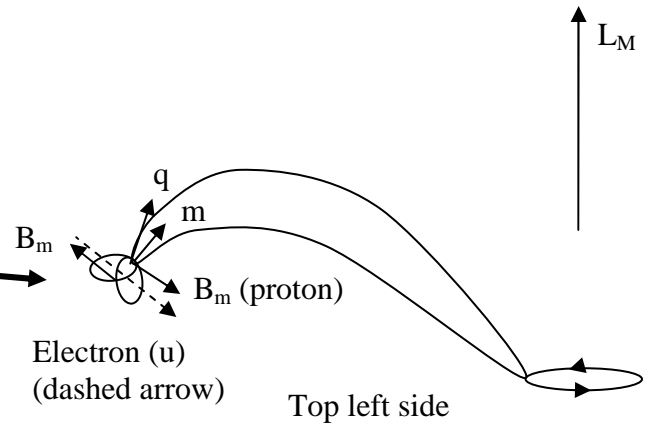


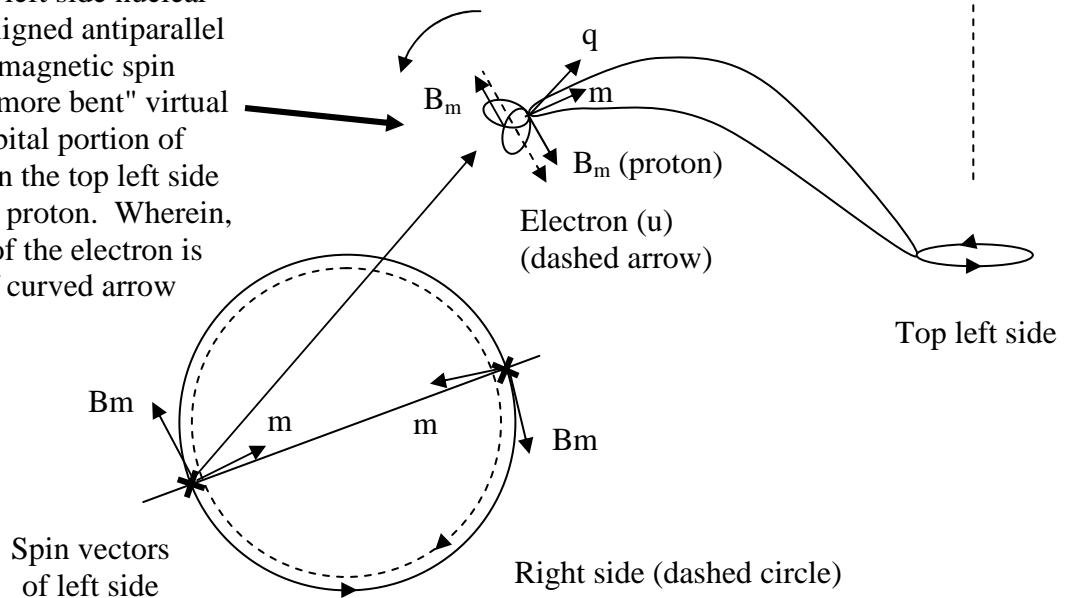
FIG. 49B

Still yet another example of the present unified field theory showing how electrons behave in atoms is illustrated in figure (50) which shows why electrons move outward from orbitals of lower to higher positional potential energy in atoms upon absorbing energy. Wherein, figure (50) shows an electron oscillating with its left hand microscopic magnetic spin (B_m) antiparallel with the microscopic magnetic spin of a "somewhat more bent" virtual particle path of the top left hand screw side of a nuclearly bonded proton (lower portion of the drawing), and shows the respective spin vector alignment of a quantum during absorption. Wherein, the quantum produces spin vector rotations in the electron so that the spin vectors of the electron rotate towards the alignment of the spin vectors of the "even more bent" virtual particle path on an orbital higher in positional potential energy, such that the electron then propagates on the respective orbital higher in positional potential energy while aligning with the magnetic fields in its environment. (Note that a similar process would occur for elevating an electron in a hydrogen atom, i.e., a non-nuclearly bonded proton.)

Inverted electron propagating into the page with the microscopic magnetic spin vector (B_m) of a bottom left side nuclear virtual particle path aligned antiparallel with the microscopic magnetic spin vector (B_m) of an "even more bent" virtual particle path on an orbital portion of greater positional PE on the top left side of the nuclearily bonded proton.



Inverted electron propagating into the page with the microscopic magnetic spin (B_m) of a bottom left side nuclear virtual particle path aligned antiparallel with the microscopic magnetic spin (B_m) of a "somewhat more bent" virtual particle path on an orbital portion of lesser positional PE on the top left side of a nuclearily bonded proton. Wherein, the mass spin vector of the electron is rotated in direction of curved arrow upon acceleration.



A matter quantum propagating into the page

Here, a quantum is absorbed by an electron in the extranuclear region of an orbital. Wherein, the directions of rotation for increases in positional potential energy for the virtual particle paths of the proton are in the same direction as the direction of rotation for an increase in mass for the electron. Thus, the electron is accelerated by the quantum, and then couples with the virtual particle paths of an orbital at a different (greater) positional potential energy level, such that the electron then propagates on the respective orbital higher in positional potential energy while aligning with the magnetic fields in its environment (wherein only certain details of the absorption of the left side of the quantum are shown).

FIG. 50

Next, the combinability (phase) of the virtual particle paths of molecularly bonded protons is considered to occur according to their respective spin vector directions and effective interactions including electric repulsion and magnetic attraction by their respectively less and more bent virtual particle paths with respectively involved electrically charged particles. Figures (51A) (top view) and (51B) (side view) show sigma and pi molecular bonding orbital portions due to electrons on respectively resulting virtual particle paths (in agreement, in general, with convention).

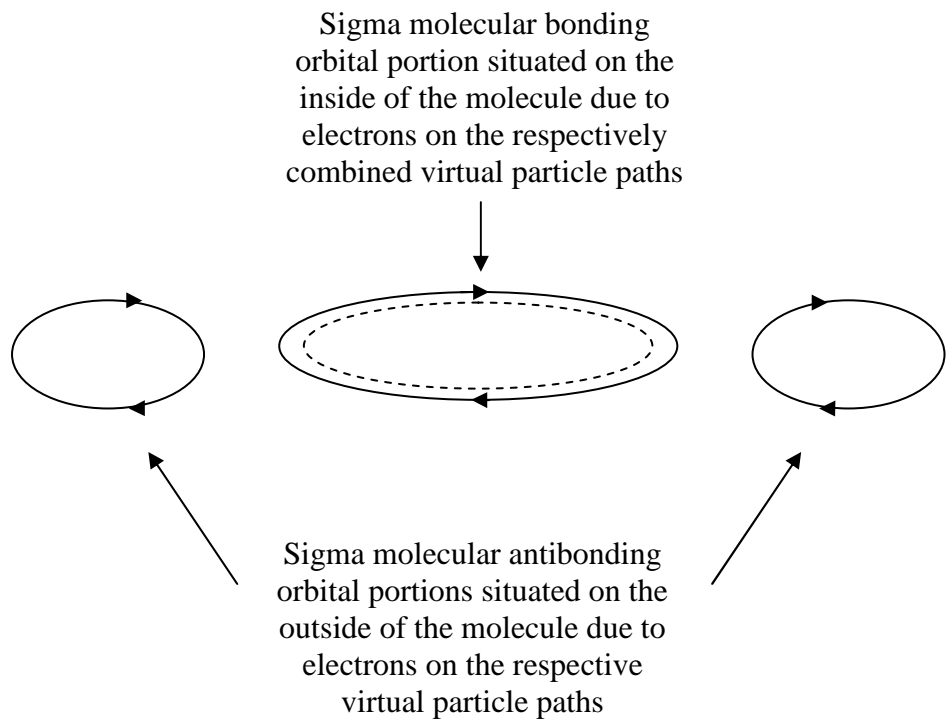


FIG. 51A

Pi molecular bonding orbital portions situated on the inside of the molecule due to electrons on the respectively combined virtual particle paths

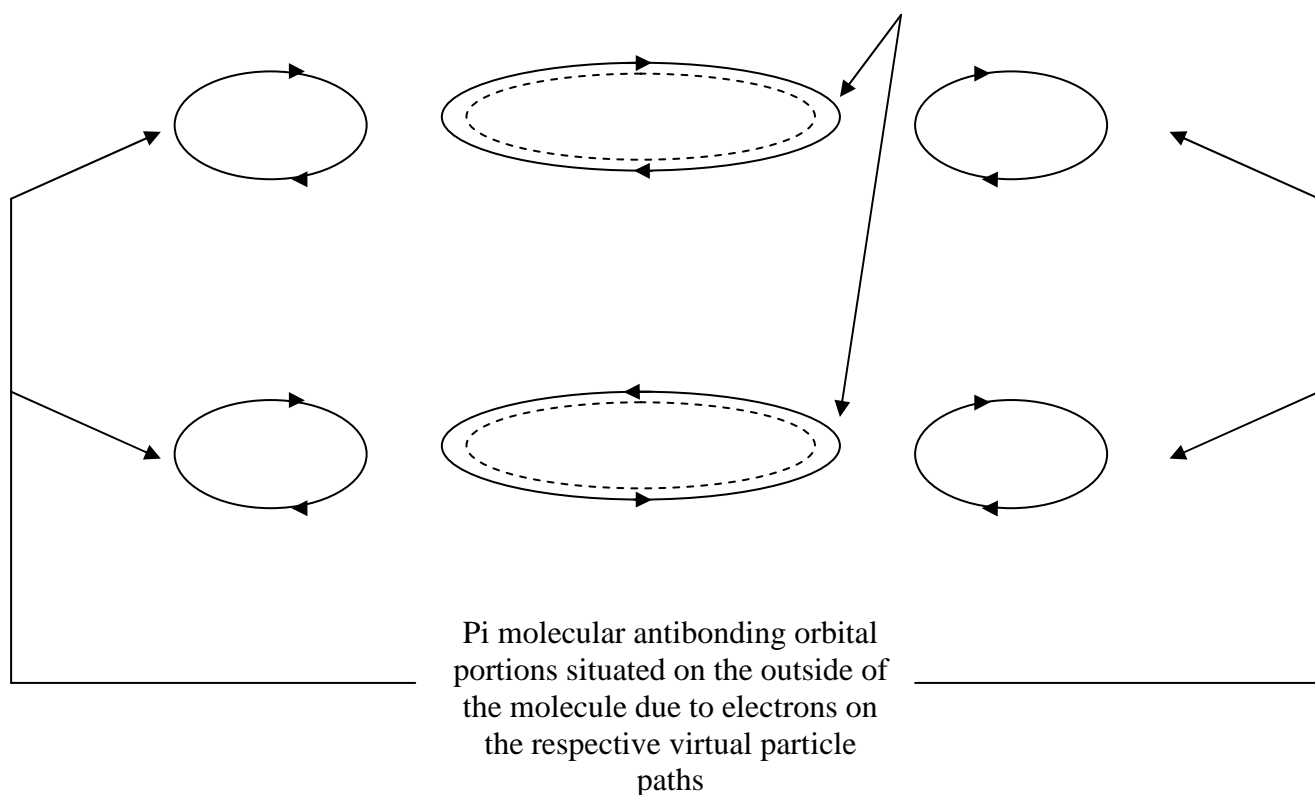


FIG. 51B

PARTICLE TRANSMUTATION AND GENERATION:

Now, it is considered the vast diversity of particles which are produced in particle physics have a cause which transcends conventional theory, and, if understood, would change the approach of conventional particle physics in its efforts to discover the underlying structure and function of mass-energy, and ultimately the universe. Respectively, the cause of such a vast diversity of particles as such is considered to simply relate to the manifestations which are produced by the acceleration and deceleration of the mass-energy of the unified field presented herein.

Accordingly, first, in certain types of accelerations, a particle can transmute from one type of particle into another type of particle. For example, in one such type of "transmutational acceleration," the top and bottom sides of an electrically charged particle reflect almost totally together so as to change into an electrically neutral particle. The transmutation of an electron and a positron into a matter and antimatter electromagnetic field quantum, respectively, upon annihilation is one example. In this case, the annihilating matter and antimatter are considered to interact in a symmetric manner so as to eliminate a significant extent of the eccentricities (including a significant extent of the bends) in their respective virtual particle path bands, such that the virtual particle paths of the top and bottom sides of each electrically charged particle (e.g., the electron and positron in the example) converge, narrow, and project forward. Wherein, the virtual particles on the top side and the virtual particles on the bottom side of the respectively produced quanta consequentially propagate away (while interacting) with translational velocity (c).

It is considered that in another type of acceleration, that a neutral particle can produce two particles of opposite spin and opposite charge while conserving electric charge, etc. as shown in figure (52). Wherein, for example, the top and bottom sides of an effectively electrically neutral gamma ray could, upon deceleration,

open so as to produce an electron, in which case the top and bottom sides of the electron thus produced would split such that one portion would flip over so as to produce a positron of the opposite spin and opposite electric charge, and the other portion would continue in the form of an electron as in the case of pair production. Note that it is considered that a matter quantum differs from an antimatter quantum according to the different top and bottom screw rotations, different top and bottom microscopic magnetic spin (B_m) directions, etc., similar to how a negatively and a positively electrically charged particle differ. However, it is considered that an antimatter quantum can act in a manner which is equivalent to that of a matter quantum by the top and bottom sides flipping over, for example, upon being absorbed by an electron. Here, nevertheless, the production of oppositely charged particles (including the production of matter and antimatter) from an electrically neutral particle can be more profoundly understood by such a process.

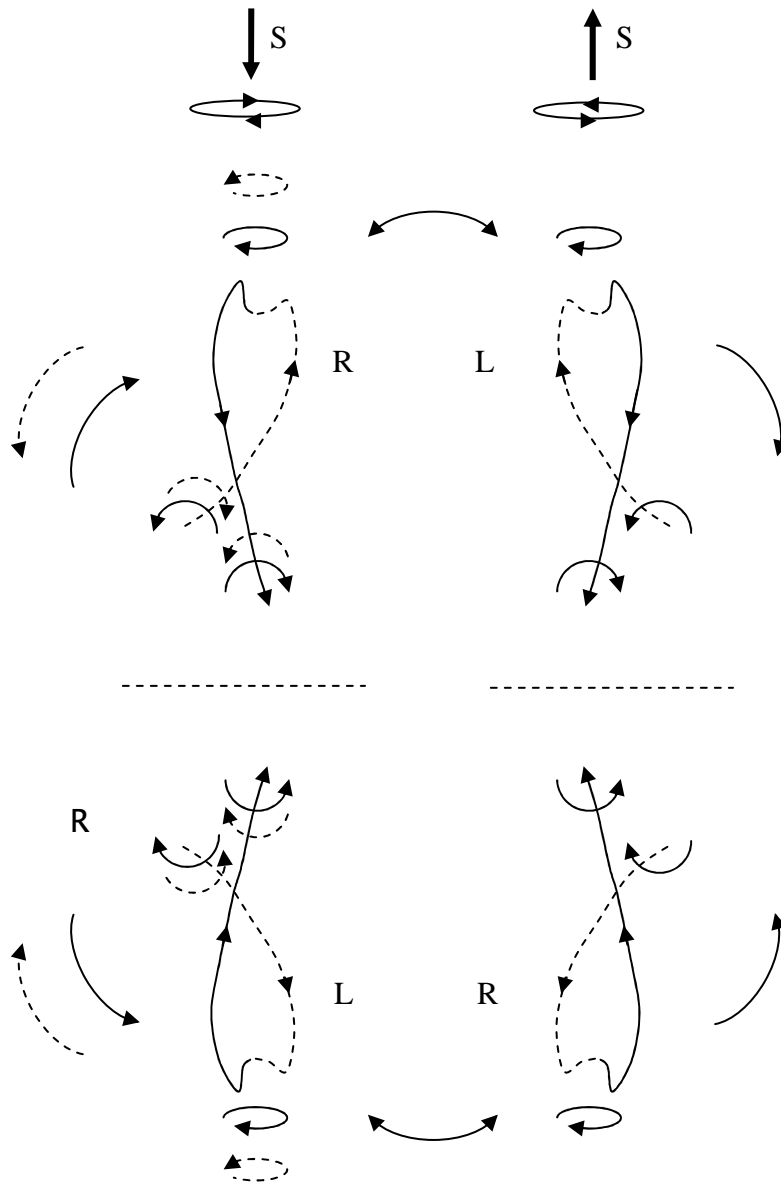


FIG. 52

In yet another type of acceleration, it is considered that a given electrically charged particle can cause the emission of another particle (e.g., during an oscillation). Wherein, in one such acceleration, the top and bottom sides of the electrically charged particle would emit a particle from the nuclear region which would have top and bottom sides which are almost totally reflected together (e.g., as with an electromagnetic field

quantum). In which case, the top and bottom right and left hand screws of the emitted particle would be the same as the particle which emitted it yet with bands of virtual particle paths with spin vectors of different alignment (and eccentricity), such that the emitted particle would have neither an effective nuclear region nor an effective bend in its extranuclear field, and thus have neither an effective mass nor electromagnetically attract or repel in a effective manner (but electromagnetically, electrically, and gravitationally interact as mentioned previously).

In still yet another type of acceleration, the dipole pattern of electromagnetic radiation can be emitted by the virtual particles on the virtual particle paths of an accelerated electrically charged particle (e.g., a non-relativistically accelerated electron). Wherein, the structure and function of a virtual particle is considered analogous to that of an accelerated electrically charged particle as stated above. While in even still yet another type of acceleration, the forwardly directed pattern of electromagnetic radiation from a relativistically accelerated electron in a synchrotron is considered to be produced by the virtual particles on the virtual particle paths of the forwardly aligned top and bottom sides of the respectively accelerated electron as the electron follows a helical course while effectively propagating forward in the magnetic field of the synchrotron.

CONCLUSION:

In conclusion, one unifying general function for a unified field has been provided with the application of Planck units which produces equations which not only unify all of the conventional fields and respective forces, but also unifies mass-energy and electric charge with "spacetime," and in result includes quantum field theory and relativity as well. Accordingly, the unifying principles were applied in a description of the geometry (including internal structure) and functionality of certain aspects of the unified field including the geometry and functionality of electromagnetic, gravitational, and nuclear interaction, the geometry and

functionality of Lorentz transformations, and the structure and function of elementary particles (including antiparticles), atoms, molecules, and bodies of astronomical dimensions. In broadening, the resulting unified field theory proposes to provide a basis for describing and solving problems in unified terms in other areas of physics which include subject matter which pertains to relevant "probabilistic" phenomena, chaos, big bang theory, and, in general, the universe as a whole. While furthermore, it is proposed that the principles of the unified field theory presented are also applicable as a means of describing and solving problems in unified terms in other areas of the sciences.